

N71-33719
NASA CR-121473

NATIONAL AERONAUTICS AND SPACE ADMINISTRATION

Technical Memorandum 33-486

*Use of Derived Forcing Functions at Centaur Main
Engine Cutoff in Predicting Transient Loads on
Mariner Mars '71 and Viking Spacecraft*

M. R. Trubert

J. R. Chisholm

W. H. Gayman

CASE FILE
COPY

JET PROPULSION LABORATORY
CALIFORNIA INSTITUTE OF TECHNOLOGY
PASADENA, CALIFORNIA

June 28, 1971

NATIONAL AERONAUTICS AND SPACE ADMINISTRATION

Technical Memorandum 33-486

*Use of Derived Forcing Functions at Centaur Main
Engine Cutoff in Predicting Transient Loads on
Mariner Mars '71 and Viking Spacecraft*

M. R. Trubert

J. R. Chisholm

W. H. Gayman

**JET PROPULSION LABORATORY
CALIFORNIA INSTITUTE OF TECHNOLOGY
PASADENA, CALIFORNIA**

June 28, 1971

Prepared Under Contract No. NAS 7-100
National Aeronautics and Space Administration

ACKNOWLEDGEMENT

The analyses relating to the predictions of Viking spacecraft response at MECO were funded by NASA Langley Research Center, and were under the cognizance of Dr. John P. Raney and Mr. Larry Pinson.

The work described in this report was performed by the Engineering Mechanics Division of the Jet Propulsion Laboratory.

CONTENTS

I.	Introduction	1
II.	Mathematical Models	1
	A. Centaur Launch Vehicle Model	1
	B. Mariner Mars '71 Spacecraft Model	1
	C. Viking Spacecraft Model	2
III.	Computer Analysis	2
	A. Computer Programs	2
	B. Mariner '71/Centaur Composite Vehicle	2
	C. Viking/Centaur Composite Vehicle	3
IV.	Discussion	4
V.	Conclusion	5
	References	6
	Tables	
1.	Centaur MECO torsional model for Viking spacecraft – gridpoints, station locations and moments of inertia.	7
2.	Centaur MECO lateral model Viking spacecraft – gridpoints, station locations, weights and moments of inertia	8
3.	Centaur MECO longitudinal model for Viking spacecraft – gridpoints, station locations and weights	9
4.	Centaur MECO lateral model for Viking spacecraft – spring constants	10
5.	Centaur MECO longitudinal model for Viking spacecraft – spring constants	11
6.	Centaur MECO torsional model for Viking spacecraft – spring constants	12
7.	Natural frequencies, damping and elastic-rigid coupling matrix [M_{ER}] for the Mariner '71 spacecraft	13
8.	Rigid body mass matrix [M_{RR}] for the Mariner '71 spacecraft	14
9.	Elastic-rigid coupling matrix [M_{ER}] for Viking spacecraft model	15

CONTENTS (Cont'd)

Tables (Cont'd)

10.	Rigid body weight matrix $[M_{RR}]$ for Viking spacecraft model	16
11.	ϕ_{1r} and ϕ_{1e} matrices for MECO Mariner '71/Centaur model	17
12.	ϕ_{2r} and ϕ_{2e} matrices for MECO Mariner '71/Centaur model	18
13.	Rigid body mass matrix $[M_{rr}]$ for Mariner '71/Centaur model	19
14.	ϕ_{1r} and ϕ_{1e} matrices for MECO Viking/Centaur model	20
15.	ϕ_{2r} and ϕ_{2e} matrices for MECO Viking/Centaur model	22
16.	Rigid body mass matrix $[M_{rr}]$ for Viking/Centaur model	24

Figures

1.	Centaur vehicle model for Viking model	25
2.	Gridpoint 12, Centaur-Mariner Mars '71 acceleration response in X-direction at base of Centaur adapter predicted from the forcing function obtained from Mariner VI (AC-20) MECO flight data	26
3.	Gridpoint 12, Centaur-Mariner Mars '71 acceleration response in Y-direction at base of Centaur adapter predicted from the forcing function obtained from Mariner VI (AC-20) MECO flight data	27
4.	Gridpoint 12, Centaur-Mariner Mars '71 acceleration response in Z-direction at base of Centaur adapter predicted from the forcing function obtained from Mariner VI (AC-20) MECO flight data	28
5.	Gridpoint 12, Centaur-Mariner Mars '71 rotational acceleration response in θ_x -direction at base of Centaur adapter predicted from the forcing function obtained from Mariner VI (AC-20) MECO flight data . . .	29
6.	Gridpoint 12, Centaur-Mariner Mars '71 rotational acceleration response in θ_y -direction at base of Centaur adapter predicted from the forcing function obtained from Mariner VI (AC-20) MECO flight data . . .	30
7.	Gridpoint 12, Centaur-Mariner Mars '71 torsional acceleration response in θ_z -direction at base of Centaur adapter predicted from the forcing function obtained from Mariner VI (AC-20) MECO flight data . . .	31
8.	Gridpoint 12, Centaur-Mariner Mars '71 acceleration response in X-direction at base of Centaur adapter predicted from the forcing function obtained from Mariner VII (AC-19) MECO flight data	32
9.	Gridpoint 12, Centaur-Mariner Mars '71 acceleration response in Y-direction at base of Centaur adapter predicted from the forcing function obtained from Mariner VII (AC-19) MECO flight data	33

CONTENTS (Cont'd)

Figures (Cont'd)

10.	Gridpoint 12, Centaur-Mariner Mars '71 acceleration response in Z-direction at base of Centaur adapter predicted from the forcing function obtained from Mariner VII (AC-19) MECO flight data	34
11.	Gridpoint 12, Centaur-Mariner Mars '71 rotational acceleration response in θ_x -direction at base of Centaur adapter predicted from the forcing function obtained from Mariner VII (AC-19) MECO flight data	35
12.	Gridpoint 12, Centaur-Mariner Mars '71 rotational acceleration response in θ_y -direction at base of Centaur adapter predicted from the forcing function obtained from Mariner VII (AC-19) MECO flight data	36
13.	Gridpoint 12, Centaur-Mariner Mars '71 torsional acceleration response in θ_z -direction at base of Centaur adapter predicted from the forcing function obtained from Mariner VII (AC-19) MECO flight data	37
14.	Gridpoint 12, Mariner Mars '71 reaction force in X-direction at base of Centaur adapter predicted from the forcing function derived from Mariner VI (AC-20) MECO flight data	38
15.	Gridpoint 12, Mariner Mars '71 reaction force in Y-direction at base of Centaur adapter predicted from the forcing function derived from Mariner VI (AC-20) MECO flight data	39
16.	Gridpoint 12, Mariner Mars '71 reaction force in Z-direction at base of Centaur adapter predicted from the forcing function derived from Mariner VI (AC-20) MECO flight data	40
17.	Gridpoint 12, Mariner Mars '71 reaction moment in θ_x -direction at base of Centaur adapter predicted from the forcing function derived from Mariner VI (AC-20) MECO flight data	41
18.	Gridpoint 12, Mariner Mars '71 reaction moment in θ_y -direction at base of Centaur adapter predicted from the forcing function derived from Mariner VI (AC-20) MECO flight data	42
19.	Gridpoint 12, Mariner Mars '71 reaction moment in θ_z -direction at base of Centaur adapter predicted from the forcing function derived from Mariner VI (AC-20) MECO flight data	43
20.	Gridpoint 12, Mariner Mars '71 reaction force in X-direction at base of Centaur adapter predicted from the forcing function derived from Mariner VII (AC-19) MECO flight data	44
21.	Gridpoint 12, Mariner Mars '71 reaction force in Y-direction at base of Centaur adapter predicted from the forcing function derived from Mariner VII (AC-19) MECO flight data	45

CONTENTS (Cont'd)

Figures (Cont'd)

22.	Gridpoint 12, Mariner Mars '71 reaction force in Z-direction at base of Centaur adapter predicted from the forcing function derived from Mariner VII (AC-19) MECO flight data	46
23.	Gridpoint 12, Mariner Mars '71 reaction moment in θ_x -direction at base of Centaur adapter predicted from the forcing function derived from Mariner VII (AC-19) MECO flight data	47
24.	Gridpoint 12, Mariner Mars '71 reaction moment in θ_y -direction at base of Centaur adapter predicted from the forcing function derived from Mariner VII (AC-19) MECO flight data	48
25.	Gridpoint 12, Mariner Mars '71 reaction moment in θ_z -direction at base of Centaur adapter predicted from the forcing function derived from Mariner VII (AC-19) MECO flight data	49
26.	Gridpoint 8, Viking acceleration response in X-direction at base of Viking truss adapter predicted from the forcing function derived from Mariner VI (AC-20) MECO flight data	50
27.	Gridpoint 8, Viking acceleration response in Y-direction at base of Viking truss adapter predicted from the forcing function derived from Mariner VI (AC-20) MECO flight data	51
28.	Gridpoint 8, Viking acceleration response in Z-direction at base of Viking truss adapter predicted from the forcing function derived from Mariner VI (AC-20) MECO flight data	52
29.	Gridpoint 8, Viking rotational acceleration response in θ_x -direction at base of Viking truss adapter predicted from the forcing function derived from Mariner VI (AC-20) MECO flight data	53
30.	Gridpoint 8, Viking rotational acceleration response in θ_y -direction at base of Viking truss adapter predicted from the forcing function derived from Mariner VI (AC-20) MECO flight data	54
31.	Gridpoint 8, Viking torsional acceleration response in θ_z -direction at base of Viking truss adapter predicted from the forcing function derived from Mariner VI (AC-20) MECO flight data	55
32.	Gridpoint 8, Viking acceleration response in X-direction at base of Viking truss adapter predicted from the forcing function derived from Mariner VII (AC-19) MECO flight data	56
33.	Gridpoint 8, Viking acceleration response in Y-direction at base of Viking truss adapter predicted from the forcing function derived from Mariner VII (AC-19) MECO flight data	57

CONTENTS (Cont'd)

Figures (Cont'd)

34.	Gridpoint 8, Viking acceleration response in Z-direction at base of Viking truss adapter predicted from the forcing function derived from Mariner VII (AC-19) MECO flight data	58
35.	Gridpoint 8, Viking rotational acceleration response in θ_x -direction at base of Viking truss adapter predicted from the forcing function derived from Mariner VII (AC-19) MECO flight data	59
36.	Gridpoint 8, Viking rotational acceleration response in θ_y -direction at base of Viking truss adapter predicted from the forcing function derived from Mariner VII (AC-19) MECO flight data	60
37.	Gridpoint 8, Viking torsional acceleration response in θ_z -direction at base of Viking truss adapter predicted from the forcing function derived from Mariner VII (AC-19) MECO flight data	61
38.	Gridpoint 8, Viking reaction force in X-direction at base of Viking truss adapter predicted from the forcing function derived from Mariner VI (AC-20) MECO flight data	62
39.	Gridpoint 8, Viking reaction force in Y-direction at base of Viking truss adapter predicted from the forcing function derived from Mariner VI (AC-20) MECO flight data	63
40.	Gridpoint 8, Viking reaction force in Z-direction at base of Viking truss adapter predicted from the forcing function derived from Mariner VI (AC-20) MECO flight data	64
41.	Gridpoint 8, Viking reaction moment in θ_x -direction at base of Viking truss adapter predicted from the forcing function derived from Mariner VI (AC-20) MECO flight data	65
42.	Gridpoint 8, Viking reaction moment in θ_y -direction at base of Viking truss adapter predicted from the forcing function derived from Mariner VI (AC-20) MECO flight data	66
43.	Gridpoint 8, Viking reaction moment in θ_z -direction at base of Viking truss adapter predicted from the forcing function derived from Mariner VI (AC-20) MECO flight data	67
44.	Gridpoint 8, Viking reaction force in X-direction at base of Viking truss adapter predicted from the forcing function derived from Mariner VII (AC-19) MECO flight data	68
45.	Gridpoint 8, Viking reaction force in Y-direction at base of Viking truss adapter predicted from the forcing function derived from Mariner VII (AC-19) MECO flight data	69

CONTENTS (Cont'd)

Figures (Cont'd)

46.	Gridpoint 8, Viking reaction force in Z-direction at base of Viking truss adapter predicted from the forcing function derived from Mariner VII (AC-19) MECO flight data	70
47.	Gridpoint 8, Viking reaction moment in θ_x -direction at base of Viking truss adapter predicted from the forcing function derived from Mariner VII (AC-19) MECO flight data	71
48.	Gridpoint 8, Viking reaction moment in θ_y -direction at base of Viking truss adapter predicted from the forcing function derived from Mariner VII (AC-19) MECO flight data	72
49.	Gridpoint 8, Viking reaction moment in θ_z -direction at base of Viking truss adapter predicted from the forcing function derived from Mariner VII (AC-19) MECO flight data	73

ABSTRACT

The disturbing forcing functions of the Centaur engines at Main Engine Cutoff derived from acceleration flight data of the Mariner Mars '69 spacecraft are used to predict acceleration and reaction forces and moments near the base of Mariner Mars '71 and Viking spacecraft. Mathematical dynamic models of the Mariner Mars '71 and Viking spacecraft and the Centaur launch vehicle modified for the Viking model are presented. Discussion concerning the method and the accuracy of the results are given.

I. INTRODUCTION

Ref. 1 describes the synthesis of engine forcing functions at Centaur Main Engine Cutoff (MECO) from acceleration measurements in flight, and from computed modal characteristics of the Mariner Mars '69, OAO-II, and ATS composite space vehicles.

Ref. 1 also gives derivations of equations for computing the acceleration response and the reaction forces and moments at the base of a new spacecraft at Centaur MECO.

This memorandum applies techniques and data generated in Ref. 1 to the predictions of acceleration responses and reaction forces and moments at appropriate planes near the base of Mariner Mars '71 and Viking spacecraft. The only engine forcing functions used are those derived from Mariner VI and Mariner VII data, as bases were found to invalidate forcing functions obtained from OAO-II and ATS data.

II. MATHEMATICAL MODELS

A. Centaur Launch Vehicle Model

The Centaur model of Ref. 1 was used without modification for the Centaur/Mariner '71 composite analysis. However, the above Centaur model was modified for the Centaur/Viking analysis to include the stub-adapter pertinent to the Viking spacecraft (Ref. 2). The modified lumped mass model is given in Fig. 1. The modified weight and stiffness properties are given in Tables 1 through 6.

B. Mariner Mars '71 Spacecraft Model

The Mariner Mars '71 spacecraft model was a set of fifteen cantilever normal modes. Seven normal modes were obtained from a modal survey conducted on the Mariner '71 development test model (DTM) without

solar panels and cantilevered on the floor at the base of the Centaur adapter (Ref. 3). Four solar panel modes and four slosh modes were subsequently added to the measured modes to form a fifteen-mode model. The rigid body mass matrix $[M_{RR}]$, the elastic-rigid coupling matrix $[M_{ER}]$ and natural frequencies $[\omega_n]$ were generated for these fifteen modes. These matrices are shown in Tables 7 and 8. The modes are normalized such that the generalized mass matrix $[M_{EE}]$ is unity.

C. Viking Spacecraft Model

The model used for the Viking spacecraft was also a set of cantilever normal modes. The mass matrix $[M_{RR}]$, the elastic-rigid coupling matrix $[M_{ER}]$ and the natural frequencies $[\omega_n]$ were obtained from previous analyses performed by JPL on the original Viking model presented in Ref. 4. The $[M_{RR}]$, $[M_{ER}]$, and $[\omega_n]$ matrices for the model are given in Tables 9 and 10. The generalized mass matrix $[M_{EE}]$ is unity.

III. COMPUTER ANALYSIS

A. Computer Programs

The same computer programs as in Ref. 1 were used for all the numerical computations. The JPL SAMIS computer program was used for the normal mode analysis, and the JPL RECEP computer program was used for the frequency domain calculations.

B. Mariner '71/Centaur Composite Vehicle

As in Ref. 1 the modal combination method was used for the modal analysis of the composite vehicle. The mass matrix $[M_{RR}]$, the elastic-rigid matrix $[M_{ER}]$ and the natural frequencies $[\omega_n]$ relative to the Mariner Mars '71 spacecraft were combined with the Centaur model of Ref. 1 to give the free-free normal modes of the composite vehicle needed to

compute $[H^2(\omega)]$ in Eq. (15) of Ref. 1. The resulting modal data at the gimbal axis and the base of the Centaur adapter are shown in Tables 11 through 13. Again the generalized mass $[M_{EE}]$ is unity.

The transfer function matrix $[H^2(\omega)]$ was computed using the above modal data and a modal damping of $\xi_n = .03$ for all modes.

The Fourier transform $\{F(\omega)\}$ of the forcing function obtained in Ref. 1 for Mariners VI and VII flights was used to compute a prediction of the response $\{A^2(\omega)\}$ at the base of the Centaur adapter (gridpoint 12, Fig. 1 of Vol. I) making use of Eq. (15) of Ref. 1. Figs. 2 through 13 show the time histories and the Fourier transforms of the responses.

The reaction forces and moments were then computed by Eqs. (25) and (26) of Ref. 1 using the responses $\{A^2(\omega)\}$ determined above. The $[M_{RR}]$, $[M_{ER}]$ and $[\omega_n]$ matrices needed for Eq. (25) were those indicated in Tables 7 and 8. Measured modal dampings (Table 7) were used in Eq. (24). Figs. 14 through 25 show the time histories and the Fourier transforms of the reaction forces and moments.

C. Viking/Centaur Composite Vehicle

The same procedure as outlined above for the Mariner '71/Centaur composite vehicle was applied for the Viking/Centaur composite vehicle. Tables 14 through 16 show the modal data relative to the gimbal axis and the base of the truss adapter.

Only the two forcing functions obtained from Mariners VI and VII flights were used to compute the responses at the base of the truss adapter. Figs. 26 through 37 show the time histories and the Fourier transforms of these responses.

These responses were then applied as an input to determine the reaction forces and moments at the base of the truss adapter, (gridpoint

8, Fig. 1). A modal damping $\xi_n = .03$ was chosen for the Viking model. Figs. 38 through 49 show the time histories and the Fourier transforms of the reaction forces and moments. Coordinate system is given in Fig. 1 of Ref. 1.

IV. DISCUSSION

Section V of Ref. 1 comments on the sensitivity of the "inverse method" of deriving the engine forcing functions to the fidelity in structural modeling. In the application of forcing functions so derived to predictions of MECO response at the base of a new spacecraft (e.g., Mariner Mars '71 and Viking), the overall accuracy is affected not only by errors in $\{F(\omega)\}$, but by errors in the new transfer function matrix $[H^2(\omega)]$.

It is hypothesized that, if the only errors in the computed matrices $[H^1(\omega)]$ and $[H^2(\omega)]$ were ascribable to errors in computed *modal frequencies* the results of such a two-stage analysis would yield conservative results in $\{a^2(t)\}$ and $\{g(t)\}$. However, the fact that errors in natural frequency are generally accompanied by errors in *mode shape* precludes a conjecture that the results are *always* conservative. The limited scope of this effort has not permitted an investigation of these aspects.

It is to be emphasized that the basic techniques employed in the work leading to Ref. 1 and to this document are generalizations of the approach, reported in Ref. 5, that dealt with one-dimensional solutions easily manageable.

However, the generalization from the one-dimensional solution (one component) to the three-dimensional solution (six components) has been accompanied by the delicate problem of management of an enormous amount of data which has proved to be a real complication in the whole effort.

In retrospect, the authors endorse, in concept, the methods employed but improvements in structural modeling are needed together with words of caution concerning the data management.

Techniques described in Ref. 6, in combination with those described herein, could be expected to produce a materially higher confidence in the quality of the desired information but only at a considerably increased cost of flight test instrumentation, data processing and dynamic analysis.

V. CONCLUSION

The predicted "base" acceleration responses and reaction forces and moments reported herein for Mariner Mars '71 spacecraft and Viking spacecraft at Centaur Main Engine Cutoff are considered realistic and, probably, conservative. The methods employed in the predictions are considered theoretically sound and computationally "well-behaved"; they need only upgraded "input" to enhance their usefulness.

REFERENCES

1. Trubert, M. R., Chisholm, J. R., and Gayman, W. H., "Use of Centaur/Spacecraft Flight Data in the Synthesis of Forcing Functions at the Centaur Main Engine Cutoff During Boost of Mariner '69, OAO-II and ATS Spacecraft," Technical Memorandum 33-487, Vols. I and II, Jet Propulsion Laboratory, Pasadena, Calif. (in process).
2. T-IIID Centaur Loads Data Book, Vol. I, Book I, Martin Marietta Corporation, Denver Division, December 1969.
3. Freeland, R. E., "Mariner Mars 1971 Unique Structural Analysis and Tests," Report No. 610-176, Jet Propulsion Laboratory, Pasadena, 26 March 1971.
4. Garba, J. A., Bamford, R. M., and Wada, B. K., "Viking 1975 Structural Dynamic Model I for Loads Analyses," Viking Project Document 611-14, Jet Propulsion Laboratory, Pasadena 6 July 1970.
5. Trubert, M. R., "A Fourier Transform Technique for the Prediction of Torsional Transients for a Spacecraft from Flight Data of Another Spacecraft Using the Same Booster," Technical Memorandum No. 33-350, Jet Propulsion Laboratory, Pasadena, 15 October 1967.
6. Wagner, R. G., and Rubin, S., "Detection of Titan Pogo Characteristics by Analysis of Random Data," (ASME Special Publication: "Stochastic Processes in Dynamical Problems," 1969 Winter Annual Meeting, Los Angeles, California).

Table 1. Centaur MECO Torsional Model for Viking Spacecraft - Gridpoints, Station Locations and Moments of Inertia

Gridpoint	Station (in.)	Inertia (lb-in ²)
8	143.0	0.2521 E7
12	122.0	0.1559 E7
13	141.0	0.1247 E6
14	149.0	0.1551 E6
15	168.0	0.5930 E6
16	199.3	0.2300 E6
17	229.3	0.2499 E6
18	264.0	0.2758 E6
19	294.0	0.4164 E6
20	324.0	0.7243 E6
21	361.0	0.3665 E6
64	369.0	0.2546 E6
65	389.0	0.7525 E6
66	409.0	0.7551 E6
67	433.5	0.1224 E6

Table 2. Centaur MECO Lateral Model Viking Spacecraft – Gridpoints, Station Locations, Weights and Moments of Inertia

Gridpoint	Station (in)	Weight (lb)	Inertia, (lb-in. ²)	
			Ix	Iy
8	143.0	702.14	0.1260 E7	0.1260 E7
12	122.0	202.0	0.7794 E6	0.7794 E6
13	141.0	233.0	0.6236 E5	0.6236 E6
14	149.0	79.0	0.7755 E5	0.7755 E5
15	168.0	440.28	0.2965 E6	0.2965 E6
16	199.3	93.0	0.1150 E6	0.1150 E6
17	229.3	93.0	0.1250 E6	0.1250 E6
18	264.0	91.0	0.1379 E6	0.1379 E6
19	294.0	91.0	0.2082 E6	0.2082 E6
20	324.0	273.0	0.3080 E6	0.3080 E6
21	361.0	507.0	0.1695 E6	0.6765 E6
66	387.0	270.0	0.2542 E6	0.2603 E6
67	403.0	561.0	0.9006 E6	0.4509 E6
68	398.9	197.7	-	-
69	337.0	-	-	-
70	437.2	524.4	-	-

Table 3. Centaur MECO Longitudinal Model for Viking Spacecraft - Gridpoints, Station Locations and Weights

Gridpoint	Station (in.)	Weight (lb)
8	193.0	702.14
9	-	-
10	-	819.0
11	-	754.0
12	122.0	202.10
13	141.0	233.0
14	149.0	79.0
15	168.0	440.28
16	199.3	93.0
17	229.3	93.0
18	264.0	91.0
19	294.0	91.0
20	324.0	273.0
21	361.0	507.0

Table 4. Centaur MECO Lateral Model for Viking Spacecraft –
Spring Constants

Gridpoint 1	Gridpoint 2	Stiffness (Pitch and Yaw)			
		EI_1 (10^{12} lb-in. ²)	EI_2 (10^{12} lb-in. ²)	KAG_1 (10^8 lb)	KAG_2 (10^8 lb)
8	15	0.479	0.479	0.456	0.456
12	13	0.055	0.203	0.122	0.221
13	14	0.0818	0.122	0.221	0.238
14	15	0.122	0.214	0.238	0.264
15	16	0.312	0.312	0.335	0.335
16	17	0.312	0.312	0.335	0.335
17	18	0.312	0.312	0.335	0.335
18	19	0.312	0.312	0.335	0.335
19	20	0.312	0.312	0.335	0.335
20	21	0.312	0.312	0.335	0.335
21	69	0.384	0.179	0.423	0.254
21	66	0.384	0.131	0.423	0.338
66	67	0.131	0.217	0.338	0.198
67	68	0.000000305	0.00000059	—	—
67	70	0.0001904	0.0001838	—	—

Table 5. Centaur MECO Longitudinal Model for Viking Spacecraft -
Spring Constants

Gridpoint 1	Gridpoint 2	Stiffness K (10^6 lb/in.)
8	15	10.6
12	13	100.0
13	14	100.0
14	15	0.50
15	16	4.57
16	17	4.72
17	18	4.05
18	19	4.72
19	20	4.72
20	21	3.83
21	9	8.91
21	10	-0.33
9	10	0.61
10	11	20.0

Table 6. Centaur MECO Torsional Model for Viking Spacecraft -
Spring Constants

Gridpoint 1	Gridpoint 2	Stiffness $10^{10} \frac{K}{\text{in.-lb/Rad}}$
8	15	1.31
12	13	0.3672
13	14	0.8292
14	15	0.7290
15	16	0.6169
16	17	0.6374
17	18	0.5464
18	19	0.6169
19	20	0.6169
20	21	0.5168
21	64	3.168
64	65	0.8496
65	66	0.1296
66	67	0.00082

Table 7. Natural Frequencies, Damping and Elastic-Rigid Coupling Matrix [MER] for the Mariner '71 Spacecraft (Units: lb, in., sec)

	Frequency Hz	Damping	X	Y	Z	θ_x	θ_y	θ_z
1	1.5	1 E-01	0.746	0.000	0.000	0.000	-57.536	8.900
2	1.5	1 E-01	0.000	0.746	0.000	57.536	0.000	8.900
3	2.5	1 E-01	0.456	0.000	0.000	0.000	-35.196	-5.450
4	2.5	1 E-01	0.000	0.456	0.000	35.196	0.000	-5.450
5	9.82	1	0.385	-0.442	-0.002	-42.572	-37.340	-0.372
6	9.86	1	-0.396	-0.364	0.000	-35.754	38.936	0.283
7	10.63	1	-0.000	0.002	0.000	0.111	0.007	0.014
8	10.83	1	0.000	-0.001	0.039	-0.028	-0.003	-0.130
9	15.38	7 E-02	-1.546	0.902	-0.244	71.962	118.946	-1.575
10	17.47	7 E-02	1.026	1.654	-0.142	120.404	-70.926	4.909
11	29.3	6 E-02	0.158	-0.371	-1.635	-10.673	-3.361	-1.252
12	36.05	9 E-02	-0.024	-0.310	0.954	-2.840	-7.298	-9.330
13	36.58	3 E-02	-0.179	-0.045	0.159	-1.660	-2.171	-2.674
14	47.32	3 E-02	0.336	0.173	0.341	8.264	3.992	33.813
15	66.53	3 E-02	0.423	-0.135	-0.066	-0.115	0.500	-0.023

Table 8. Rigid Body Mass Matrix $[M_{RR}]$ for the Mariner '71 Spacecraft (Units lb, in., sec)

	X	Y	Z	θ_x	θ_y	θ_z
X	5.55	0.00	0.00	0.00	-368.80	9.74
Y	0.00	5.55	0.00	368.80	0.00	9.75
Z	0.00	0.00	5.55	-9.74	-9.75	0.00
θ_x	0.00	368.80	-9.74	28782.80	456.00	756.00
θ_y	-368.80	0.00	-9.75	456.00	28832.80	-822.84
θ_z	9.74	9.75	0.00	756.00	-822.84	2539.00

Table 9. Elastic-Rigid Coupling Matrix $[M_{ER}]$ For Viking Spacecraft Model
(Units: lb, in., sec)

Frequency Hz	X	Y	Z	θ_x	θ_y	θ_z
1.592	0.31745+02	0.82582+00	0.45736-01	-0.96378+02	0.37109+04	-0.15326+03
1.599	0.80792+00	-0.31243+02	-0.10618-01	0.36960+04	0.94292+02	-0.76675+01
1.614	-0.10621+01	-0.16903+00	-0.61075-02	0.23771+02	-0.14434+03	-0.48422+03
1.616	-0.30968-02	-0.20282+00	0.13190-01	0.35559+01	-0.77127+00	-0.14098+02
4.064	0.24804+01	-0.79282+02	-0.13278+00	0.11877+05	0.34529+03	-0.43702+03
4.184	-0.78171+02	-0.31798+01	-0.32042+00	0.45183+03	-0.10850+05	0.23322+03
5.812	0.39609+01	-0.17841+02	0.23645-01	0.20561+04	0.65153+03	0.21023+04
7.087	-0.17287+02	-0.62622+00	0.28178+01	0.80793+02	-0.61618+04	-0.60580+02
8.407	0.34451+00	0.76924+00	0.28198+00	0.47545+03	-0.22422+02	0.53173+03
8.485	-0.84336-01	0.17660+01	-0.13511+00	-0.66923+03	0.91391+01	-0.77518+02
9.192	-0.36113+00	-0.18782+01	-0.15981+01	-0.29029+04	-0.40156+01	-0.11383+04
9.937	0.10321+01	0.35381+01	-0.14227+01	-0.23827+04	0.61636+02	0.12800+04
10.833	0.16912+01	-0.17387+01	0.68125+01	0.17190+03	0.24138+03	0.90985+00
11.680	0.24122+01	0.30714+00	0.57769+00	0.22890+02	0.33192+03	0.34020+03
11.988	-0.17628+01	0.19312+01	0.97735+01	-0.22070+03	-0.12782+03	-0.51944+02
12.241	-0.10851+02	-0.57452+00	0.76287+01	0.66159+02	-0.16123+04	0.89363+02
12.360	-0.31548+00	0.99155-02	0.51329+00	-0.25892+02	-0.45767+02	0.31447+02
12.493	-0.49819+01	-0.33594+00	0.66078+01	0.55008+02	-0.69820+03	0.17868+02
13.314	0.25052+01	0.11226+00	0.45265+02	0.85089+01	0.42697+03	0.14163+02
13.621	-0.50776-01	0.12120+01	-0.33165+01	-0.50603+03	-0.18329+03	0.37595+03
13.818	-0.16381-01	0.45873+00	-0.46904-01	-0.39428+02	0.11290+02	0.36487+01
13.877	0.51293+00	0.92069+00	-0.88528+00	-0.42390+03	-0.54743+02	0.24734+03
14.398	0.48001+01	-0.45288-02	0.26188+01	0.21483+03	0.28488+03	-0.14487+03
14.626	0.13424+01	0.10774+00	0.11377+01	-0.13047+03	0.14487+03	-0.14233+03
15.025	-0.17636+01	-0.22612+00	-0.13173+01	-0.30588+02	-0.50494+02	0.94481+02
15.068	0.11399+01	0.23955+00	0.71651+00	0.49200+02	0.67454+02	-0.11452+03
15.145	0.32144+01	0.34322-01	0.28548+01	-0.33977+00	0.20564+03	-0.78454+01
15.547	-0.75285-01	0.31283-01	-0.20399+00	-0.18059+02	-0.93800+00	0.13639+01
15.725	0.22454+00	0.49233+00	-0.12996+01	-0.25314+03	0.27322+02	-0.48776+01
16.059	-0.62144+00	-0.21153+00	-0.45300+01	0.10810+02	0.16510+03	0.27937+02
16.626	-0.43714+00	0.37710+01	0.27792+02	-0.10259+04	-0.67566+02	-0.65942+01
17.065	0.37137+00	-0.64456+00	-0.58364+02	0.11624+03	-0.34153+02	0.10222+02
17.474	-0.63502+00	0.14666+01	0.14389+02	0.10946+03	-0.33710+02	-0.12578+03
17.558	0.10407+01	-0.23898+01	0.12024+02	-0.36190+02	0.10197+03	0.17879+03
17.915	-0.10566+01	-0.15393+01	-0.45448+01	0.12739+03	-0.26828+02	0.11815+02
18.455	0.38077+00	0.48153+01	0.13710+02	-0.75143+03	0.77079+02	0.15268+03
19.238	0.49376-01	-0.18302+00	0.23653+01	0.24572+02	0.55679+01	0.46832+01
19.700	-0.30816-01	0.30438+00	0.95537+01	-0.41323+03	-0.38840+01	0.27601+02
20.469	-0.56222+00	-0.80848+00	0.97695+00	0.20196+03	-0.13033+03	-0.56553+02
21.855	-0.21539+01	-0.15825+00	0.68523+01	-0.18804+03	-0.76461+03	-0.19769+02
22.402	-0.14216+01	0.91081-01	-0.78558+01	0.31033+03	-0.43540+03	0.16119+03
22.661	-0.16187+01	0.20119+00	-0.59527+01	0.40436+03	-0.53745+03	-0.64435+02
23.730	-0.21745+01	0.35092+00	-0.52420+00	-0.43441+03	-0.66979+03	-0.19566+02
25.577	-0.13402+01	-0.13964+00	0.95504+00	0.74473+02	-0.53991+03	0.12940+02
26.095	-0.51601+00	0.18649+00	-0.50230-01	-0.76746+02	-0.15928+02	-0.64826+01
27.310	-0.19144+00	-0.44744+00	0.11840+01	0.24442+03	-0.39276+02	-0.21605+02
28.475	0.77175+00	-0.26665+00	0.43227+01	0.40480+02	0.93846+02	-0.32465+02
29.112	0.71787+00	0.11601+01	-0.17509+01	-0.21039+03	0.14059+03	0.13575+03
30.555	-0.62315+00	-0.33161+00	0.18490+00	0.55398+02	-0.13142+03	0.78617+01
30.889	-0.36885+01	0.29334-01	0.38156+01	-0.15755+02	-0.76518+03	0.25921+02
32.837	0.39172+00	-0.16293+01	0.32343+01	0.99752+02	0.89774+02	0.13263+03
36.000	-0.40061+00	-0.47639-01	-0.17422+00	-0.75161+01	-0.10702+03	0.21241+01
36.348	0.32295-01	0.35992+00	0.26419+01	0.27117+02	0.10868+02	-0.14928+02
37.330	0.16989+00	0.22645-01	0.87641+01	0.30502+02	0.48224+02	-0.41262+01
38.704	-0.51194-01	-0.10441+01	-0.55111+00	0.83969+03	-0.11896+02	0.35501+02
42.490	-0.50478+00	0.31716+00	-0.76595+01	-0.14822+03	-0.12278+03	-0.10486+02
42.892	-0.21325+00	-0.31443+00	-0.45009+01	0.11571+03	-0.49189+02	0.35226+02
45.263	0.52545-01	0.72694+00	0.69585+00	-0.22120+03	0.20297+02	0.18244+02
57.423	-0.75094-01	-0.54718+00	0.29332+00	0.20619+03	-0.95336+01	-0.10301+02
62.184	0.23350-01	0.73138+00	0.20183+01	-0.26740+03	-0.30659+00	-0.10359+01

Table 10. Rigid Body Weight Matrix $[M_{RR}]$ for Viking Spacecraft Model
 (Units: lb, in., sec.)

	X	Y	Z	θ_x	θ_y	θ_z
X	0.77491+04	-0.14262+00	-0.16183-01	0.20706+02	0.11142+07	-0.13297+05
Y	-0.14263+00	0.77489+04	-0.14297-01	-0.11142+07	-0.20175+02	0.41847+04
Z	-0.16183-01	-0.14314-01	0.77504+04	0.13297+05	-0.42100+04	-0.22274+00
θ_x	0.20704+02	-0.11142+07	0.13297+05	0.17831+09	-0.38594+05	-0.62734+06
θ_y	0.11142+07	-0.20176+02	-0.42100+04	-0.38594+05	0.17657+09	-0.15194+07
θ_z	-0.13297+05	0.41847+04	-0.22270+00	-0.62735+06	-0.15194+07	0.89057+07

Table 11. ϕ_{1r} and ϕ_{1e} Matrices For MECO Mariner '71/Centaur Model
(Units lb, in., sec)

	Frequency, Hz	X	Y	Z	θ_x	θ_y	θ_z
ϕ_{1r}	0.0	0.10000+01					
	0.0		0.10000+01				
	0.0		0.00000	0.10000+01			
	0.0		0.00000	0.00000	0.10000+01		
	0.0		0.00000	0.00000	0.00000	0.10000+01	0.00000
	0.0		0.00000	0.00000	0.00000	0.00000	0.10000+01
ϕ_{1e}	1.557	-0.60367-03	-0.65422-03	0.31727-04	-0.12336-04	0.11337-04	-0.64953-07
	1.563	-0.70299-03	0.65039-03	0.82817-05	0.11395-04	0.12473-04	-0.29770-04
	2.539	0.44692-03	0.40254-03	-0.23129-04	0.76368-05	-0.84377-05	-0.70447-07
	2.543	-0.37951-03	0.41784-03	0.31038-05	0.84245-05	0.75692-05	0.19770-04
	10.024	-0.66420-03	-0.32267-03	0.77867-04	-0.57831-05	0.11244-04	0.93527-06
	10.051	-0.31544-03	0.68006-03	-0.32916-04	0.11985-04	0.52977-05	0.26986-05
	10.630	0.32359-07	0.14535-05	-0.28048-06	0.47542-07	0.75231-09	-0.25540-07
	10.831	-0.22708-05	-0.12333-05	0.12343-03	-0.31768-08	0.22804-07	-0.32787-06
	15.922	0.23897-04	0.18660-04	-0.11090-04	-0.22663-06	0.61040-06	0.57504-04
	17.622	-0.33112-02	-0.79349-02	0.57173-03	0.20447-05	-0.10328-04	0.89886-05
	18.171	-0.75036-02	0.57431-02	0.19332-03	0.84019-05	-0.45724-05	-0.27827-05
	21.659	0.80390-02	0.54658-02	0.15174-02	0.43336-04	-0.64017-04	0.10517-04
	25.671	-0.40980-02	0.68906-02	0.14922-02	0.78050-04	0.54490-04	-0.11591-04
	28.720	0.30257-03	0.21636-02	-0.65881-02	0.30158-04	-0.89916-05	0.22894-05
	32.678	0.96606-02	-0.57124-03	-0.42078-03	-0.10399-04	-0.31295-04	0.75302-05
	35.647	0.11546-02	0.14040-03	0.23136-03	0.78356-05	-0.13402-04	-0.30918-04
	36.005	0.27151-02	0.56261-03	0.76076-03	0.23789-04	-0.33071-04	-0.80702-05
	36.708	0.18816-02	0.10715-03	0.26336-03	0.90442-05	-0.23827-04	-0.90522-05
	38.639	-0.20604-04	0.87406-02	-0.33149-04	0.30537-04	-0.11909-05	-0.65606-05
	44.792	0.62756-03	0.22225-02	0.30362-02	0.25107-04	-0.12658-04	-0.14197-03
	48.964	0.41311-03	-0.14764-02	0.50153-02	-0.15430-04	-0.27423-05	0.15616-03
	65.000	-0.19374-02	0.13083-02	-0.25628-04	0.28877-04	0.39586-04	-0.64518-05
	66.825	-0.19037-02	-0.14463-02	0.23218-02	-0.24722-04	0.17138-04	-0.51026-03
	77.847	-0.15454-01	-0.19970-02	0.54638-02	-0.35455-04	0.29668-03	0.38789-04

Table 12. ϕ_{2r} and ϕ_{2e} Matrices for MECO Mariner '71/Centaur Model
(Units: lb, in., sec)

	Frequency, Hz	X	Y	Z	θ_x	θ_y	θ_z
ϕ_{2r}	0.0	1.0	0.00000	0.00000	0.00000	0.28099+03	0.00000
	0.0	0.00000	1.0	0.00000	-0.28099+03	0.00000	0.00000
	0.0	0.00000	0.00000	0.10000+01	0.00000	0.00000	0.00000
	0.0	0.00000	0.00000	0.00000	0.10000+01	0.00000	0.00000
	0.0		0.00000	0.00000	0.00000	0.10000+01	0.00000
	0.0		0.00000	0.00000	0.00000	0.00000	0.10000+01
	0.0	0.00000	0.00000	0.00000	0.00000	0.00000	0.10000+01
ϕ_{2e}	1.557	0.25789-02	0.28088-02	0.31704-04	-0.12274-04	0.11280-04	-0.69077-07
	1.563	0.27985-02	-0.25480-02	0.82912-05	0.11334-04	0.12411-04	-0.29721-04
	2.539	-0.19181-02	-0.17378-02	-0.23081-04	0.75346-05	-0.83255-05	-0.62852-07
	2.543	0.17419-02	-0.19438-02	0.31265-05	0.83135-05	0.74649-05	0.19680-04
	10.024	0.23382-02	0.12199-02	0.71492-04	-0.40785-05	0.78425-05	0.75032-06
	10.051	0.10974-02	-0.25137-02	-0.29398-04	0.83288-05	0.36450-05	0.25802-05
	10.630	0.23951-06	-0.11233-04	-0.25014-06	0.38340-07	0.11091-08	-0.22443-07
	10.831	0.32055-05	-0.16523-06	0.10839-03	0.45021-08	0.12612-07	-0.29515-06
	15.922	0.18011-03	-0.60993-04	-0.78046-05	0.77694-06	0.29972-07	0.81096-04
	17.622	-0.38280-02	-0.42895-02	0.36928-03	-0.34054-04	0.13399-04	0.80831-05
	18.171	-0.44193-02	0.87154-03	0.12949-03	0.25473-04	0.32434-04	-0.48165-05
	21.659	-0.10405-01	-0.68713-02	0.58798-03	0.20683-04	-0.32145-04	0.11645-04
	25.671	0.94897-02	-0.12844-01	0.11499-03	0.10997-04	0.79032-05	-0.35525-05
	28.720	-0.16056-02	-0.50619-02	0.23112-02	0.13388-05	-0.37294-05	0.35750-05
	32.678	-0.24377-02	0.15841-02	0.55022-03	0.18788-05	-0.46578-04	0.76056-05
	35.647	-0.20058-02	-0.14104-02	-0.96527-03	-0.24766-06	-0.45631-05	0.71057-04
	36.005	-0.50312-02	-0.37262-02	-0.37373-02	-0.16038-05	-0.12425-04	-0.19742-04
	36.708	-0.35536-02	-0.13740-02	-0.18535-02	-0.27493-05	-0.70374.05	-0.46458-05
	38.639	-0.27692-03	-0.34197-02	-0.84574-03	0.46020-04	-0.30829-05	-0.75430-05
	44.792	-0.15100-02	-0.19224-02	0.98586-02	-0.79657-05	0.10022-04	0.48233-05
	48.964	-0.54257-03	0.48460-03	0.10447-01	0.15270-04	-0.59005-05	-0.31209-04
	65.000	0.98749-03	-0.70573-03	-0.52119-04	-0.87744-05	-0.17511-04	0.11318-04
	66.825	0.22539-03	0.12970-02	0.15650-03	0.61010-04	-0.25661-04	0.46494-03
	77.847	-0.83819-02	-0.79089-03	-0.20610-02	0.47343-04	-0.30868-03	-0.46639-04

Table 13. Rigid Body Mass Matrix $[M_{R}]$ for Mariner '71/Centaur Model (Units: lb, in., sec)

	X	Y	Z	θ_x	θ_y	θ_z
X	0.16281+02	-0.13375-09	0.22673-05	-0.24977-03	0.31655+04	-0.16585+02
Y	-0.13375-09	0.16284+02	-0.43393-05	-0.31640+04	0.24980-03	0.26216+02
Z	0.22673-05	-0.43392-05	0.16333+02	16.585	-26.216	0.00000
θ_x	-0.24977-03	-0.31640+04	16.585	0.99071+06	-0.35051+03	-0.55156+04
θ_y	0.31655+04	0.24980-03	-0.49367+02	-0.35051+03	0.99088+06	-0.27378+04
θ_z	-0.16585+02	0.26216+02	0.00000	-0.55156+04	-0.27378+04	0.20416+05

Table 14. ϕ_{1r} and ϕ_{1e} Matrices For MECO Viking/Centaur Model
(Units: lb, in., sec)

	Frequency, Hz	X	Y	Z	θ_x	θ_y	θ_z
ϕ_{1r}	0.0	1.0					
	0.0		1.0				
	0.0			1.0			
	0.0				1.0		
	0.0					1.0	
	0.0						1.0
ϕ_{1e}	1.616	0.10112-06	0.18966-04	-0.11913-05	0.61772-07	0.32098-09	-0.20309-06
	1.625	0.25841-04	-0.35203-04	0.94225-06	-0.93832-07	0.24324-06	0.26023-04
	1.670	-0.32006-03	-0.71760-05	-0.14981-04	-0.36706-07	-0.69474-05	0.58557-05
	1.673	-0.81523-06	0.32451-03	0.93016-05	-0.67025-05	0.37134-07	0.16190-05
	6.366	-0.15923-02	-0.49597-03	-0.16617-03	-0.42393-05	-0.11296-04	0.50912-04
	6.407	-0.80387-03	0.12032-02	-0.95982-04	0.11632-04	-0.36506-05	-0.10050-03
	8.441	-0.31910-04	-0.29679-03	-0.47164-04	0.80267-05	0.10630-06	-0.11637-04
	8.460	0.62495-04	-0.22337-04	0.13152-05	0.91055-06	-0.28046-06	0.21287-04
	8.978	-0.55850-04	0.13011-02	0.15011-03	-0.18130-04	0.49886-06	0.12410-04
	10.658	-0.26139-02	0.24300-03	-0.15676-03	0.30570-05	0.39571-04	-0.14413-04
	10.883	-0.14953-02	-0.88413-03	0.27799-03	-0.14302-04	0.22086-04	-0.89048-04
	11.006	0.99047-03	-0.11721-03	-0.17409-03	-0.54258-05	-0.17671-04	-0.11066-03
	11.854	0.26758-03	-0.10825-02	-0.27340-03	-0.19984-04	-0.52304-05	-0.59933-04
	11.919	-0.54755-04	-0.14090-02	-0.18939-03	-0.26007-04	0.28699-05	0.58018-04
	12.361	0.13303-04	-0.72322-04	-0.24035-05	-0.18596-05	-0.41235-06	-0.74628-05
	12.449	-0.24648-03	-0.45867-03	0.76090-04	-0.10075-04	0.41745-05	-0.48763-05
	12.548	-0.80702-04	0.30539-02	-0.16524-03	0.68536-04	0.31942-05	0.26198-04
	13.732	0.70508-04	-0.36941-03	0.10199-03	-0.98284-05	0.74990-07	0.29001-04
	13.820	-0.35521-04	-0.56168-04	-0.27638-04	-0.28208-05	0.58576-06	-0.19672-05
	13.899	0.11352-02	-0.20829-03	-0.16089-02	-0.66312-05	-0.29150-04	0.80762-05
	14.014	0.34101-03	-0.39629-03	-0.14295-02	-0.11528-04	-0.50658-05	0.30612-04
	14.090	-0.86646-03	-0.51829-03	0.63610-03	-0.15154-04	0.24826-04	0.41549-04
	14.611	-0.19757-03	0.90569-04	-0.56932-05	0.29619-05	0.95522-05	0.12306-04
	14.847	-0.52025-03	0.10475-04	0.46257-04	0.41081-06	0.25762-04	-0.63402-05
	15.045	0.49217-04	-0.49114-05	-0.15066-04	0.17202-06	-0.46496-05	0.31856-05
	15.091	0.59694-04	-0.28197-04	-0.15899-05	0.67687-07	-0.45635-05	0.14291-04
	15.547	-0.22044-06	-0.59194-05	-0.79883-05	0.31820-06	-0.46179-05	0.46220-06
	15.603	-0.95498-04	-0.19851-04	-0.13175-03	0.50145-06	-0.42644-04	0.28476-05
	15.732	0.54032-04	0.10301-03	-0.15043-04	-0.36333-05	0.84406-05	0.11144-05
	16.002	0.10762-03	-0.33420-04	-0.13773-04	0.36722-06	0.77719-05	-0.64425-04
	16.077	-0.15217-03	-0.42344-04	-0.12411-03	0.98959-06	-0.63883-05	0.33077-04
	16.735	-0.13814-03	0.20278-02	-0.29995-03	-0.97526-05	-0.21064-05	-0.14474-05
	17.454	-0.30777-04	0.20090-03	-0.25594-03	-0.90934-06	-0.20215-06	-0.63752-05
	17.653	-0.66128-03	0.90266-03	0.12804-03	-0.37519-05	-0.27351-05	-0.39026-04
	17.916	-0.53172-03	-0.19497-02	0.17405-03	-0.16621-05	-0.14135-05	0.48497-05
	18.171	0.17551-03	0.54038-02	-0.54632-03	0.13050-04	-0.13605-07	0.15145-04
19.233	0.11945-04	0.43619-03	0.22297-03	0.18878-05	-0.15032-06	-0.95707-06	
19.518	-0.38703-02	0.28376-02	-0.82479-03	0.18018-04	0.19023-04	-0.65868-05	
19.604	0.10043-01	0.14774-02	0.13431-03	0.91370-05	-0.50735-04	0.39271-05	
20.185	0.12486-02	-0.91004-02	-0.65487-03	-0.55651-04	-0.72724-05	0.87154-05	
20.636	-0.10209-02	-0.65920-02	-0.20962-03	-0.43236-04	0.68684-05	0.14495-04	
21.727	-0.17620-02	0.19635-02	0.38158-02	0.11371-04	0.11813-04	0.97360-05	
22.453	0.32569-02	0.51178-03	0.17581-02	0.35029-05	-0.24857-04	0.21101-04	
22.697	0.31265-02	0.14524-02	0.23977-02	0.90381-05	-0.24524-04	-0.10612-04	
23.852	-0.15702-02	0.25444-02	-0.54338-02	0.18003-04	0.14227-04	0.24405-05	
24.121	0.35468-02	-0.16024-04	-0.65246-02	-0.20266-06	-0.28870-04	0.25245-05	
25.638	-0.21102-02	-0.25919-03	-0.20235-03	-0.20572-05	0.18774-04	-0.28477-05	
26.100	-0.24857-03	0.31602-03	0.48920-04	0.26102-05	0.32068-05	0.65130-06	
27.318	-0.10166-03	-0.88593-03	-0.34863-03	-0.71939-05	0.12855-05	0.31399-05	
28.522	-0.32778-03	-0.14376-03	-0.11688-02	-0.15309-05	-0.46085-05	0.47059-05	
29.164	-0.21892-03	-0.86614-03	-0.42347-03	-0.88504-05	0.39573-05	0.20728-04	
30.555	-0.17425-04	0.19858-03	0.46665-04	0.22294-05	-0.33573-05	0.12525-05	
30.816	0.54941-03	0.72513-04	-0.67079-03	0.71499-06	0.13975-04	-0.39336-05	
32.845	0.49564-02	0.32734-03	0.47665-03	0.58835-05	-0.21281-04	0.19988-04	
33.016	0.89072-02	-0.20485-03	-0.18171-03	-0.35927-05	-0.41168-04	-0.90629-05	
35.685	-0.88280-05	-0.11764-03	0.21841-04	-0.72427-06	-0.25183-06	-0.26714-04	
36.002	-0.75708-03	0.11322-04	0.18546-04	0.58823-07	0.51481-05	-0.18527-06	

Table 14. ϕ_{1r} and ϕ_{1e} Matrices For MECO Viking/Centaur Model (Cont'd)
 (Units: lb, in., sec)

	Frequency, Hz	X	Y	Z	θ_x	θ_y	θ_z
ϕ_{1r}	0.0	1.0	1.0	1.0	1.0	1.0	1.0
	0.0						
	0.0						
	0.0						
	0.0						
	0.0						
ϕ_{1e}	36.329	-0.12200-03	0.25997-04	0.23856-03	-0.35415-06	0.73391-06	-0.18675-05
	37.099	-0.32808-03	-0.59304-05	0.44009-03	0.50727-06	0.22203-05	-0.52550-06
	37.829	-0.10022-03	0.17417-02	0.16249-04	-0.65750-05	0.63699-06	-0.87407-05
	39.538	-0.35436-04	-0.81449-02	-0.12979-04	-0.32105-04	0.21879-06	0.52909-05
	41.796	-0.50827-03	0.60759-03	-0.11720-02	0.35438-05	0.49874-05	-0.87259-06
	42.805	0.40851-05	-0.91820-03	-0.29901-03	-0.61579-05	-0.96460-07	-0.62473-05
	45.225	-0.46117-04	-0.11961-02	-0.24747-03	-0.92130-05	0.53593-06	0.53539-05
	49.679	-0.70422-03	0.54830-06	0.88404-02	0.55350-06	-0.14314-05	-0.24028-06
	57.424	-0.44308-04	-0.12548-02	-0.20557-03	-0.11960-04	0.82371-06	0.86703-05
	62.064	0.25668-04	0.18374-02	-0.10893-02	0.19153-04	0.11827-05	-0.11532-04
	67.442	-0.33918-03	0.26488-02	0.85152-04	0.47567-04	-0.96034-05	-0.58555-03
	85.888	0.16861-01	-0.73400-02	0.26198-02	-0.16469-03	-0.32799-03	-0.25216-04
	86.826	-0.73099-02	-0.16282-01	-0.24568-02	-0.35107-03	0.13392-03	-0.11696-03
	102.53	0.20789-03	0.41831-02	-0.13693-01	0.18458-03	0.10798-03	0.54805-04
	105.56	0.58359-02	0.54356-02	0.21894-02	0.28006-03	-0.22226-03	0.55004-04

Table 15. ϕ_{2r} and ϕ_{2e} Matrices For MECO Viking/Centaur Model
(Units: lb, in., sec)

	Frequency, Hz	X	Y	Z	θ_x	θ_y	θ_z
ϕ_{2r}	0.0	1.0				260.0	
	0.0		1.0		-260.0		
	0.0			1.0			
	0.0				1.0		
	0.0					1.0	
	0.0						1.0
ϕ_{2e}	1.616	0.18570-06	0.29282-05	-0.11902-05	0.60578-07	0.36013-09	-0.20285-06
	1.625	0.89029-04	-0.11004-04	0.94246-06	-0.92326-07	0.24236-06	0.25994-04
	1.670	-0.21253-02	0.23069-05	-0.14998-04	-0.36321-07	-0.69696-05	0.58480-05
	1.673	0.88454-05	0.20661-02	0.92947-05	-0.67242-05	0.37319-07	-0.16181-05
	6.366	-0.45177-02	0.58341-03	-0.16448-03	-0.37382-05	-0.13000-04	0.49690-04
	6.407	-0.17511-02	-0.17641-02	-0.94861-04	0.10393-04	-0.43367-05	-0.98155-04
	8.441	-0.58246-05	-0.23486-02	-0.45984-04	0.85517-05	0.70725-07	-0.11121-04
	8.460	-0.81465-05	-0.25852-03	0.12403-05	0.93174-06	-0.21551-06	0.20405-04
	8.978	0.70784-04	0.59479-02	0.14588-03	-0.20864-04	0.35130-06	0.11734-04
	10.658	0.72062-02	-0.50488-03	-0.14284-03	0.21558-05	0.30186-04	-0.13550-04
	10.883	0.39758-02	0.26727-02	0.27004-03	-0.10631-04	0.16779-04	-0.82734-04
	11.006	-0.33816-02	0.12639-02	-0.16954-03	-0.46943-05	-0.13215-04	-0.10232-03
	11.854	-0.10114-02	0.38002-02	-0.25967-03	-0.13940-04	-0.35613-05	-0.54664-04
	11.919	0.65176-03	0.48942-02	-0.17809-03	-0.18171-04	0.22127-05	0.52458-04
	12.361	-0.86939-04	0.38103-03	-0.23327-05	-0.13474-05	-0.28326-06	-0.67223-05
	12.449	0.76291-03	0.19727-02	0.72782-04	-0.68965-05	0.27199-05	-0.44887-05
	12.548	0.69058-03	-0.13448-01	-0.15565-03	0.46504-04	0.23849-05	0.24089-04
	13.732	0.10274-03	0.18939-02	0.94746-04	-0.52539-05	0.44045-06	0.24671-04
	13.820	0.99164-04	0.60732-03	-0.25352-04	-0.18791-05	0.24791-06	-0.17096-05
	13.899	-0.56473-02	0.13178-02	0.14791-02	-0.36091-05	-0.16196-04	0.68535-05
	14.014	-0.82643-03	0.22213-02	-0.13211-02	-0.55788-05	-0.19106-05	0.25593-04
	14.090	0.49112-02	0.29094-02	0.59476-03	-0.70405-05	0.13644-04	0.34424-04
	14.611	0.19947-02	-0.55493-03	-0.20999-05	0.73910-06	0.53384-05	0.97338-05
	14.847	0.52987-02	-0.69663-04	0.50977-04	0.48405-07	0.12864-04	-0.47894-05
	15.045	-0.10022-02	-0.48701-04	-0.15349-04	0.18504-06	-0.25797-05	0.22297-05
	15.091	-0.96281-03	-0.74647-04	-0.30525-05	0.65446-06	-0.23600-05	0.97545-05
	15.547	-0.91016-03	-0.72152-04	-0.87570-05	0.98798-07	-0.18692-05	-0.90089-07
	15.603	-0.93663-02	-0.15837-03	-0.13469-03	0.88730-06	-0.19121-04	-0.36153-05
	15.732	0.18681-02	0.79066-03	-0.10316-04	-0.12995-07	0.35526-05	0.29148-05
	16.002	0.16863-02	-0.84185-05	-0.94348-05	-0.59769-06	0.24386-05	-0.80502-04
	16.077	-0.15413-02	-0.28554-03	-0.11373-03	0.62594-06	-0.39161-05	0.39116-04
	16.735	-0.53537-03	0.30242-02	-0.26635-03	0.78404-05	-0.44494-06	-0.16815-05
	17.454	-0.67570-04	0.33995-03	-0.22373-03	-0.30898-06	-0.18748-07	-0.59637-05
	17.653	-0.95451-03	0.14821-02	0.11055-03	-0.17206-05	0.11342-05	-0.36163-04
	17.916	-0.60515-03	-0.71776-03	0.15038-03	-0.72814-05	0.71179-06	0.42994-05
	18.171	0.68294-04	0.11165-04	-0.47139-03	0.26482-04	-0.10107-05	0.13827-04
19.233	-0.23812-04	-0.16237-03	0.18731-03	0.20521-05	-0.12678-06	-0.78924-06	
19.518	0.21155-02	-0.24238-02	-0.67636-03	0.19129-04	0.22110-04	-0.61475-05	
19.604	-0.58240-02	-0.12112-02	0.76125-04	0.94385-05	-0.57601-04	0.58205-05	
20.185	-0.91825-03	0.68958-02	-0.53975-03	-0.48408-04	-0.70874-05	0.63587-05	
20.636	0.94064-03	0.55593-02	-0.16256-03	-0.34460-04	0.57358-05	0.10724-04	
21.727	0.16459-02	-0.12081-02	0.29960-02	0.54670-05	0.82955-05	0.76424-05	
22.453	-0.33600-02	-0.45835-03	0.13201-02	0.15892-05	-0.13288-04	0.17544-04	
22.697	-0.33177-02	-0.98944-03	0.17905-02	0.33560-05	-0.11699-04	-0.70849-05	
23.852	0.18524-02	-0.21906-02	-0.38939-02	0.54601-05	0.38747-05	0.19601-05	
24.121	-0.42022-02	0.57458-05	-0.46558-02	0.85008-07	-0.11488-04	0.29829-05	
25.638	0.25577-02	0.27045-03	-0.11211-03	-0.33881-06	0.19107-05	-0.28060-05	
26.100	0.52732-03	-0.33597-03	0.34036-04	0.35579-06	0.12843-05	0.47171-06	
27.318	0.18316-03	0.87591-03	-0.19563-03	0.33877-06	-0.60027-07	0.16796-05	
28.522	-0.77858-03	0.20430-03	-0.58032-03	-0.17260-06	-0.19296-06	0.29439-05	
29.164	0.60875-03	0.11724-02	-0.18258-03	-0.11208-06	-0.14260-05	0.11761-04	
30.555	-0.59132-03	-0.31169-03	0.10526-04	-0.15424-06	0.35241-05	0.76094-06	
30.816	0.26086-02	-0.78521-04	-0.17779-03	-0.22737-06	-0.19136-04	-0.15621-05	
32.845	-0.16912-02	-0.97498-03	-0.47236-04	0.10046-05	-0.22321-04	0.11644-04	
33.016	-0.35682-02	0.54793-03	-0.66896-04	-0.40565-06	-0.35693-04	0.14009-05	
35.685	-0.43947-04	-0.13221-04	-0.24470-04	0.94525-06	-0.58569-07	0.59104-04	
36.002	0.53350-03	0.10353-04	-0.15288-04	-0.50060-06	-0.50141-06	-0.11554-05	

Table 15. ϕ_{2r} and ϕ_{2e} Matrices For MECO Viking/Centaur Model (Cont'd)
 (Units: lb, in., sec)

	Frequency, Hz	X	Y	Z	θ_x	θ_y	θ_z
ϕ_{2r}	0.0	1.0				260.0	
	0.0		1.0		-260.0		
	0.0			1.0			
	0.0				1.0	1.0	
	0.0						1.0
ϕ_{2e}	36.329	0.86367-04	0.12965-03	-0.40723-03	-0.23876-05	-0.46053-09	-0.27662-05
	37.099	0.25129-03	-0.41177-04	-0.13573-02	-0.20262-05	-0.46266-06	-0.54421-06
	37.829	0.68337-04	0.86439-03	-0.10907-03	0.45707-04	0.37874-07	-0.85760-05
	39.538	0.33461-04	0.25676-02	-0.10335-03	-0.24589-04	-0.18907-06	0.35010-05
	41.796	0.39543-03	-0.29548-03	-0.36428-02	-0.19690-05	-0.35238-05	-0.54857-06
	42.805	-0.91721-05	0.55237-03	-0.77616-03	0.43736-05	0.16026-06	-0.26246-05
	45.225	0.26610-04	0.75400-03	-0.49073-03	0.85484-05	-0.78734-06	0.63106-06
	49.679	0.68909-03	0.12694-04	0.13644-01	-0.40205-06	-0.44984-05	-0.75736-06
	57.424	0.33070-04	0.50707-03	-0.24293-04	0.22219-04	-0.99411-06	-0.27639-05
	62.064	-0.86185-04	-0.57801-03	-0.11632-02	-0.37220-04	0.70837-06	0.59874-05
	67.442	-0.14281-03	0.14731-02	0.41933-04	-0.14581-04	0.13239-04	0.22437-03
	85.888	0.29750-02	-0.14633-02	-0.33416-03	0.86563-04	0.23029-03	-0.13777-04
	86.826	-0.12576-02	-0.25853-02	-0.61224-03	0.22199-03	-0.98254-04	0.10987-04
	102.53	-0.30589-02	0.36439-02	-0.45048-02	0.12160-03	0.18302-03	-0.19703-04
	105.56	0.51376-02	0.56664-02	-0.15678-02	0.24812-03	-0.19746-03	-0.15777-04

Table 16. Rigid Body Mass Matrix $[M_{RF}]$ for Viking/Centaur Model (Units: lb, in., sec)

	X	Y	Z	θ_x	θ_y	θ_z
X	0.31729+02	0.36891-03	0.37115-04	0.14948+00	0.94359+04	-0.41255+02
Y	0.36894-03	0.31732+02	-0.31672-04	-0.94342+04	-0.14811+00	0.27296+02
Z	0.37116-04	-0.31716-04	0.30956+02	41.255	-27.296	-0.57643-03
θ_x	0.14948+00	-0.94342+04	41.255	0.36427+07	0.57754+02	-0.64588+04
θ_y	0.94359+04	-0.14811+00	-27.296	0.57754+02	0.36384+07	-0.12056+05
θ_z	-0.41255+02	0.27296+02	-0.57632-03	-0.64588+04	-0.12056+05	0.47457+05

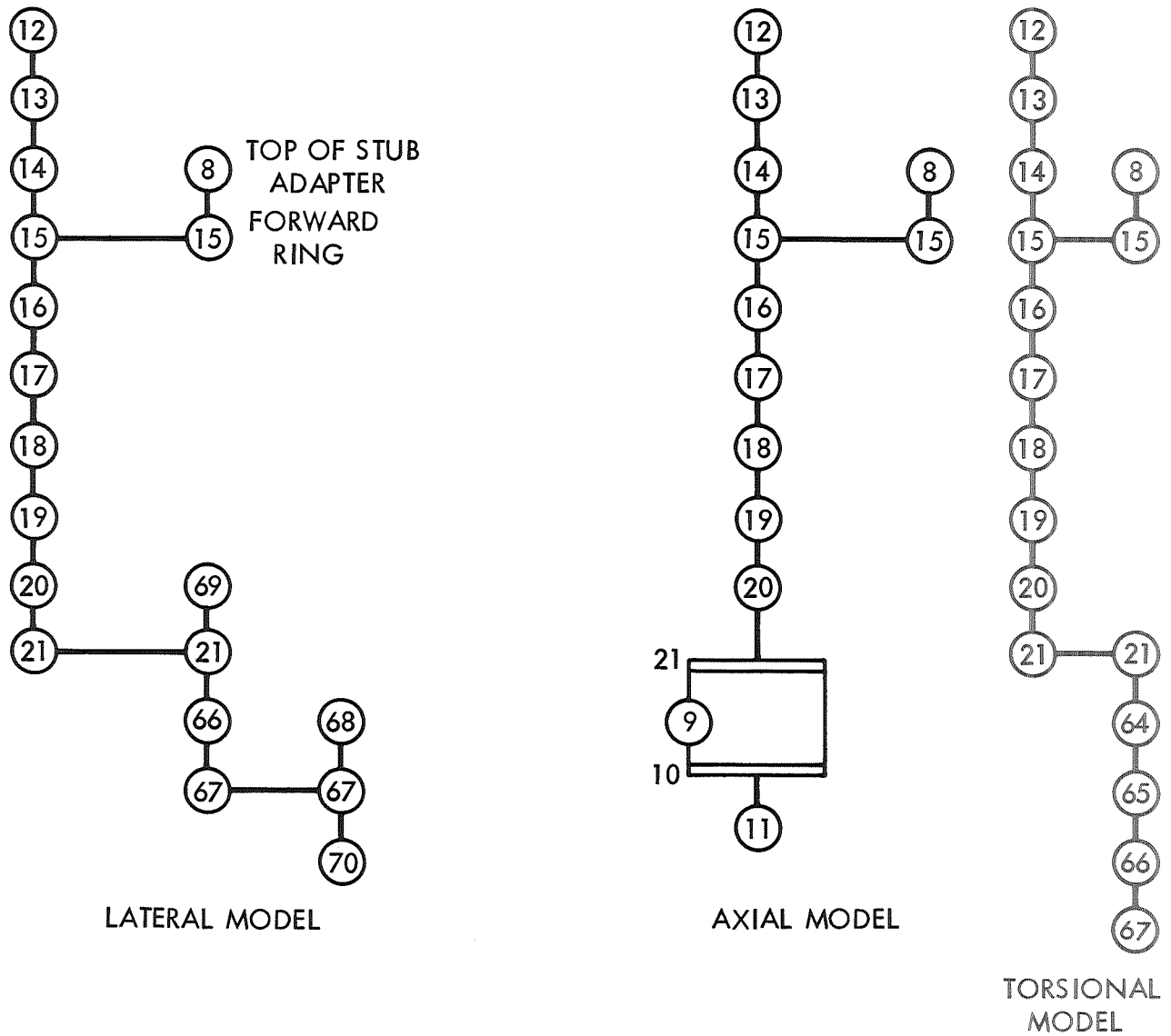
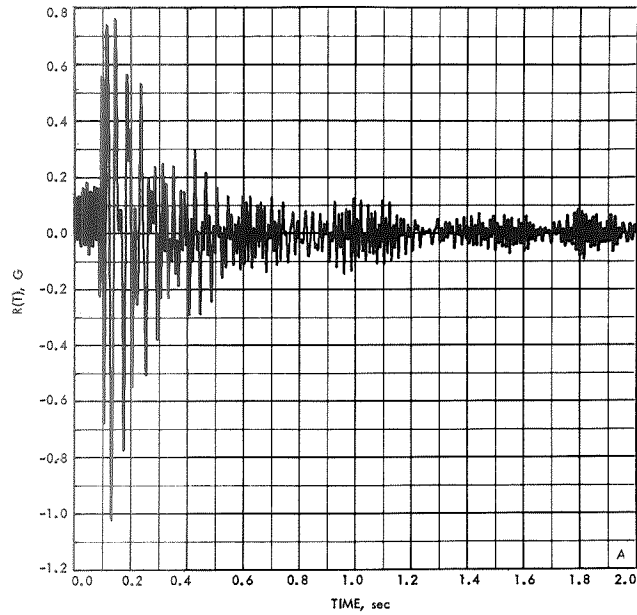


Fig. 1. Centaur vehicle model for Viking model



- A. ACCELERATION RESPONSE, TIME HISTORY
- B. ACCELERATION RESPONSE, FOURIER TRANSFORM, MODULUS
- C. ACCELERATION RESPONSE, FOURIER TRANSFORM, PHASE ANGLE

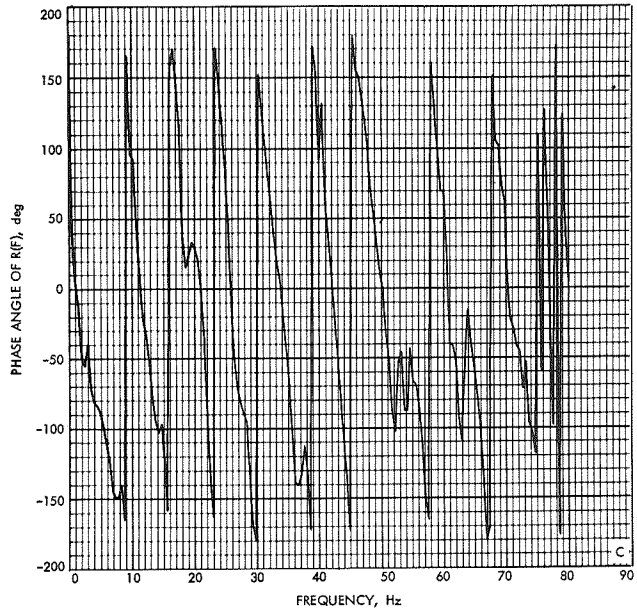
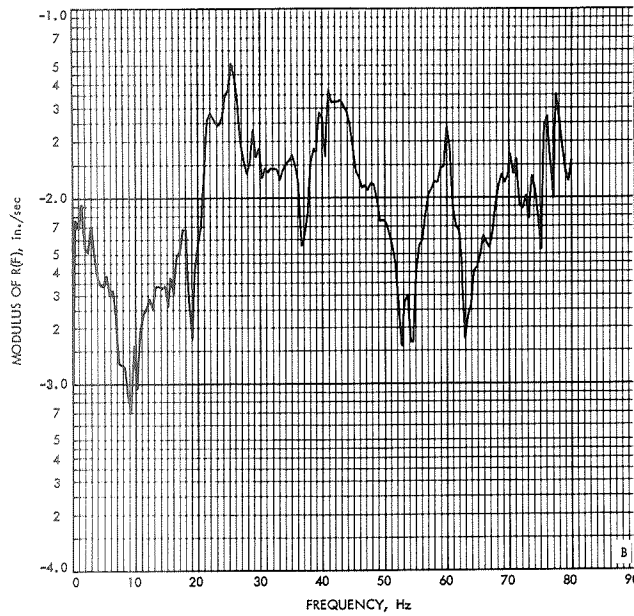
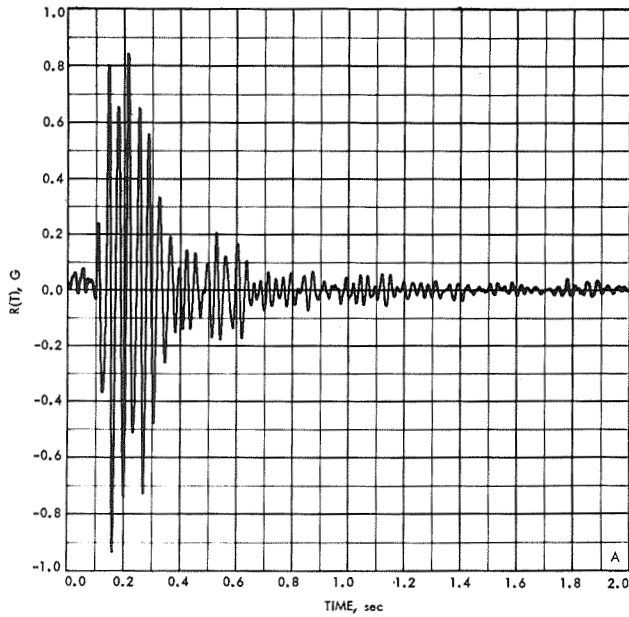


Fig. 2. Gridpoint 12, Centaur-Mariner Mars '71 acceleration response in X-direction at base of Centaur adapter predicted from the forcing function obtained from Mariner VI (AC-20) MECO flight data



- A. ACCELERATION RESPONSE, TIME HISTORY
- B. ACCELERATION RESPONSE, FOURIER TRANSFORM, MODULUS
- C. ACCELERATION RESPONSE, FOURIER TRANSFORM, PHASE ANGLE

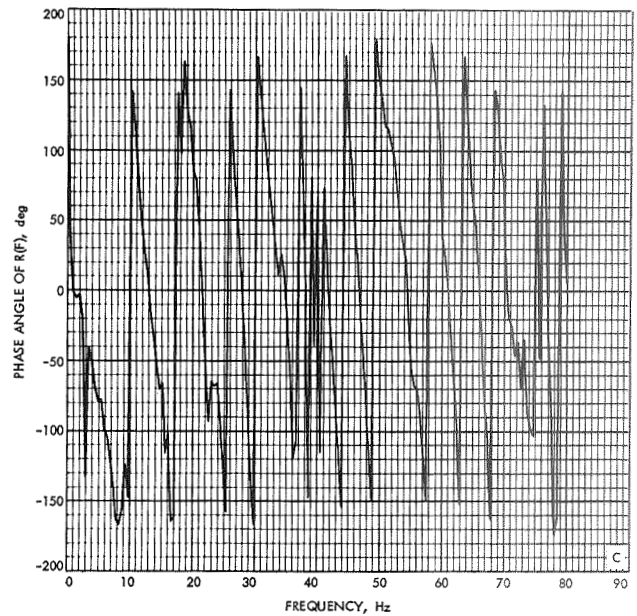
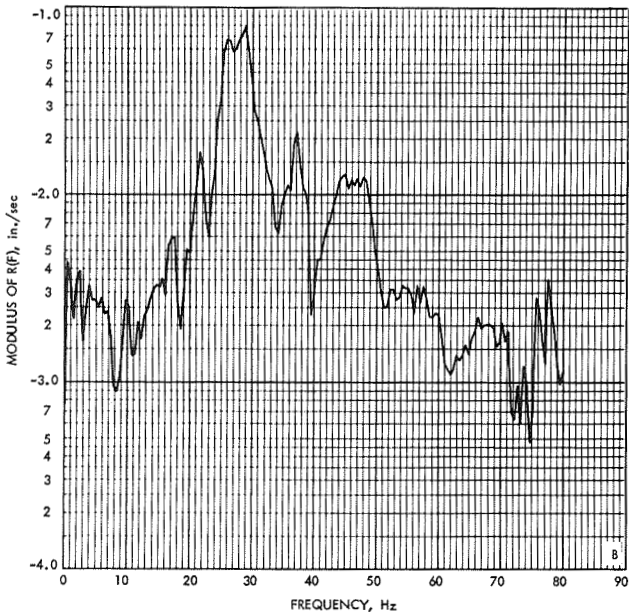
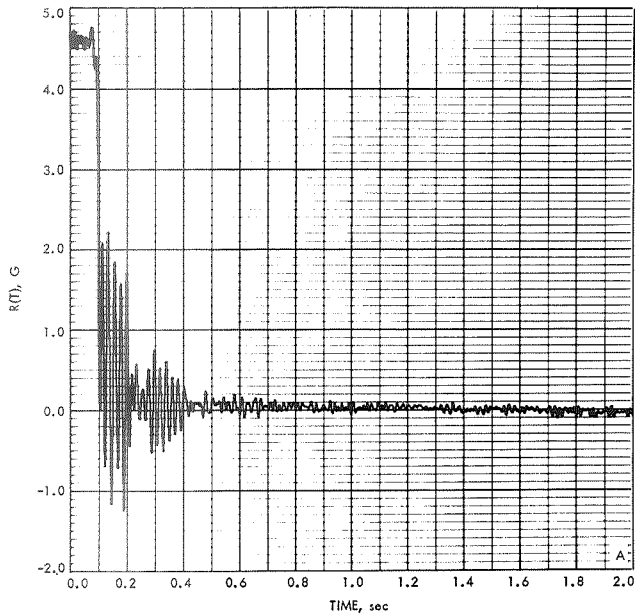


Fig. 3. Gridpoint 12, Centaur-Mariner Mars '71 acceleration response in Y-direction at base of Centaur adapter predicted from the forcing function obtained from Mariner VI (AC-20) MECO flight data



- A. ACCELERATION RESPONSE, TIME HISTORY
- B. ACCELERATION RESPONSE, FOURIER TRANSFORM, MODULUS
- C. ACCELERATION RESPONSE, FOURIER TRANSFORM, PHASE ANGLE

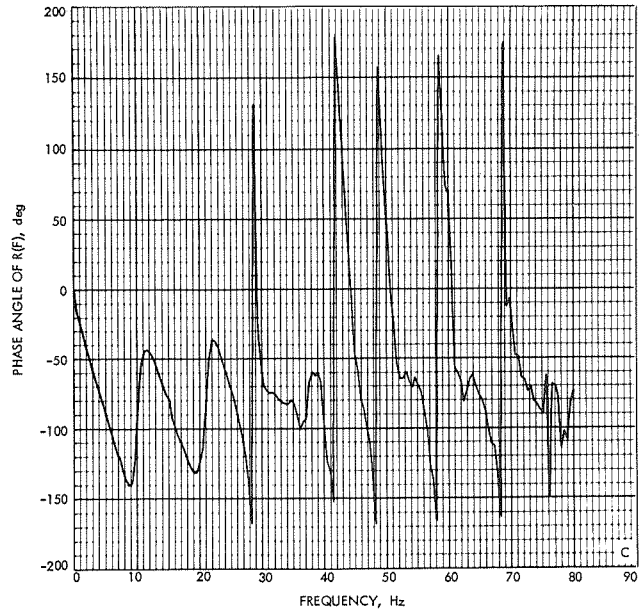
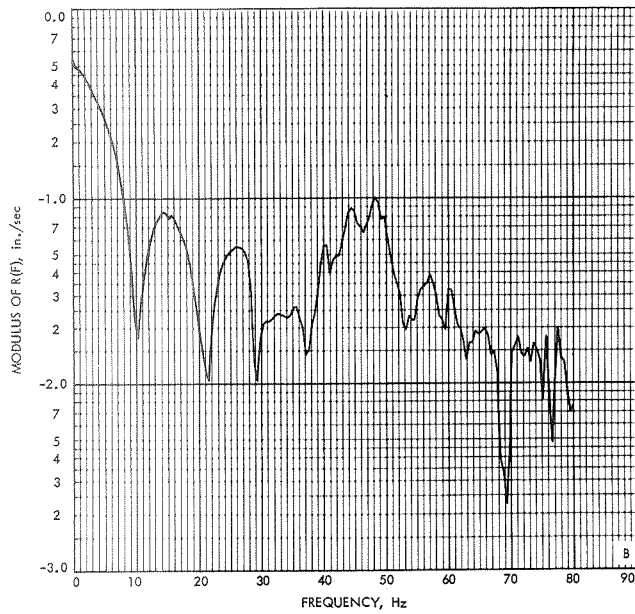


Fig. 4. Gridpoint 12, Centaur-Mariner Mars '71 acceleration response in Z-direction at base of Centaur adapter predicted from the forcing function obtained from Mariner VI (AC-20) MECO flight data

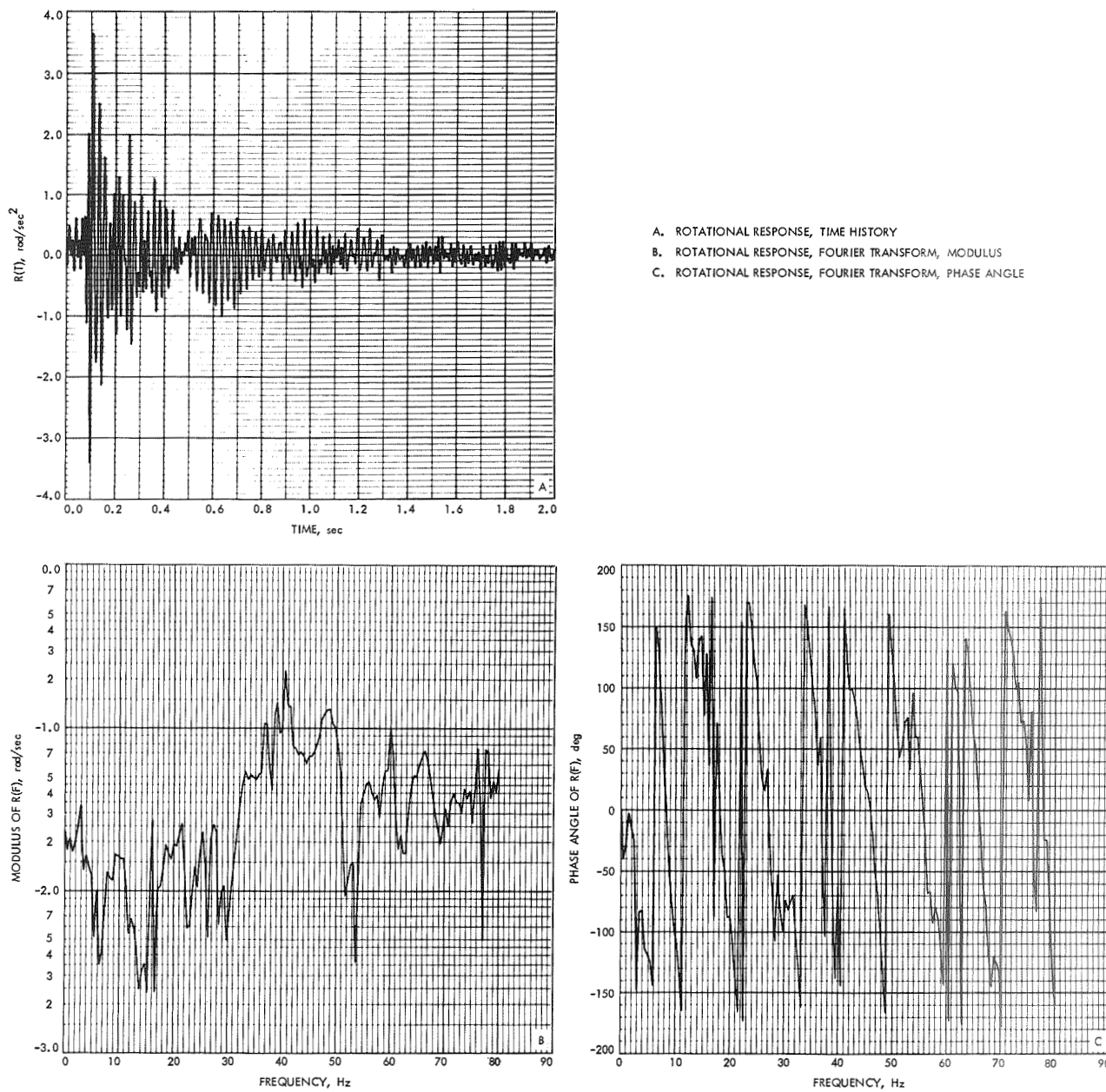
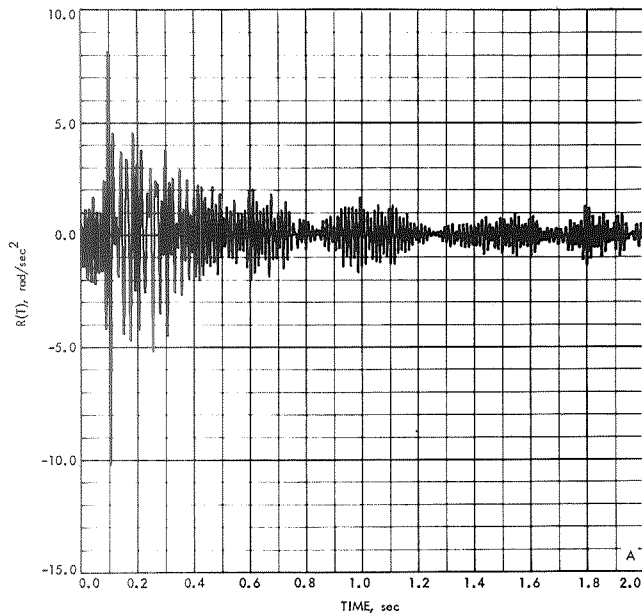


Fig. 5. Gridpoint 12, Centaur-Mariner Mars '71 rotational acceleration response in θ_x -direction at base of Centaur adapter predicted from the forcing function obtained from Mariner VI (AC-20) MECO flight data



- A. ROTATIONAL RESPONSE, TIME HISTORY
- B. ROTATIONAL RESPONSE, FOURIER TRANSFORM, MODULUS
- C. ROTATIONAL RESPONSE, FOURIER TRANSFORM, PHASE ANGLE

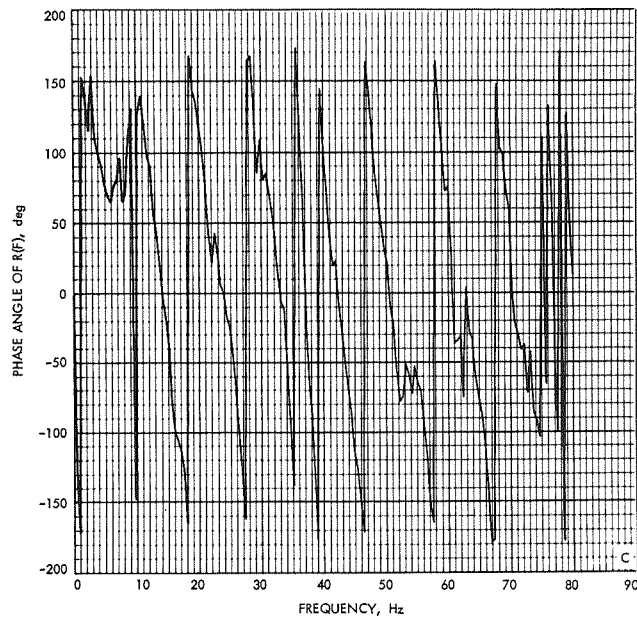
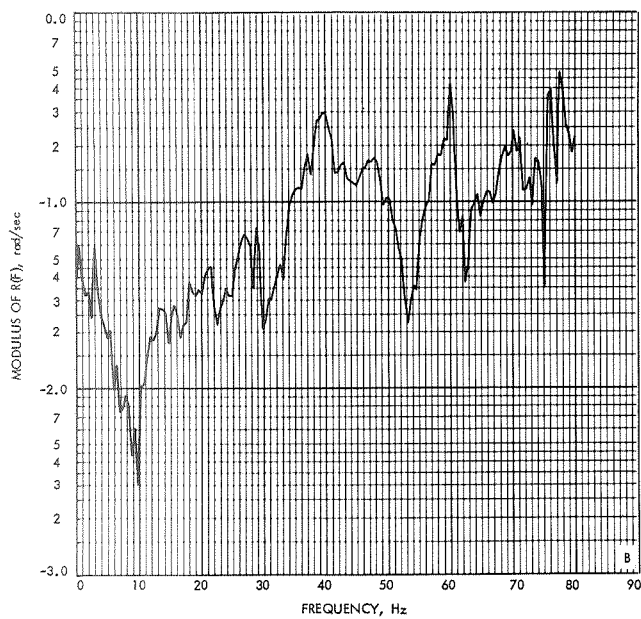
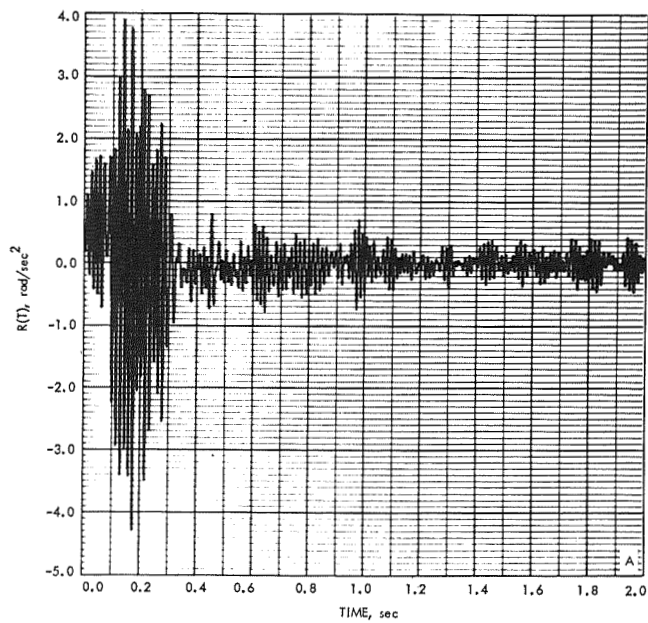


Fig. 6. Gridpoint 12, Centaur-Mariner Mars '71 rotational acceleration response in θ_y -direction at base of Centaur adapter predicted from the forcing function obtained from Mariner VI (AC-20) MECO flight data



- A. TORSIONAL RESPONSE, TIME HISTORY
- B. TORSIONAL RESPONSE, FOURIER TRANSFORM, MODULUS
- C. TORSIONAL RESPONSE, FOURIER TRANSFORM, PHASE ANGLE

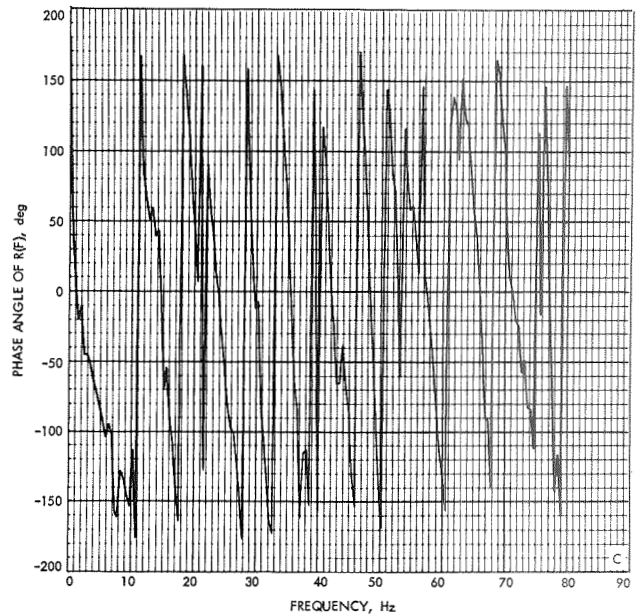
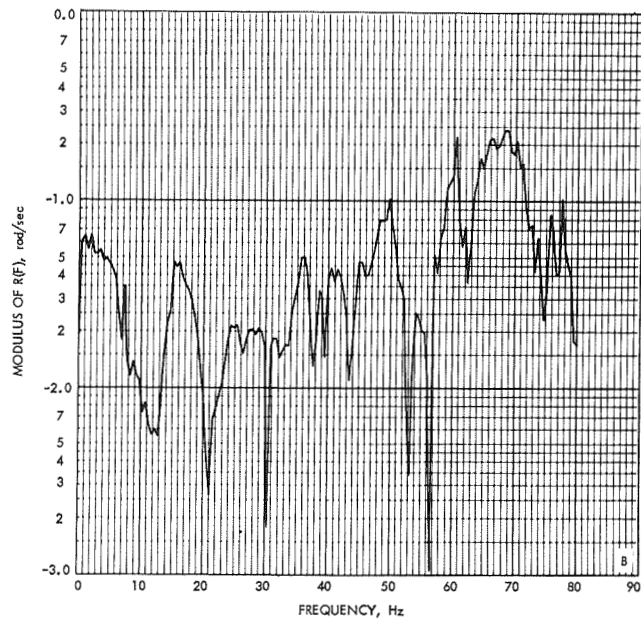
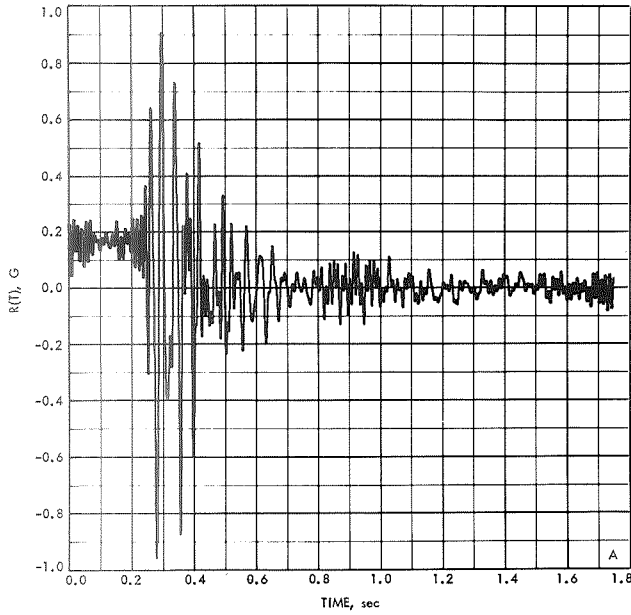


Fig. 7. Gridpoint 12, Centaur-Mariner Mars '71 torsional acceleration response in θ_z -direction at base of Centaur adapter predicted from the forcing function obtained from Mariner VI (AC-20) MECO flight data



- A. ACCELERATION RESPONSE, TIME HISTORY
- B. ACCELERATION RESPONSE, FOURIER TRANSFORM, MODULUS
- C. ACCELERATION RESPONSE, FOURIER TRANSFORM, PHASE ANGLE

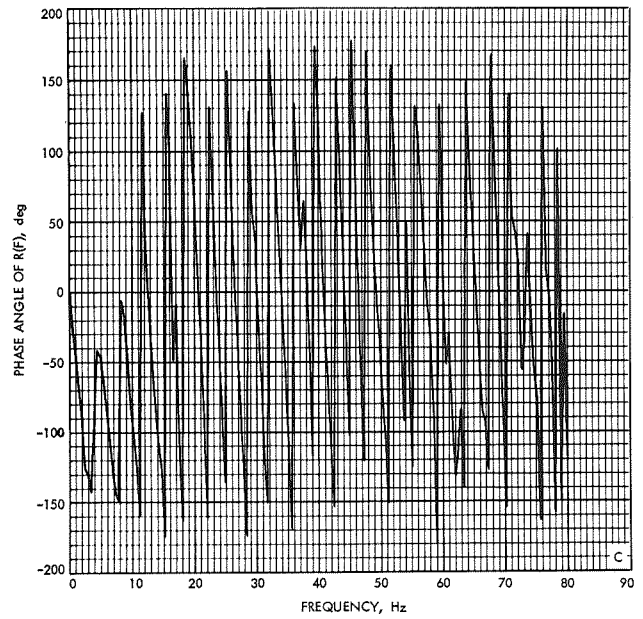
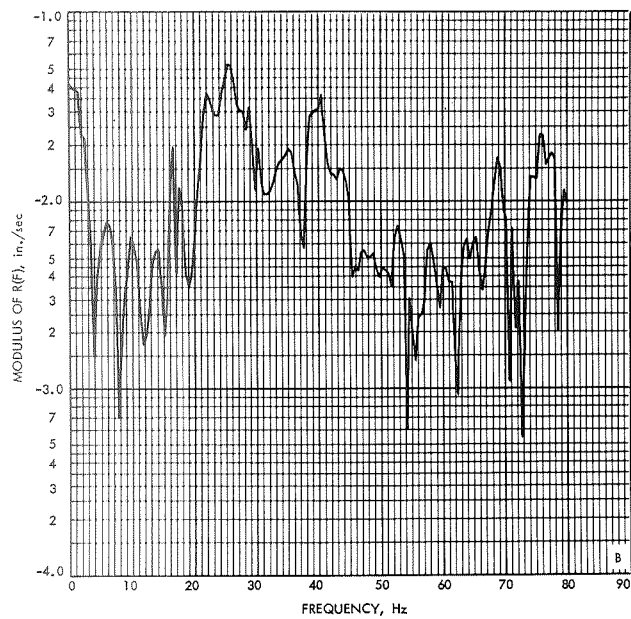
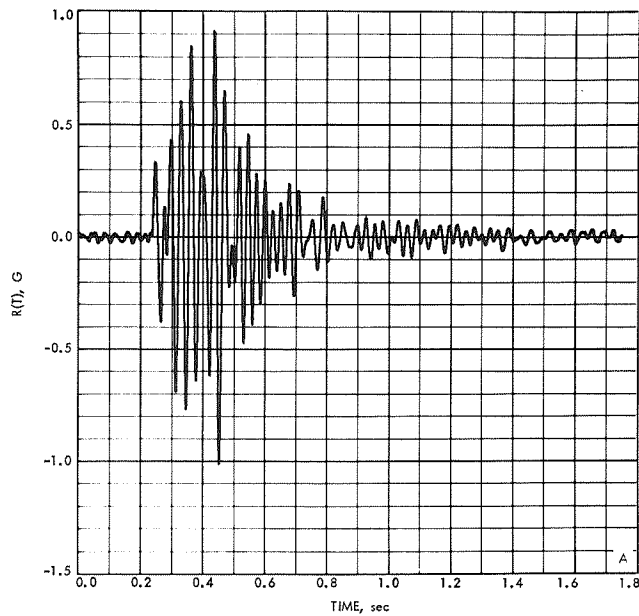


Fig. 8. Gridpoint 12, Centaur-Mariner Mars '71 acceleration response in X-direction at base of Centaur adapter predicted from the forcing function obtained from Mariner VII (AC-19) MECO flight data



- A. ACCELERATION RESPONSE, TIME HISTORY
- B. ACCELERATION RESPONSE, FOURIER TRANSFORM, MODULUS
- C. ACCELERATION RESPONSE, FOURIER TRANSFORM, PHASE ANGLE

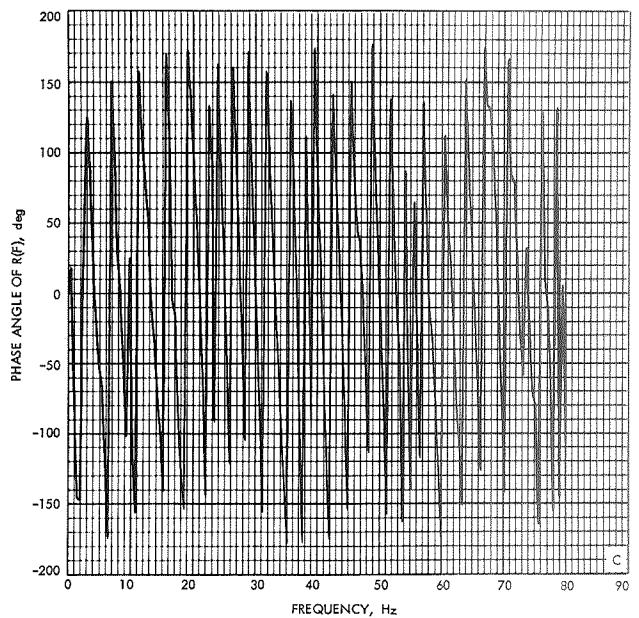
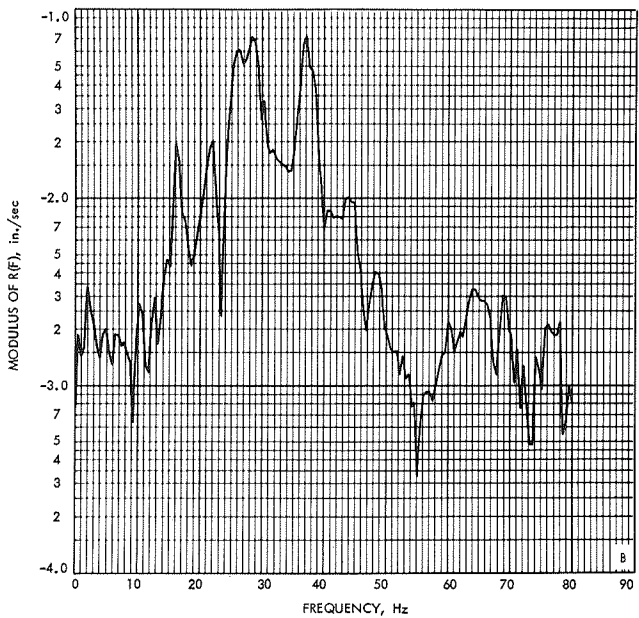
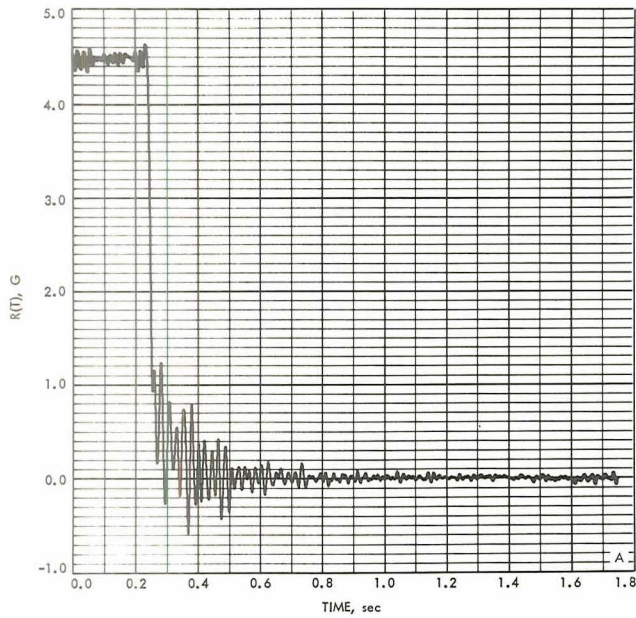


Fig. 9. Gridpoint 12, Centaur-Mariner Mars '71 acceleration response in Y-direction at base of Centaur adapter predicted from the forcing function obtained from Mariner VII (AC-19) MECO flight data



- A. ACCELERATION RESPONSE, TIME HISTORY
- B. ACCELERATION RESPONSE, FOURIER TRANSFORM, MODULUS
- C. ACCELERATION RESPONSE, FOURIER TRANSFORM, PHASE ANGLE

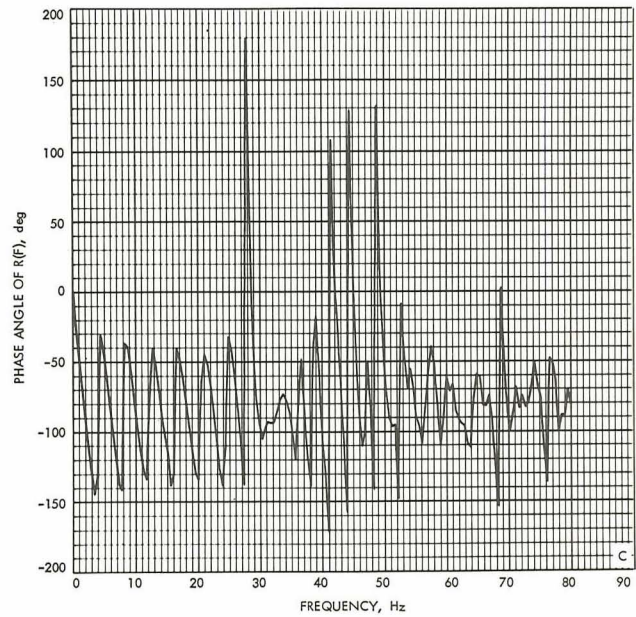
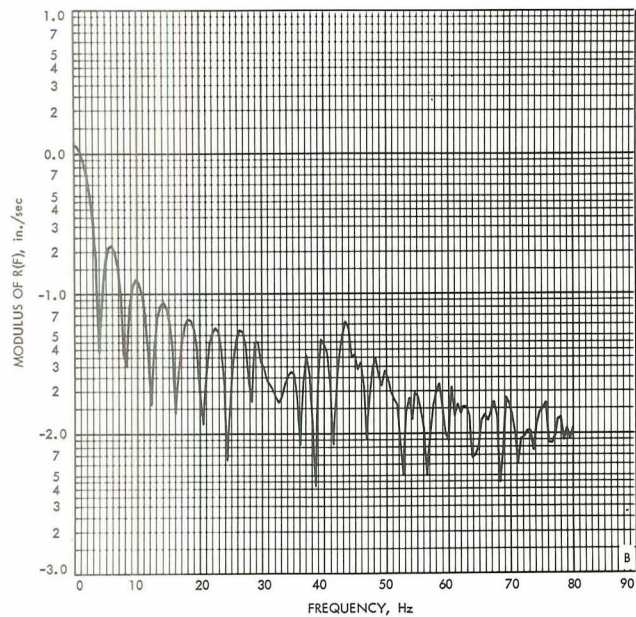
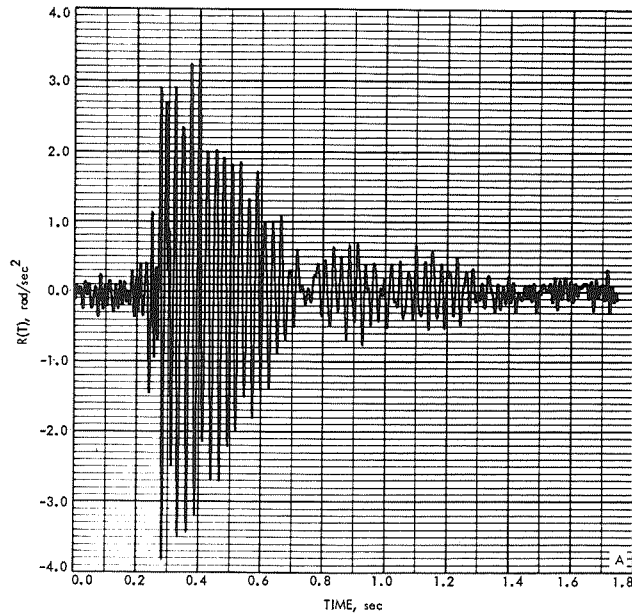


Fig. 10. Gridpoint 12, Centaur-Mariner Mars '71 acceleration response in Z-direction at base of Centaur adapter predicted from the forcing function obtained from Mariner VII (AC-19) MECO flight data



- A. ROTATIONAL RESPONSE, TIME HISTORY
- B. ROTATIONAL RESPONSE, FOURIER TRANSFORM, MODULUS
- C. ROTATIONAL RESPONSE, FOURIER TRANSFORM, PHASE ANGLE

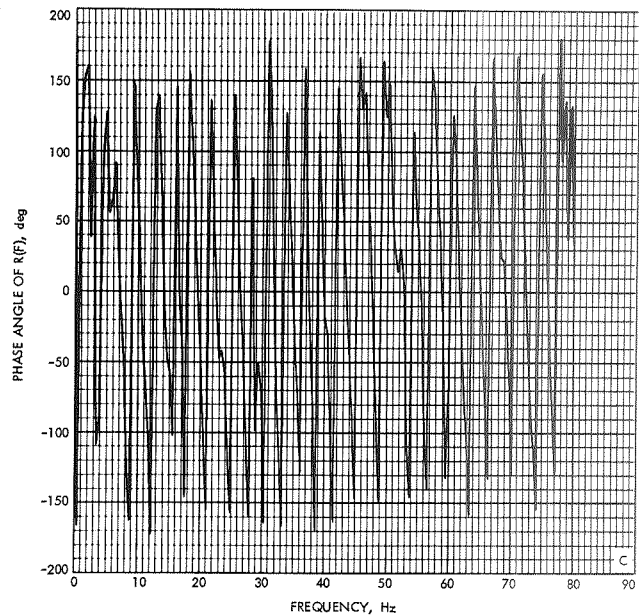
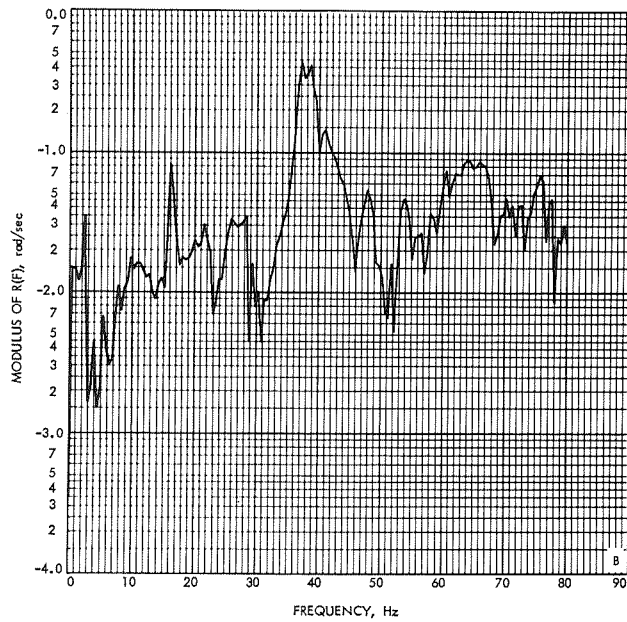
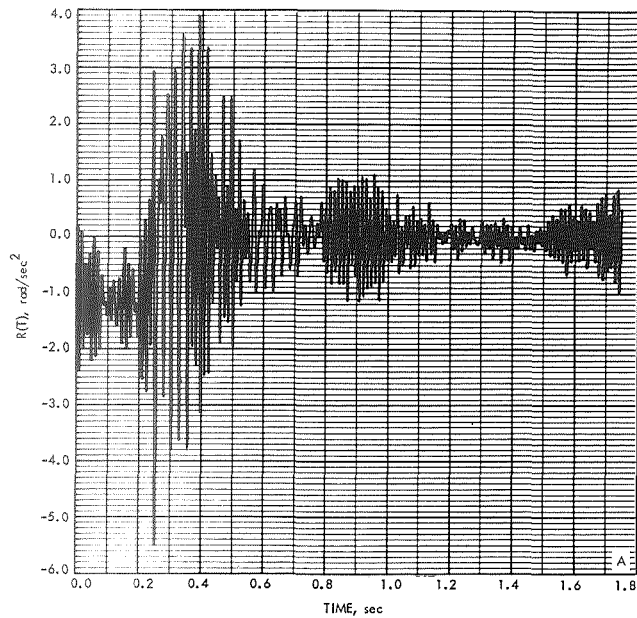


Fig. 11. Gridpoint 12, Centaur-Mariner Mars '71 rotational acceleration response in θ_x -direction at base of Centaur adapter predicted from the forcing function obtained from Mariner VII (AC-19) MECO flight data



- A. ROTATIONAL RESPONSE, TIME HISTORY
- B. ROTATIONAL RESPONSE, FOURIER TRANSFORM, MODULUS
- C. ROTATIONAL RESPONSE, FOURIER TRANSFORM, PHASE ANGLE

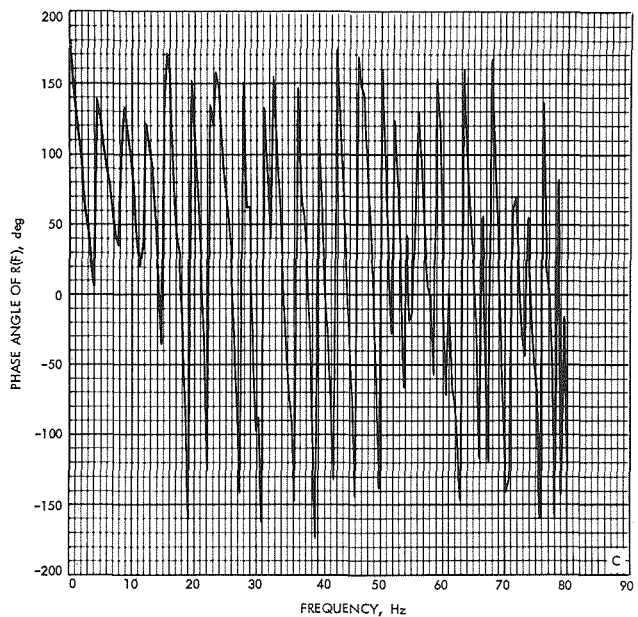
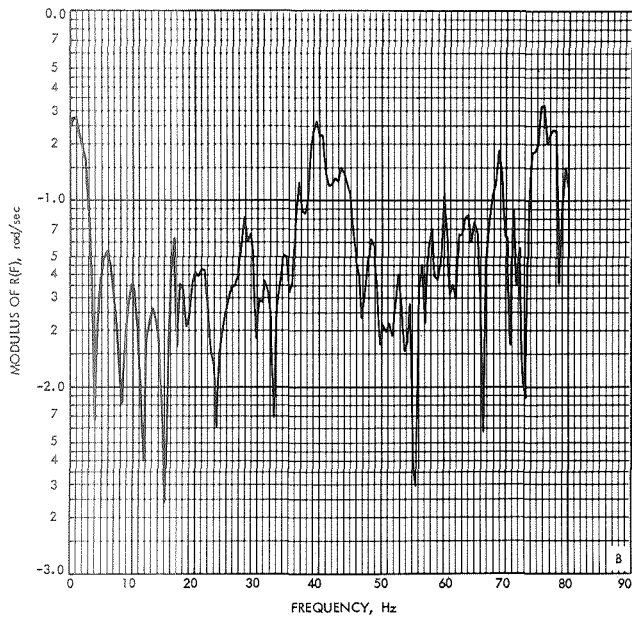
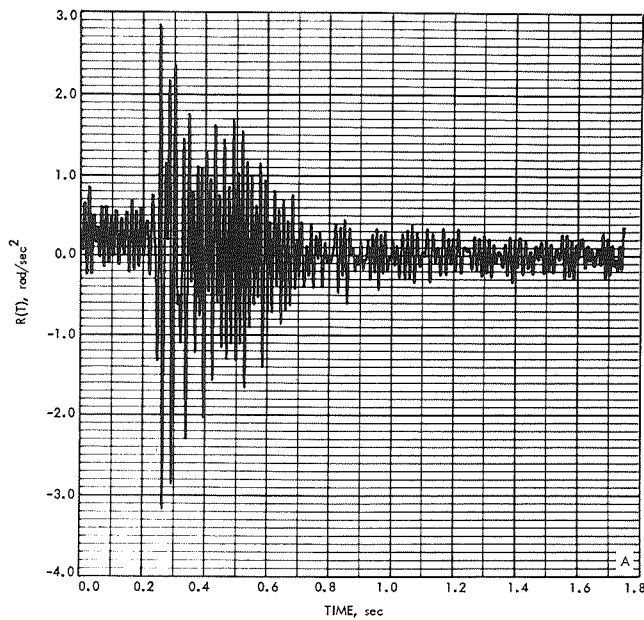


Fig. 12. Gridpoint 12, Centaur-Mariner Mars '71 rotational acceleration response in θ_v -direction at base of Centaur adapter predicted from the forcing function obtained from Mariner VII (AC-19) MECO flight data



- A. TORSIONAL RESPONSE, TIME HISTORY
- B. TORSIONAL RESPONSE, FOURIER TRANSFORM, MODULUS
- C. TORSIONAL RESPONSE, FOURIER TRANSFORM, PHASE ANGLE

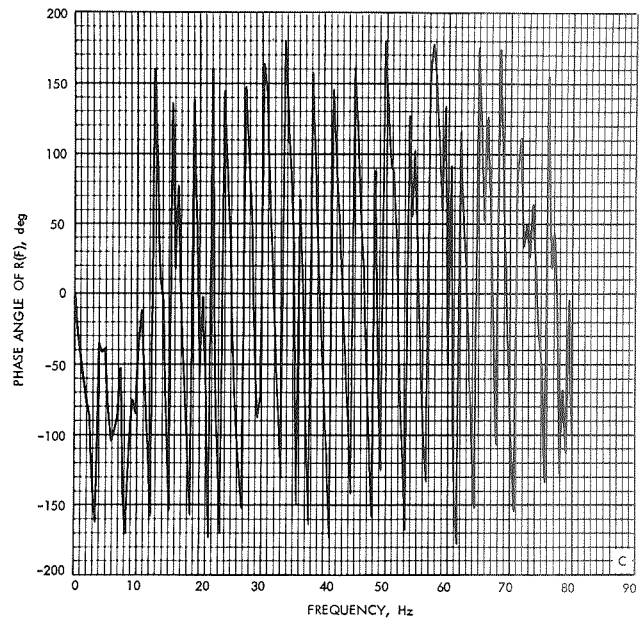
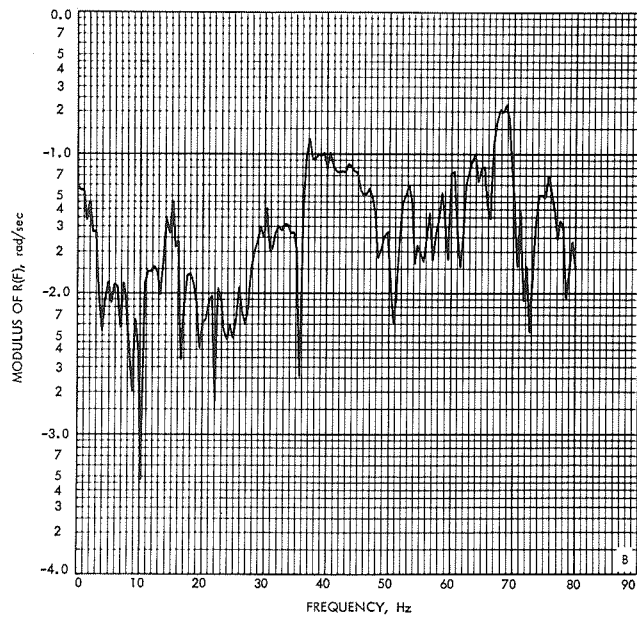
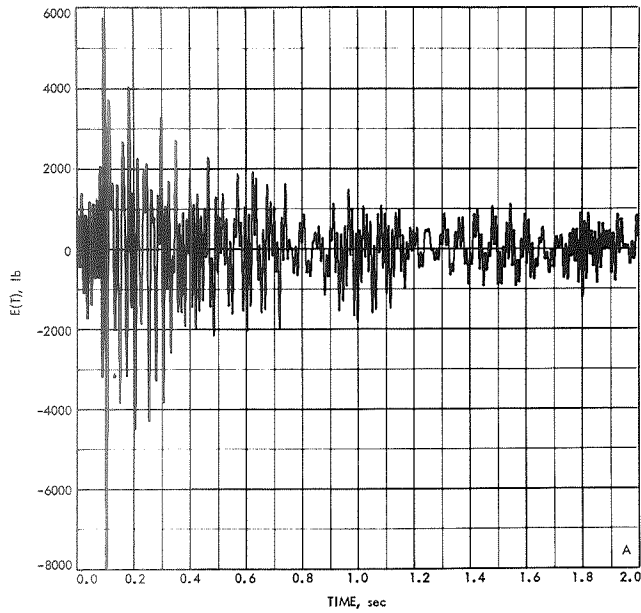


Fig. 13. Gridpoint 12, Centaur-Mariner Mars '71 torsional acceleration response in θ_z -direction at base of Centaur adapter predicted from the forcing function obtained from Mariner VII (AC-19) MECO flight data



- A. SEPARATION PLANE FORCE, TIME HISTORY
- B. SEPARATION PLANE FORCE, FOURIER TRANSFORM, MODULUS
- C. SEPARATION PLANE FORCE, FOURIER TRANSFORM, PHASE ANGLE

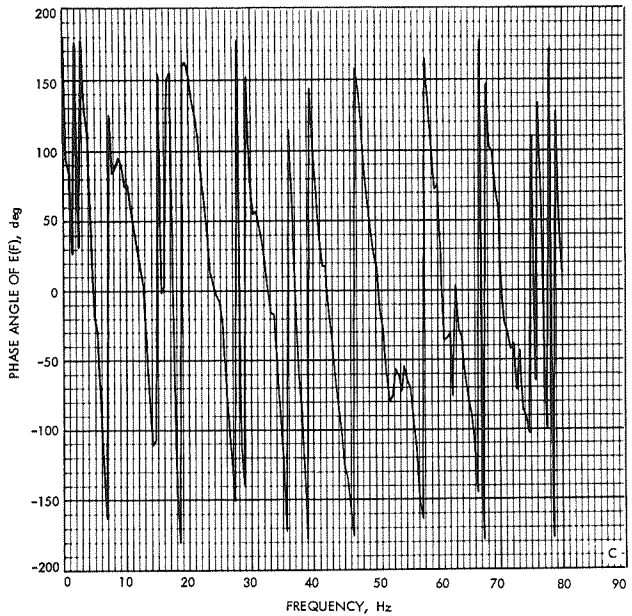
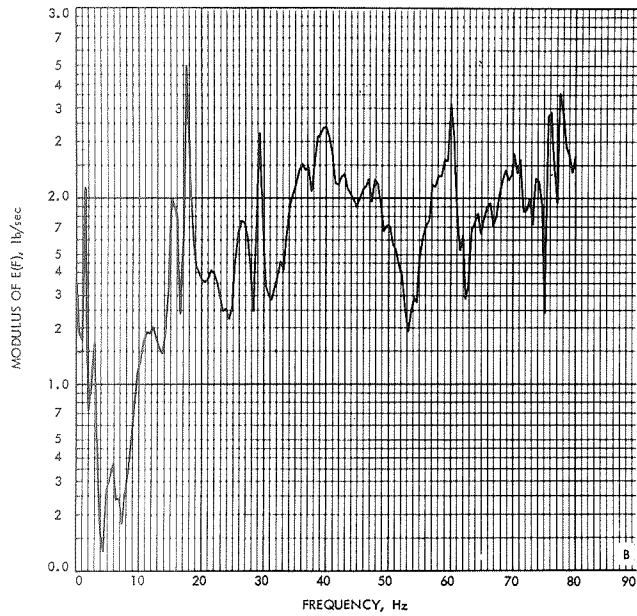
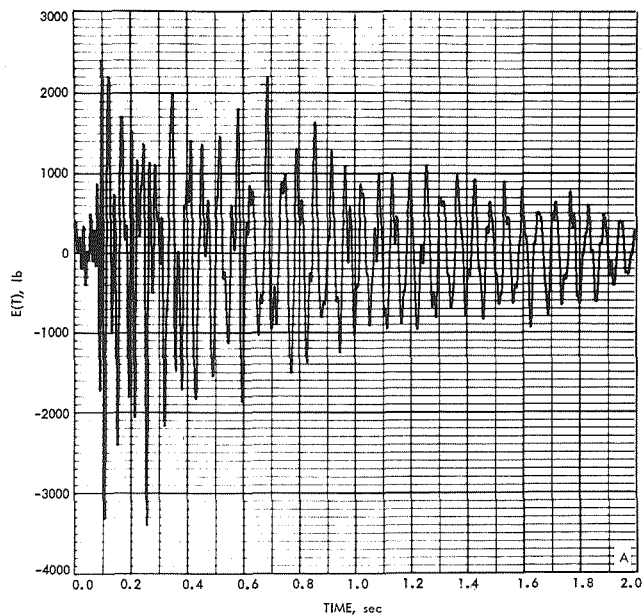


Fig. 14. Gridpoint 12, Mariner Mars '71 reaction force in X-direction at base of Centaur adapter predicted from the forcing function derived from Mariner VI (AC-20) MECO flight data



- A. SEPARATION PLANE FORCE, TIME HISTORY
- B. SEPARATION PLANE FORCE, FOURIER TRANSFORM, MODULUS
- C. SEPARATION PLANE FORCE, FOURIER TRANSFORM, PHASE ANGLE

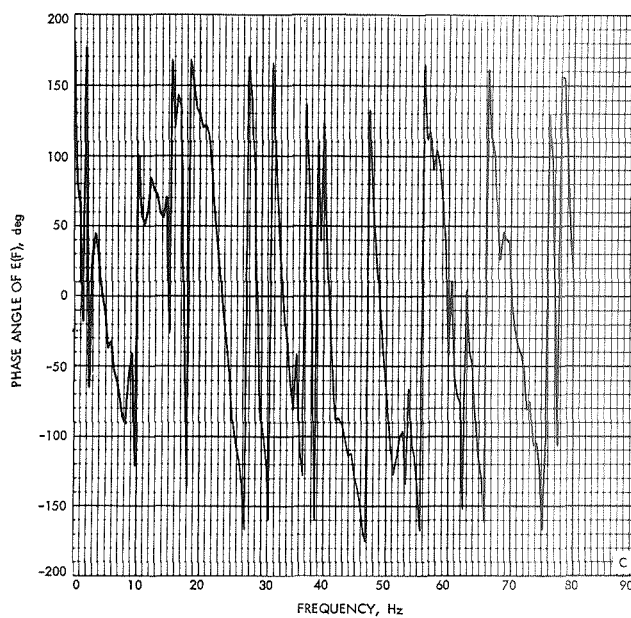
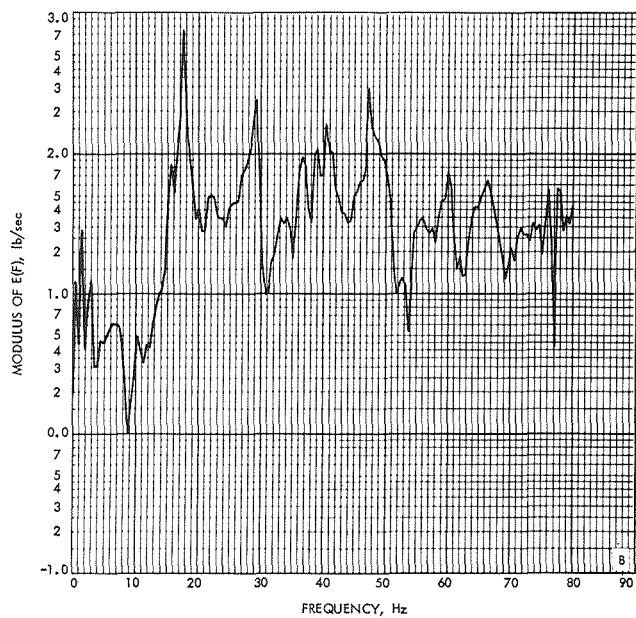
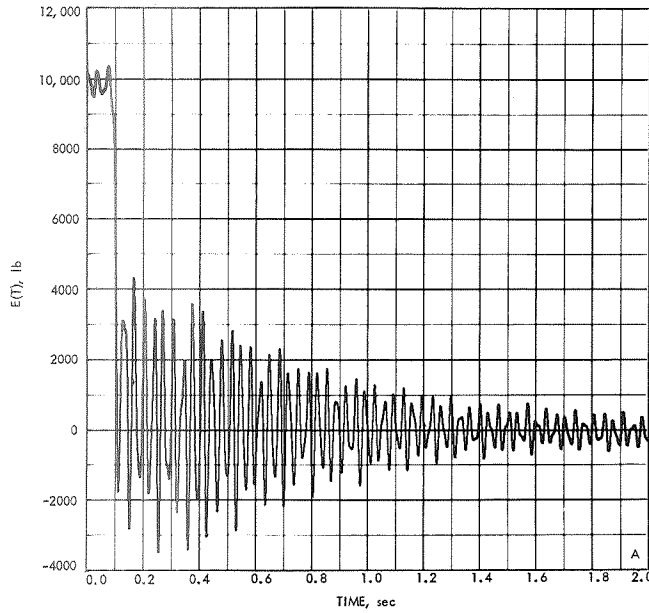


Fig. 15. Gridpoint 12, Mariner Mars '71 reaction force in Y-direction at base of Centaur adapter predicted from the forcing function derived from Mariner VI (AC-20) MECO flight data



- A. SEPARATION PLANE FORCE, TIME HISTORY
- B. SEPARATION PLANE FORCE, FOURIER TRANSFORM, MODULUS
- C. SEPARATION PLANE FORCE, FOURIER TRANSFORM, PHASE ANGLE

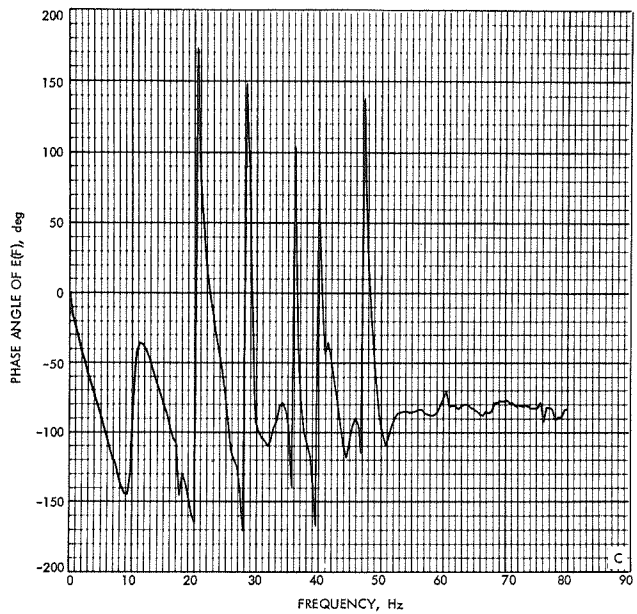
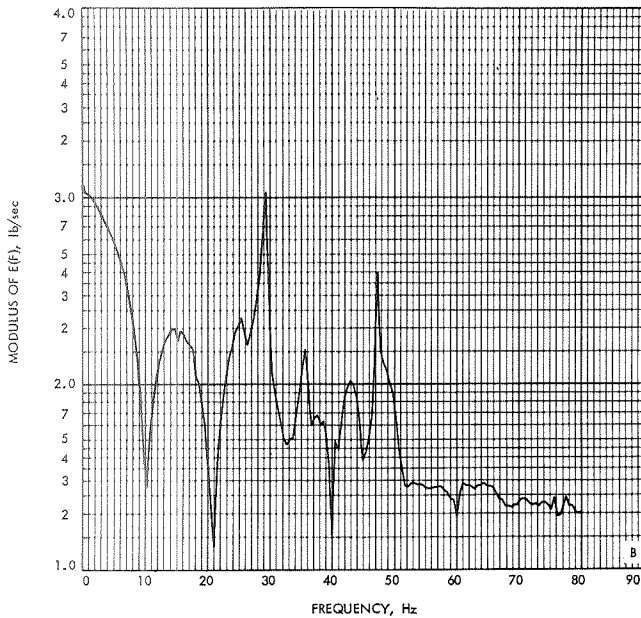
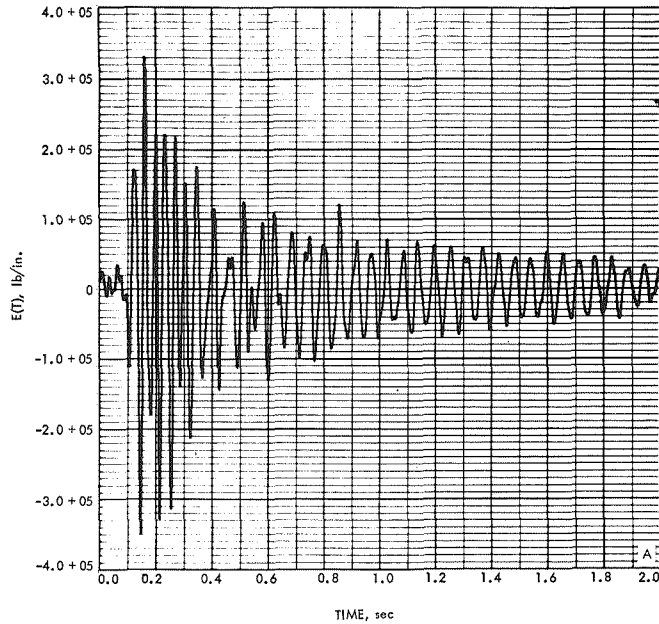


Fig. 16. Gridpoint 12, Mariner Mars '71 reaction force in Z-direction at base of Centaur adapter predicted from the forcing function derived from Mariner VI (AC-20) MECO flight data



- A. SEPARATION PLANE MOMENT, TIME HISTORY
- B. SEPARATION PLANE MOMENT, FOURIER TRANSFORM, MODULUS
- C. SEPARATION PLANE MOMENT, FOURIER TRANSFORM, PHASE ANGLE

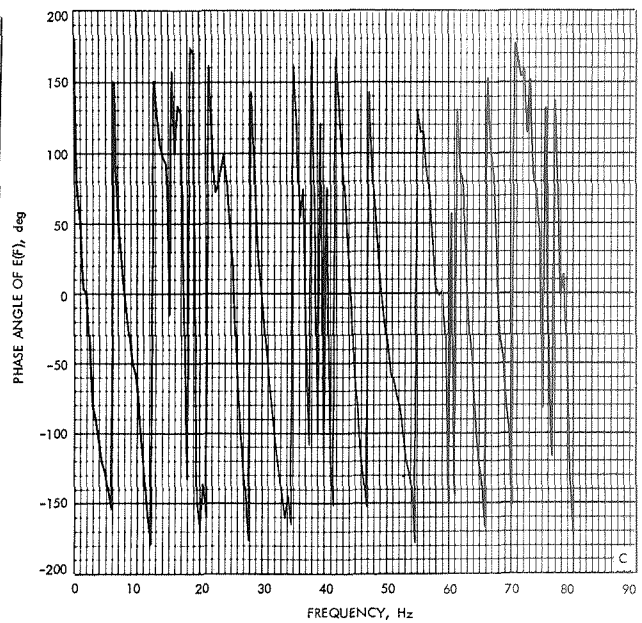
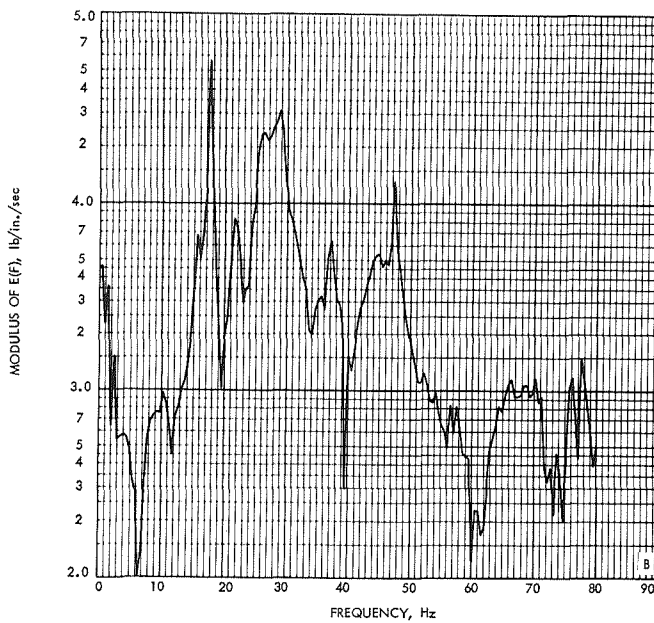
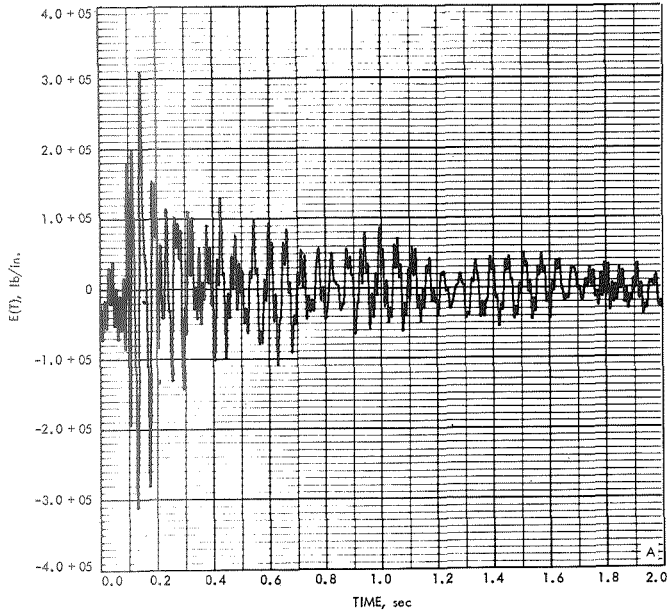


Fig. 17. Gridpoint 12, Mariner Mars '71 reaction moment in θ_x -direction at base of Centaur adapter predicted from the forcing function derived from Mariner VI (AC-20) MECO flight data



- A. SEPARATION PLANE MOMENT, TIME HISTORY
- B. SEPARATION PLANE MOMENT, FOURIER TRANSFORM, MODULUS
- C. SEPARATION PLANE MOMENT, FOURIER TRANSFORM, PHASE ANGLE

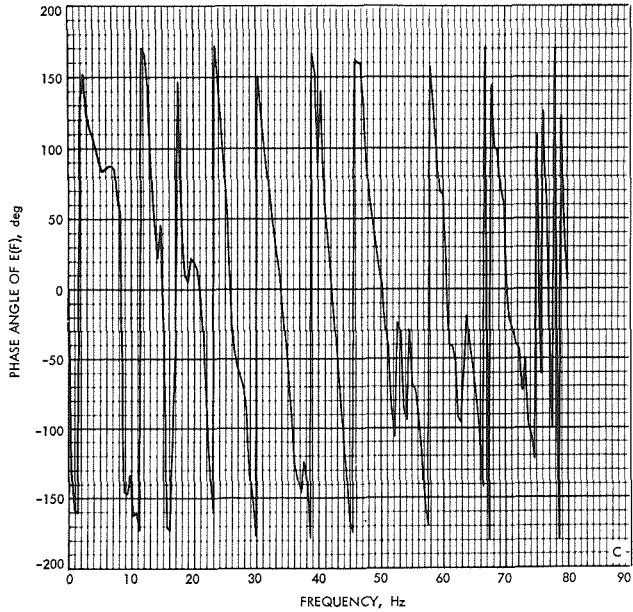
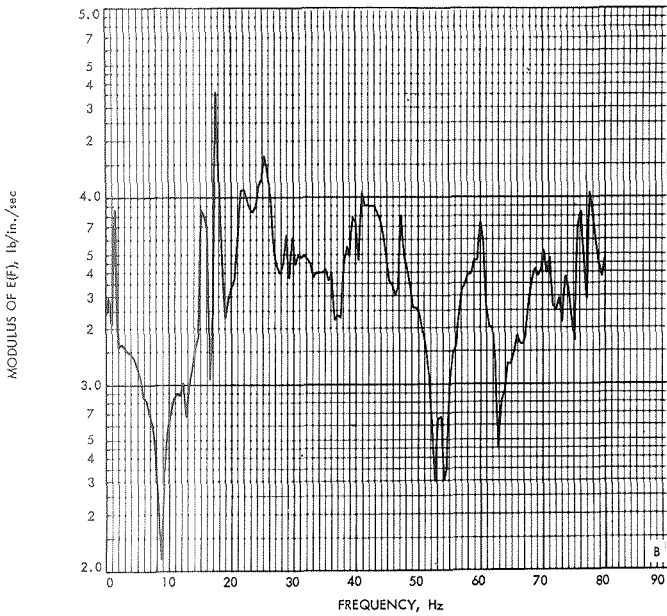
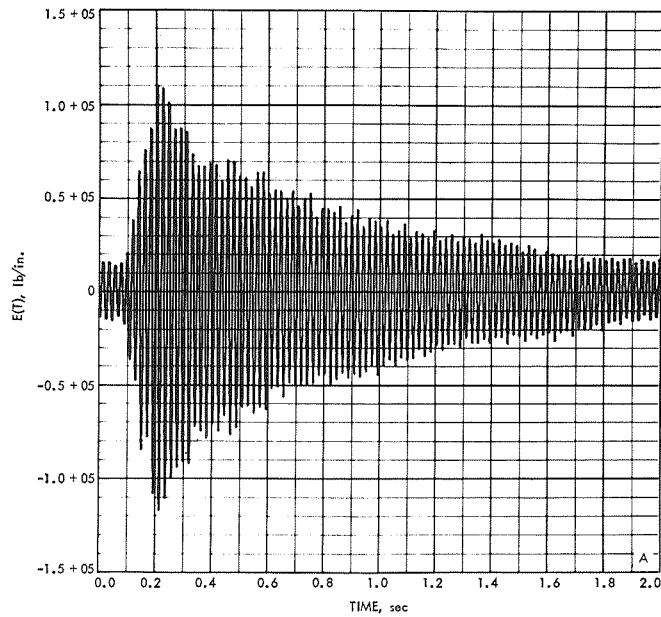


Fig. 18. Gridpoint 12, Mariner Mars '71 reaction moment in θ_y -direction at base of Centaur adapter predicted from the forcing function derived from Mariner VI (AC-20) MECO flight data



- A. SEPARATION PLANE TORQUE, TIME HISTORY
- B. SEPARATION PLANE TORQUE, FOURIER TRANSFORM, MODULUS
- C. SEPARATION PLANE TORQUE, FOURIER TRANSFORM, PHASE ANGLE

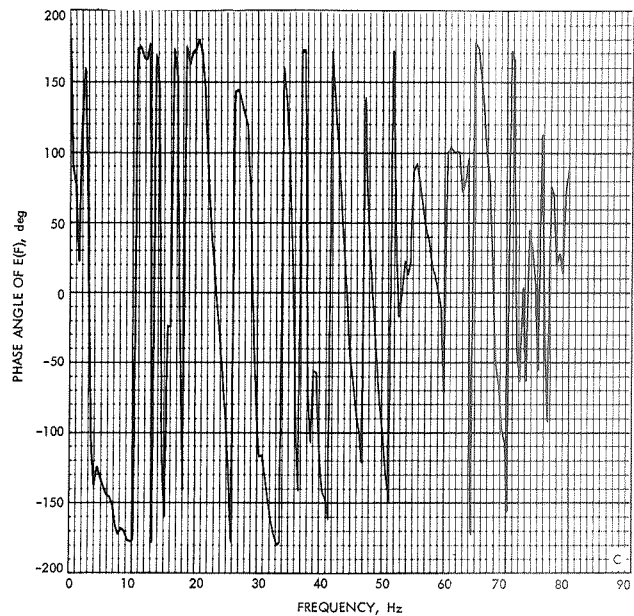
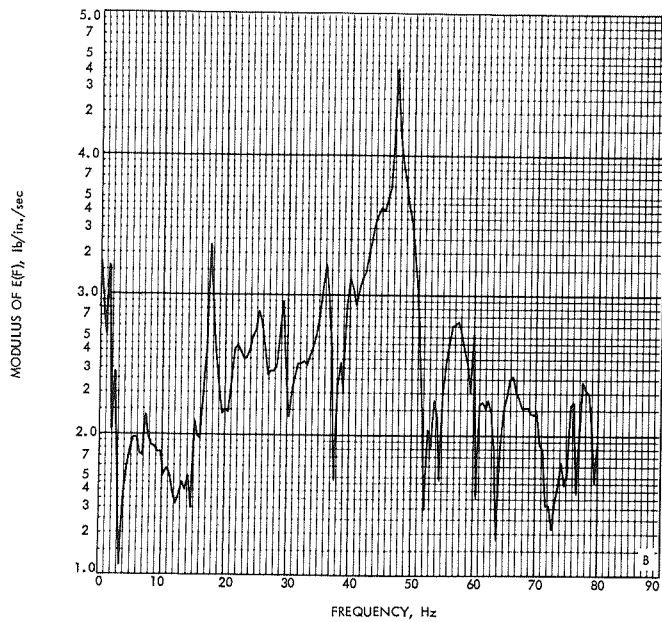


Fig. 19. Gridpoint 12, Mariner Mars '71 reaction moment in θ_z -direction at base of Centaur adapter predicted from the forcing function derived from Mariner VI (AC-20) MECO flight data

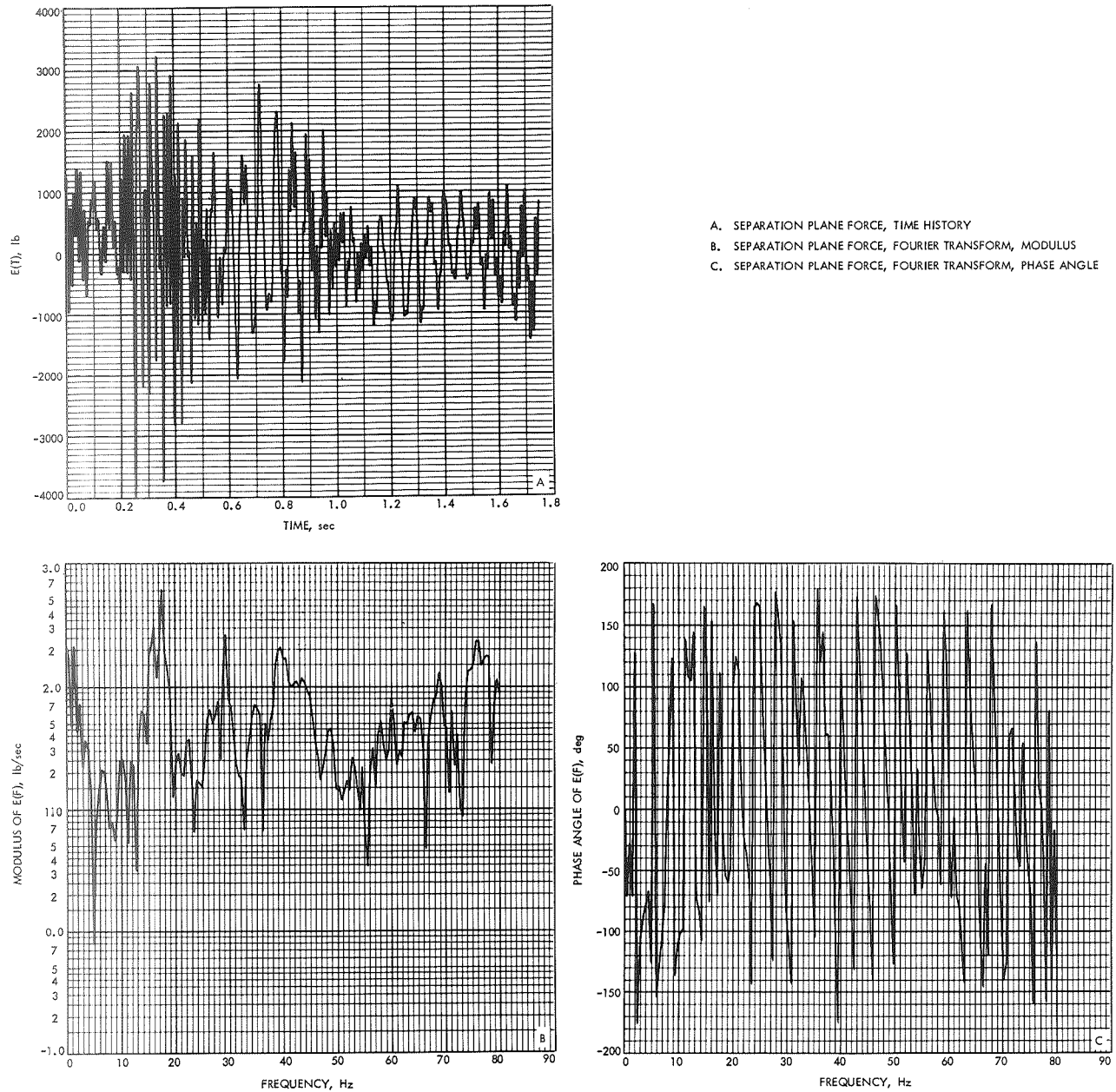
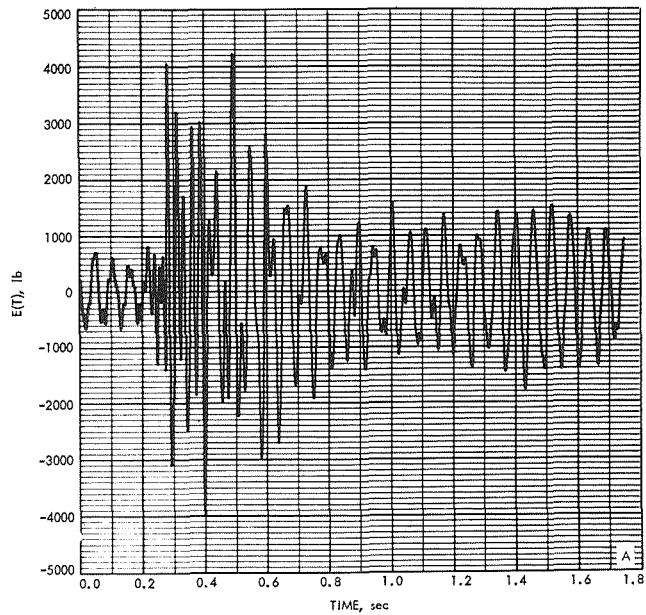


Fig. 20. Gridpoint 12, Mariner Mars '71 reaction force in X-direction at base of Centaur adapter predicted from the forcing function derived from Mariner VII (AC-19) MECO flight data



- A. SEPARATION PLANE FORCE, TIME HISTORY
- B. SEPARATION PLANE FORCE, FOURIER TRANSFORM, MODULUS
- C. SEPARATION PLANE FORCE, FOURIER TRANSFORM, PHASE ANGLE

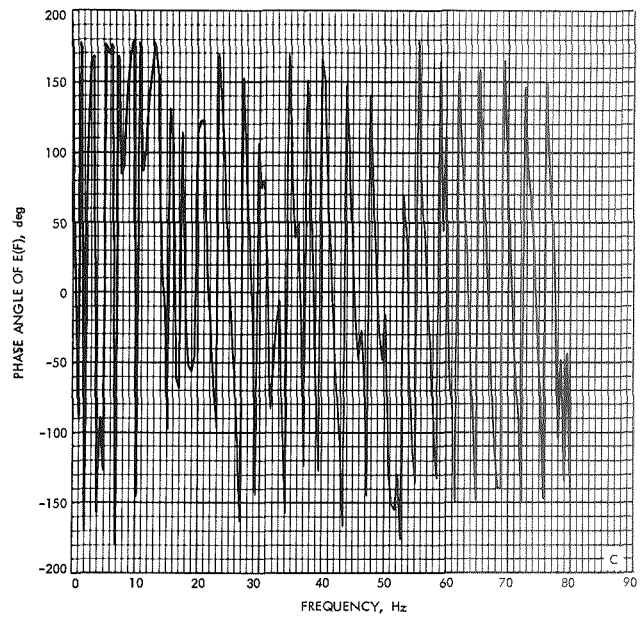
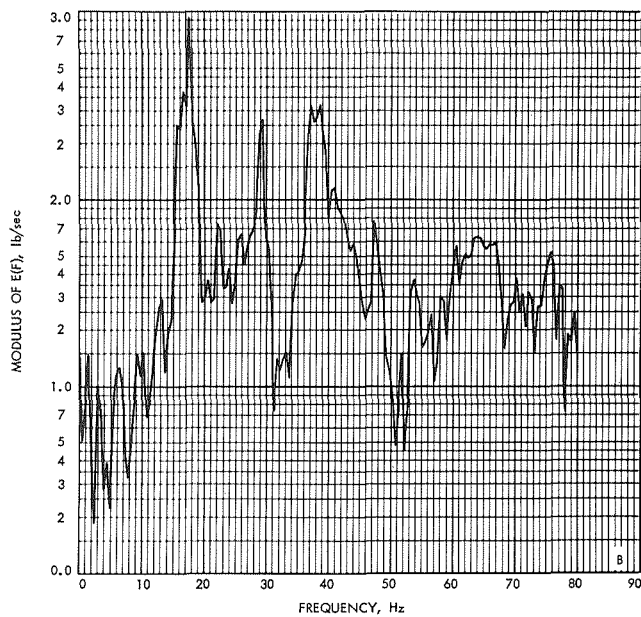
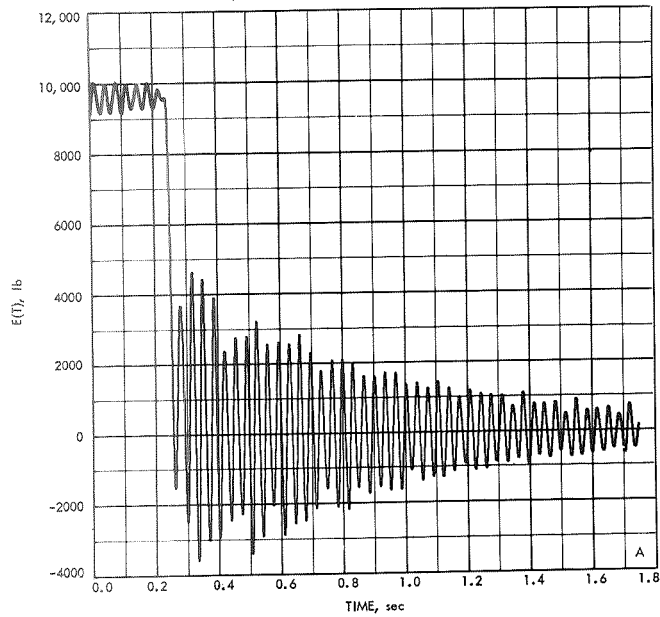


Fig. 21. Gridpoint 12, Mariner Mars '71 reaction force in Y-direction at base of Centaur adapter predicted from the forcing function derived from Mariner VII (AC-19) MECO flight data



- A. SEPARATION PLANE FORCE, TIME HISTORY
- B. SEPARATION PLANE FORCE, FOURIER TRANSFORM, MODULUS
- C. SEPARATION PLANE FORCE, FOURIER TRANSFORM, PHASE ANGLE

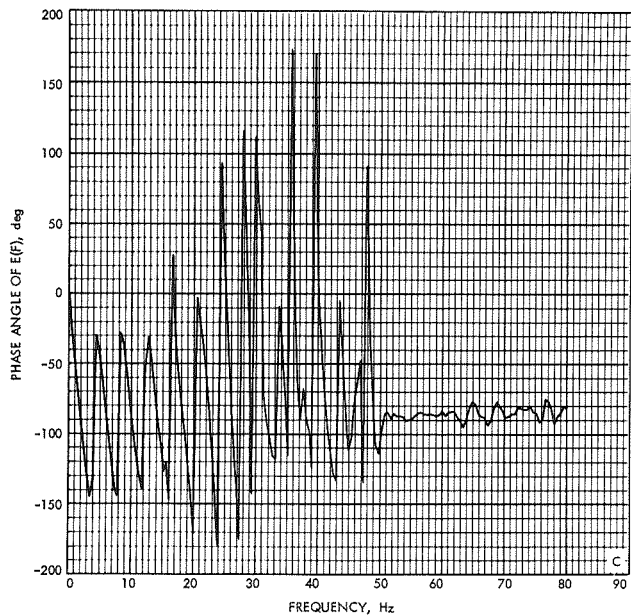
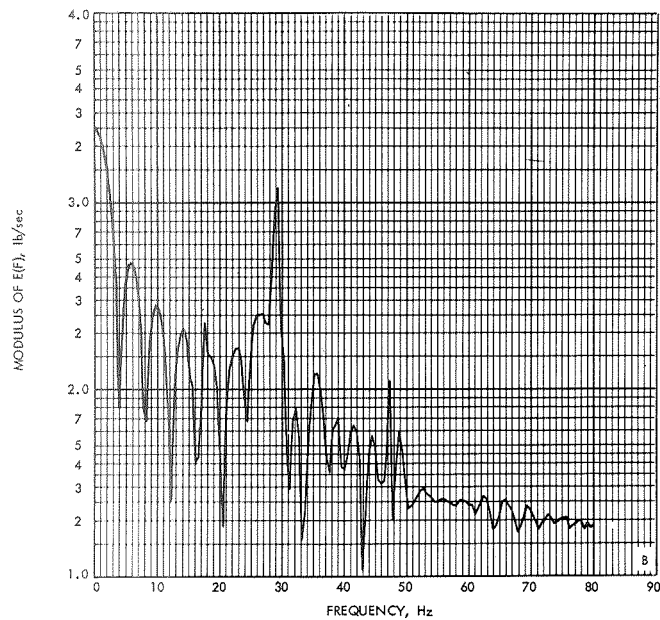
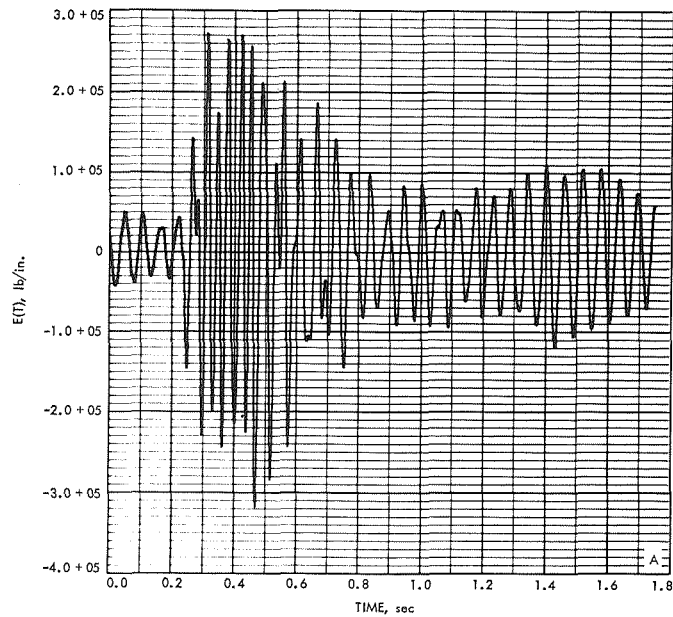


Fig. 22. Gridpoint 12, Mariner Mars '71 reaction force in Z-direction at base of Centaur adapter predicted from the forcing function derived from Mariner VII (AC-19) MECO flight data



- A. SEPARATION PLANE MOMENT, TIME HISTORY
- B. SEPARATION PLANE MOMENT, FOURIER TRANSFORM, MODULUS
- C. SEPARATION PLANE MOMENT, FOURIER TRANSFORM, PHASE ANGLE

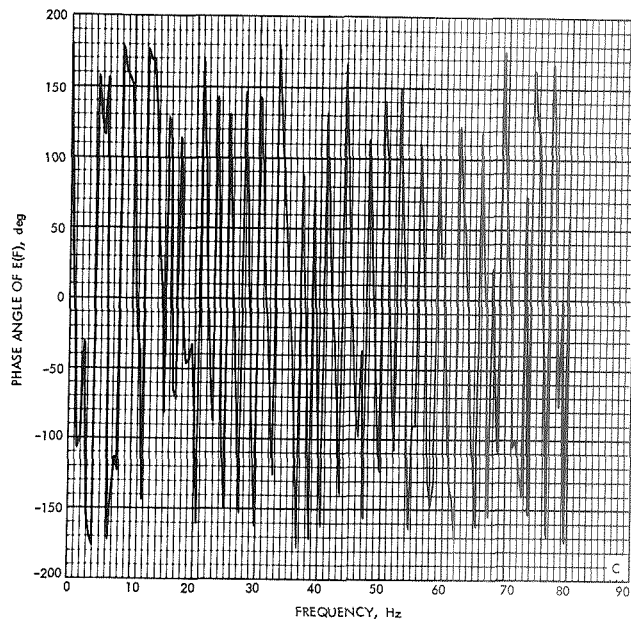
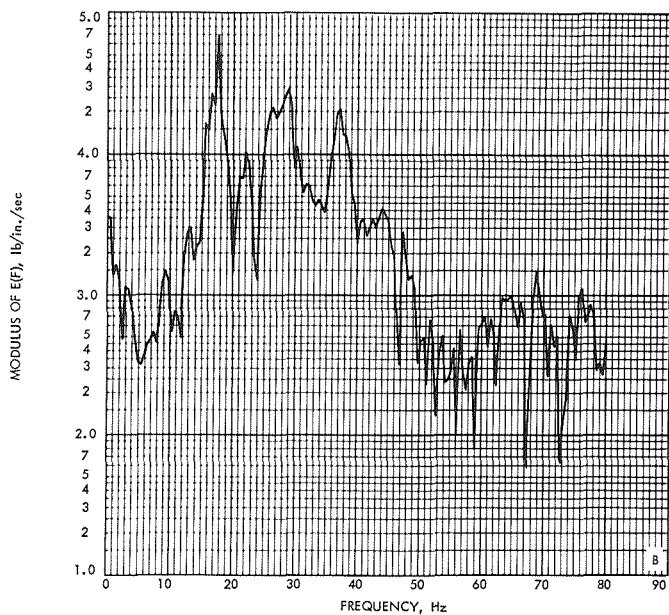
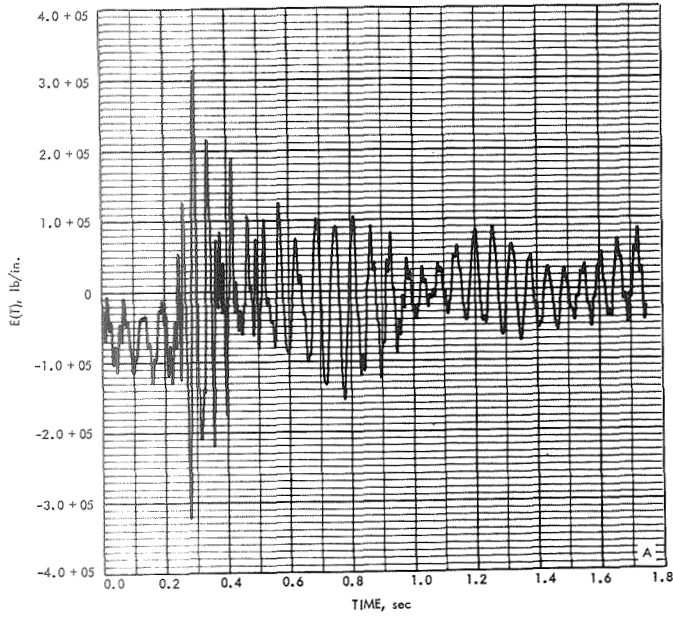


Fig. 23. Gridpoint 12, Mariner Mars '71 reaction moment in θ_x -direction at base of Centaur adapter predicted from the forcing function derived from Mariner VII (AC-19) MECO flight data



- A. SEPARATION PLANE MOMENT, TIME HISTORY
- B. SEPARATION PLANE MOMENT, FOURIER TRANSFORM, MODULUS
- C. SEPARATION PLANE MOMENT, FOURIER TRANSFORM, PHASE ANGLE

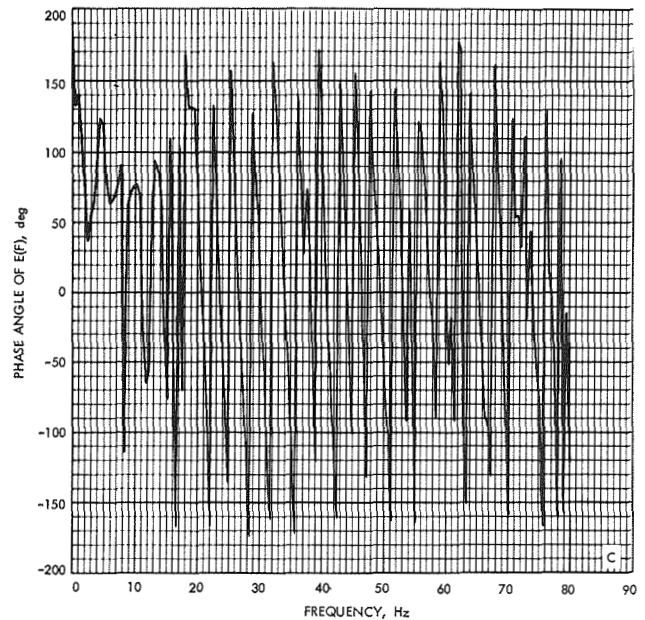
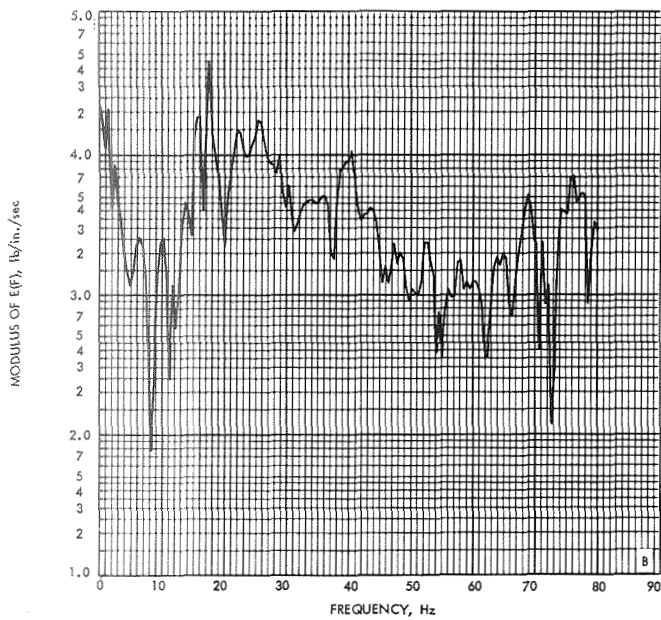
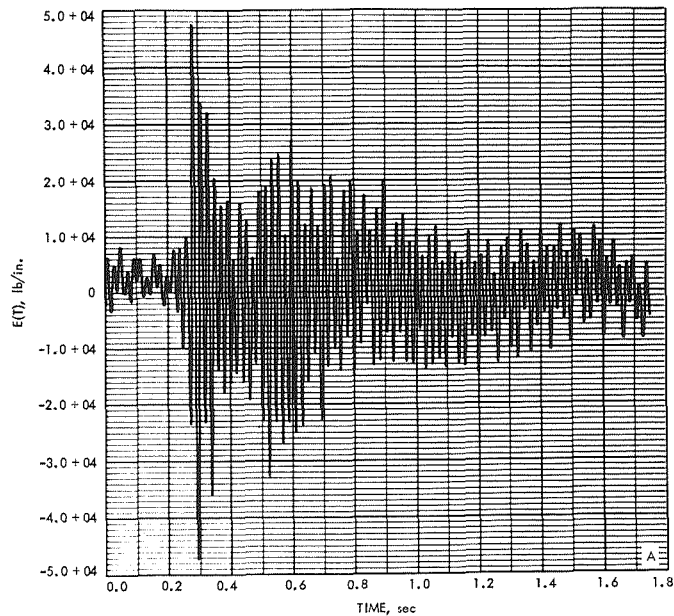


Fig. 24. Gridpoint 12, Mariner Mars '71 reaction moment in θ_y -direction at base of Centaur adapter predicted from the forcing function derived from Mariner VII (AC-19) MECO flight data



- A. SEPARATION PLANE TORQUE, TIME HISTORY
- B. SEPARATION PLANE TORQUE, FOURIER TRANSFORM, MODULUS
- C. SEPARATION PLANE TORQUE, FOURIER TRANSFORM, PHASE ANGLE

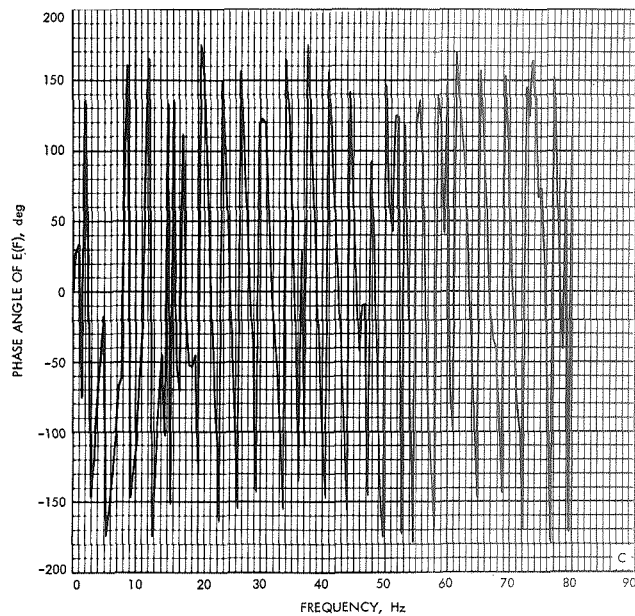
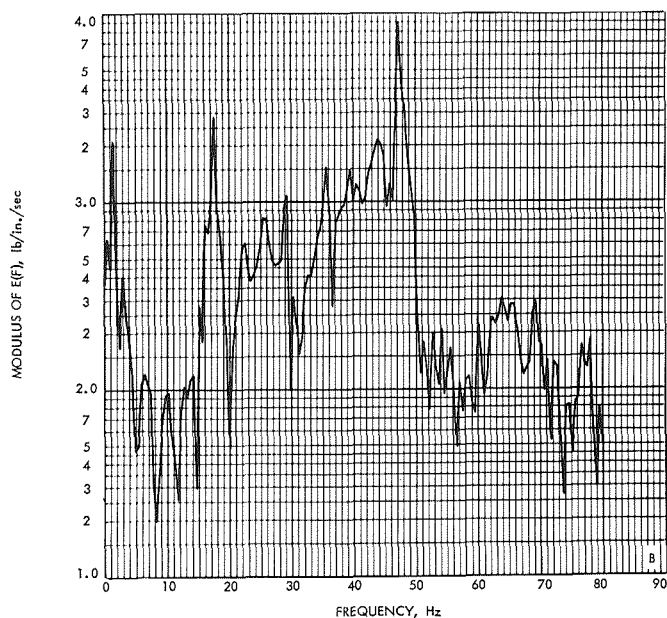
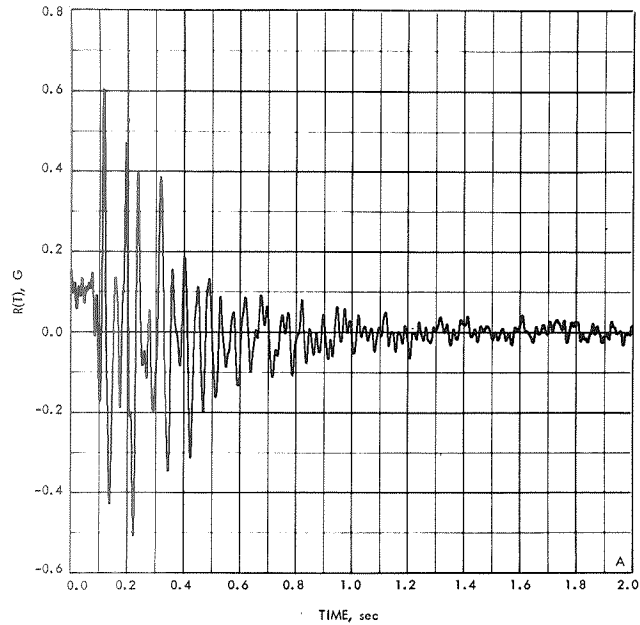


Fig. 25. Gridpoint 12, Mariner Mars '71 reaction moment in θ_z -direction at base of Centaur adapter predicted from the forcing function derived from Mariner VII (AC-19) MECO flight data



- A. VIKING ACCELERATION RESPONSE, TIME HISTORY
- B. VIKING ACCELERATION RESPONSE, FOURIER TRANSFORM
- C. VIKING ACCELERATION RESPONSE, FOURIER TRANSFORM, PHASE ANGLE

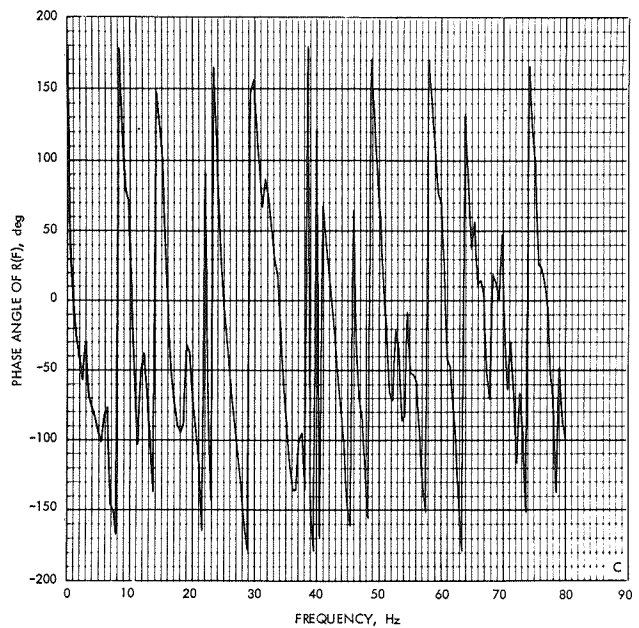
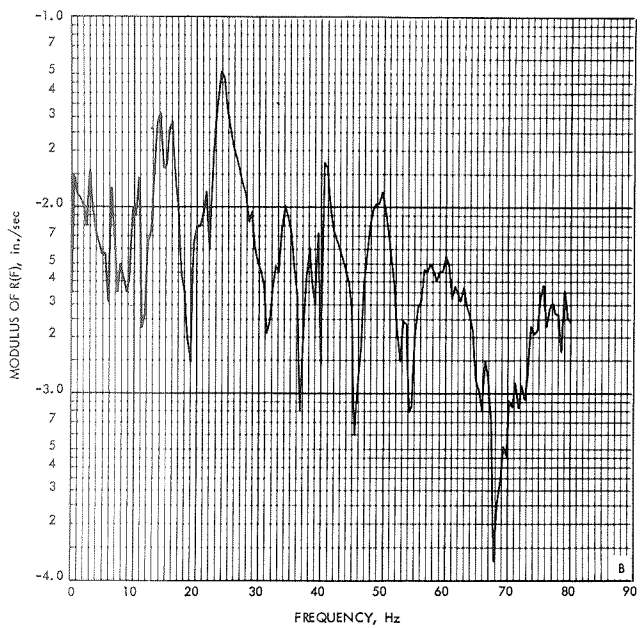
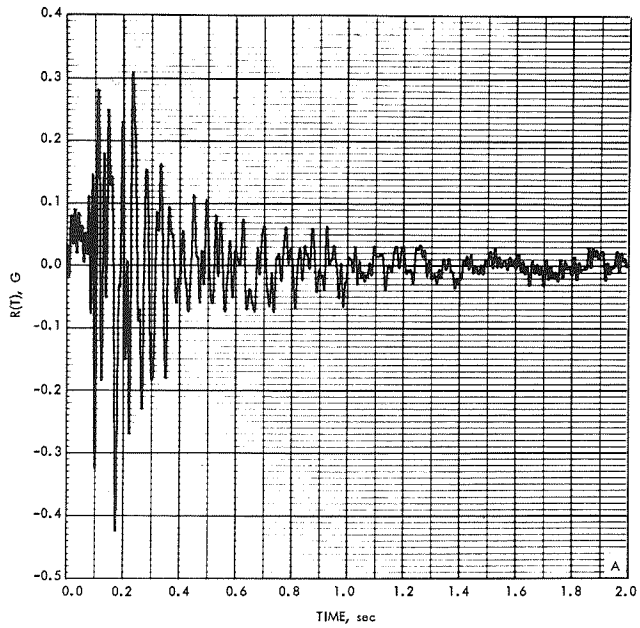


Fig. 26. Gridpoint 8, Viking acceleration response in X-direction at base of Viking truss adapter predicted from the forcing function derived from Mariner VI (AC-20) MECO flight data



- A. VIKING ACCELERATION RESPONSE, TIME HISTORY
- B. VIKING ACCELERATION RESPONSE, FOURIER TRANSFORM
- C. VIKING ACCELERATION RESPONSE, FOURIER TRANSFORM, PHASE ANGLE

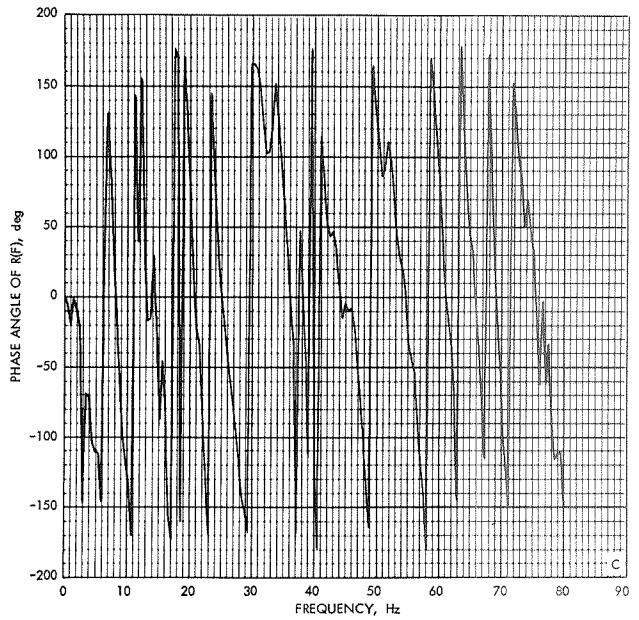
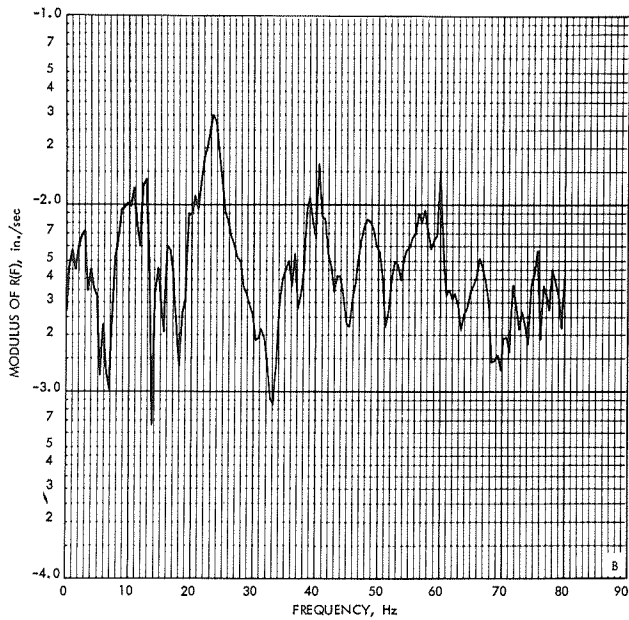
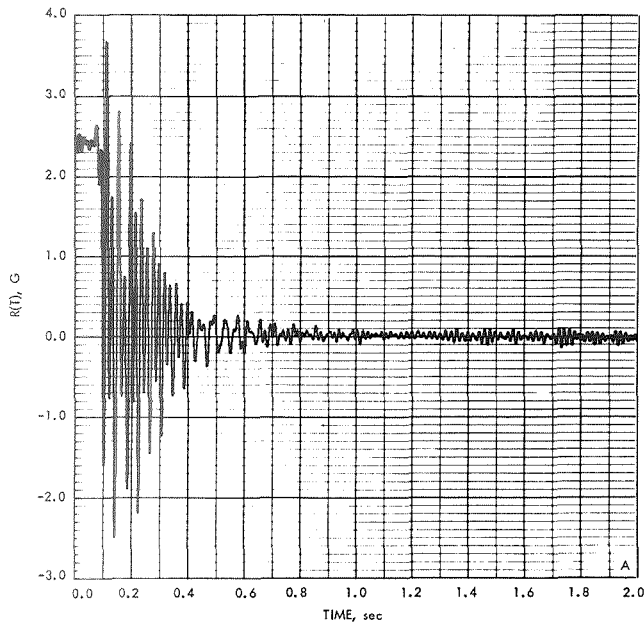


Fig. 27. Gridpoint 8, Viking acceleration response in Y-direction at base of Viking truss adapter predicted from the forcing function derived from Mariner VI (AC-20) MECO flight data



- A. VIKING ACCELERATION RESPONSE, TIME HISTORY
- B. VIKING ACCELERATION RESPONSE, FOURIER TRANSFORM
- C. VIKING ACCELERATION RESPONSE, FOURIER TRANSFORM, PHASE ANGLE

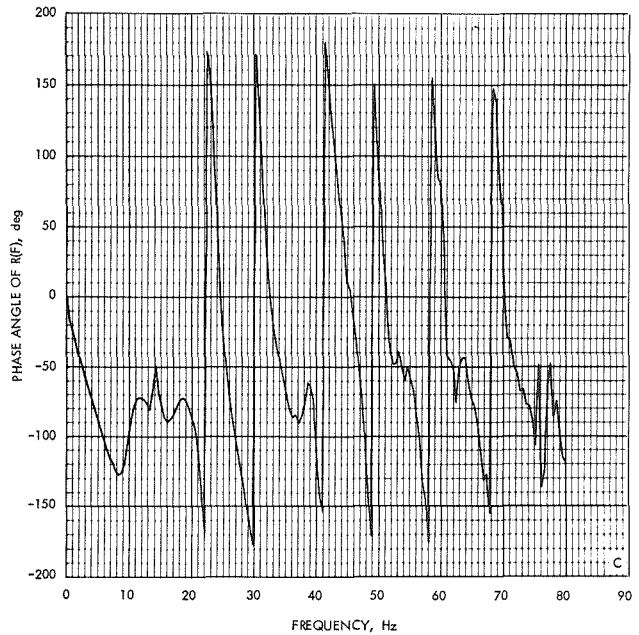
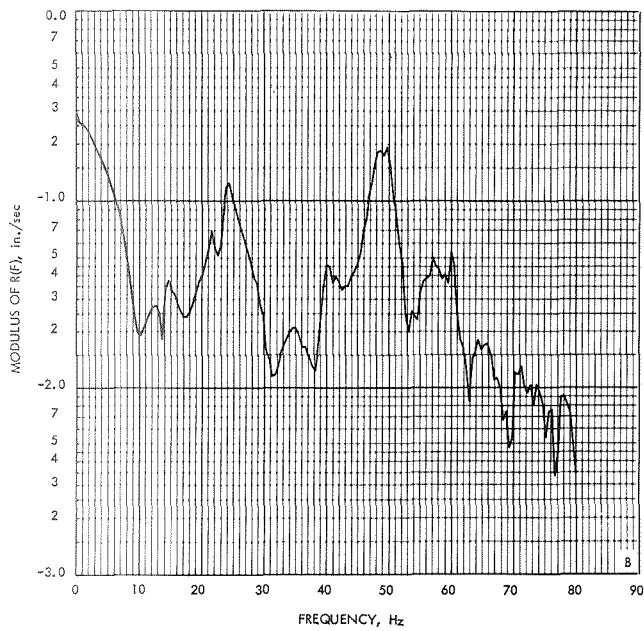
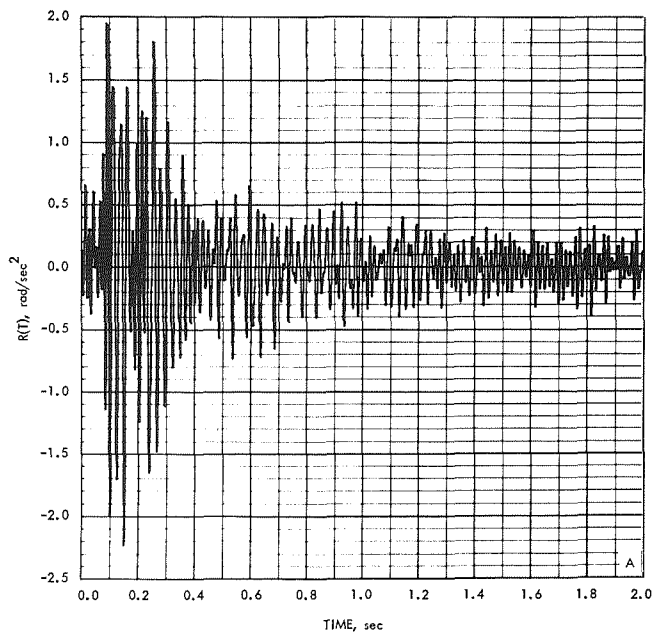


Fig. 28. Gridpoint 8, Viking acceleration response in Z-direction at base of Viking truss adapter predicted from the forcing function derived from Mariner VI (AC-20) MECO flight data



- A. VIKING ROTATIONAL RESPONSE, TIME HISTORY
- B. VIKING ROTATIONAL RESPONSE, FOURIER TRANSFORM
- C. VIKING ROTATIONAL RESPONSE, FOURIER TRANSFORM, PHASE ANGLE

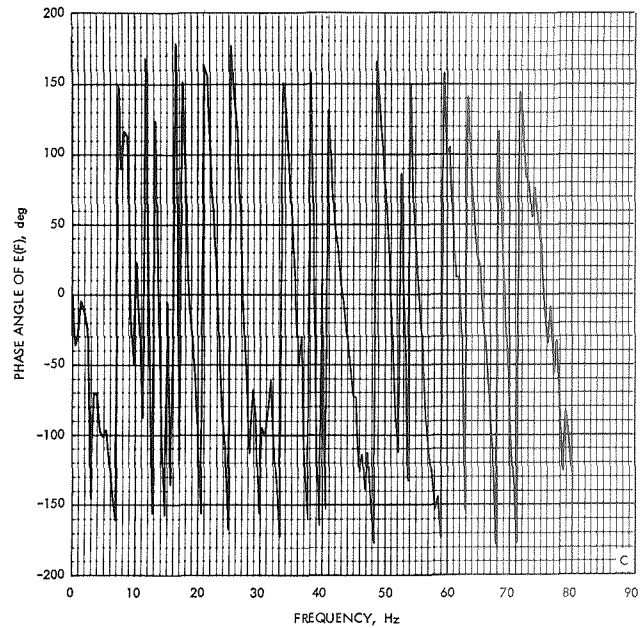
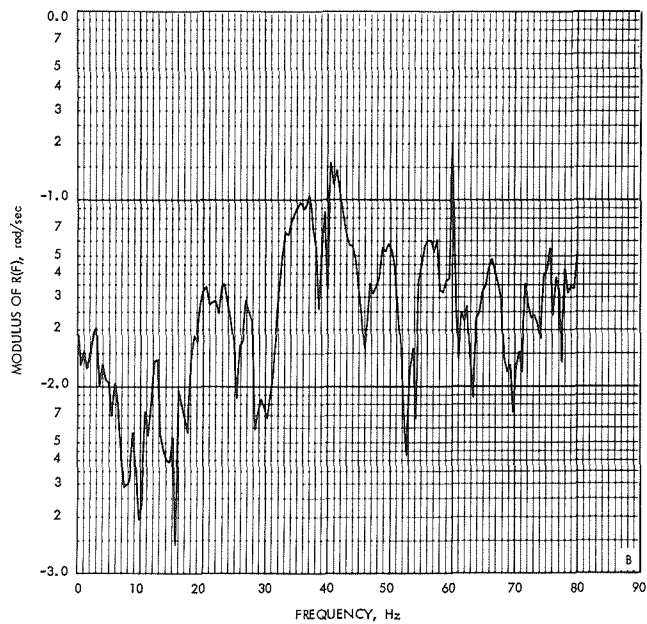
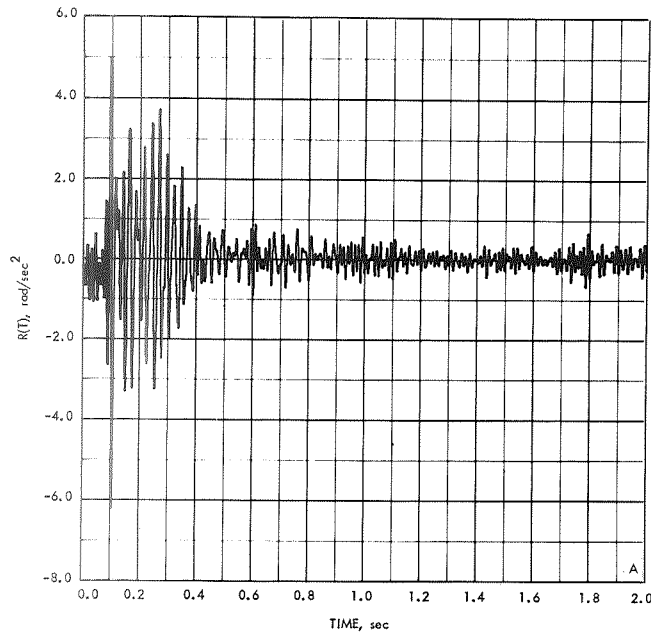


Fig. 29. Gridpoint 8, Viking rotational acceleration response in θ_x -direction at base of Viking truss adapter predicted from the forcing function derived from Mariner VI (AC-20) MECO flight data



- A. VIKING ROTATIONAL RESPONSE, TIME HISTORY
- B. VIKING ROTATIONAL RESPONSE, FOURIER TRANSFORM
- C. VIKING ROTATIONAL RESPONSE, FOURIER TRANSFORM, PHASE ANGLE

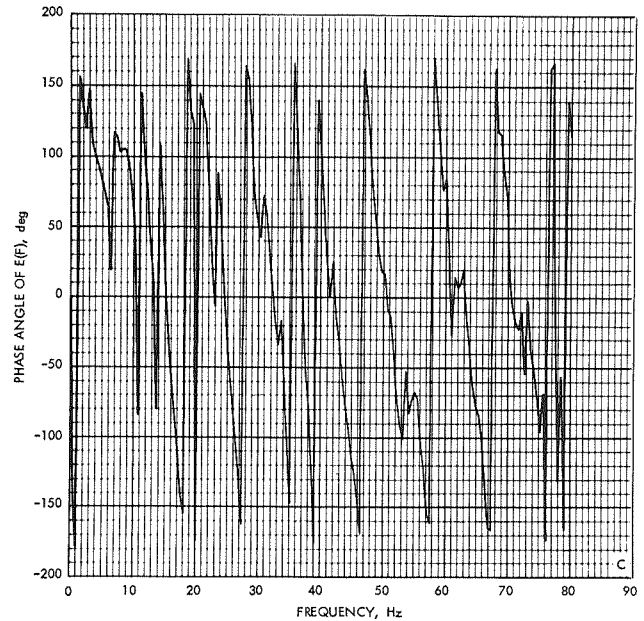
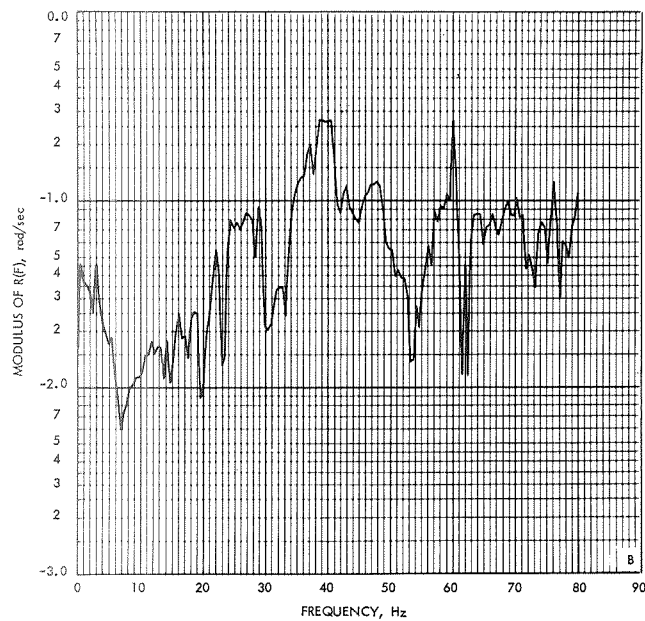
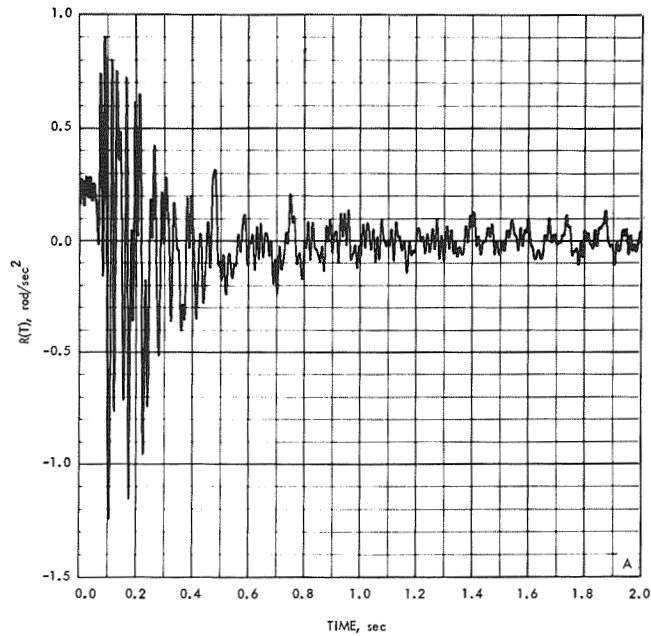


Fig. 30. Gridpoint 8, Viking rotational acceleration response in θ_y -direction at base of Viking truss adapter predicted from the forcing function derived from Mariner VI (AC-20) MECO flight data



- A. VIKING TORSIONAL RESPONSE, TIME HISTORY
- B. VIKING TORSIONAL RESPONSE, FOURIER TRANSFORM
- C. VIKING TORSIONAL RESPONSE, FOURIER TRANSFORM, PHASE ANGLE

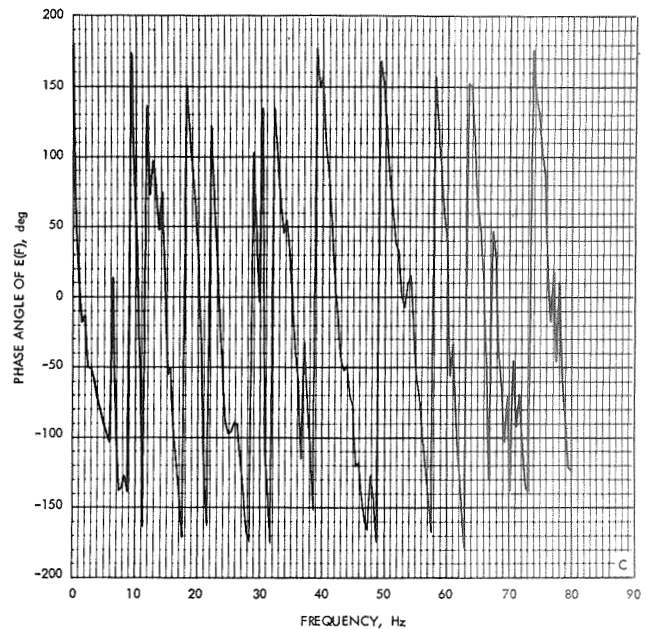
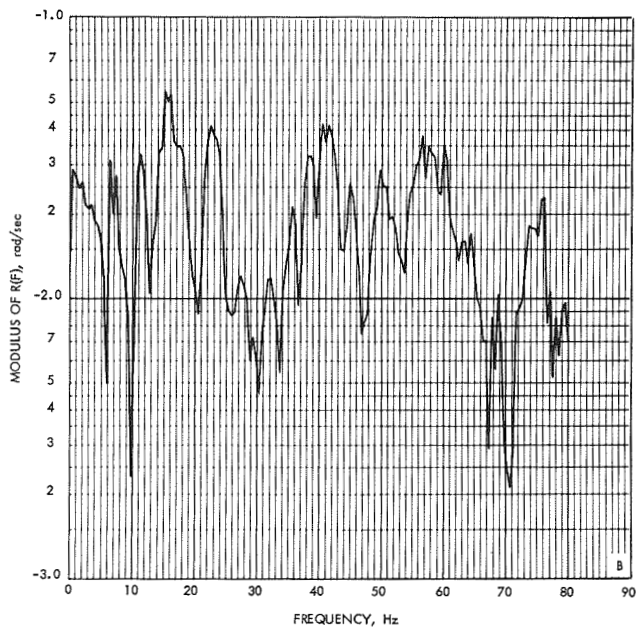
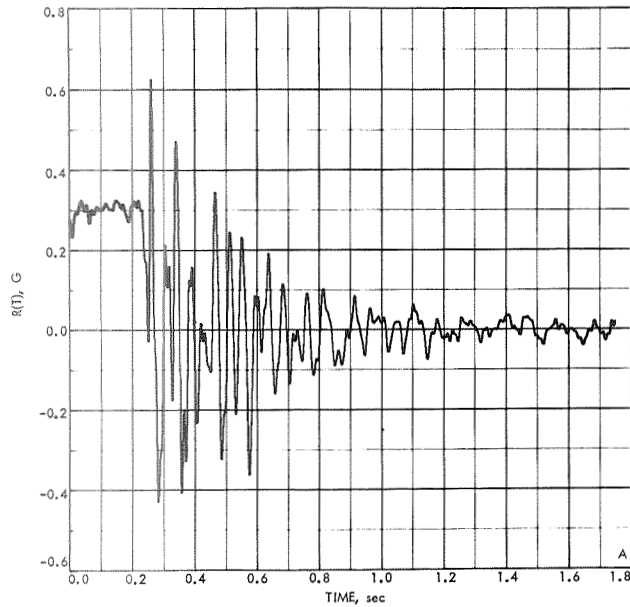


Fig. 31. Gridpoint 8, Viking torsional acceleration response in θ_z -direction at base of Viking truss adapter predicted from the forcing function derived from Mariner VI (AC-20) MECO flight data



- A. VIKING ACCELERATION RESPONSE, TIME HISTORY
- B. VIKING ACCELERATION RESPONSE, FOURIER TRANSFORM
- C. VIKING ACCELERATION RESPONSE, FOURIER TRANSFORM, PHASE ANGLE

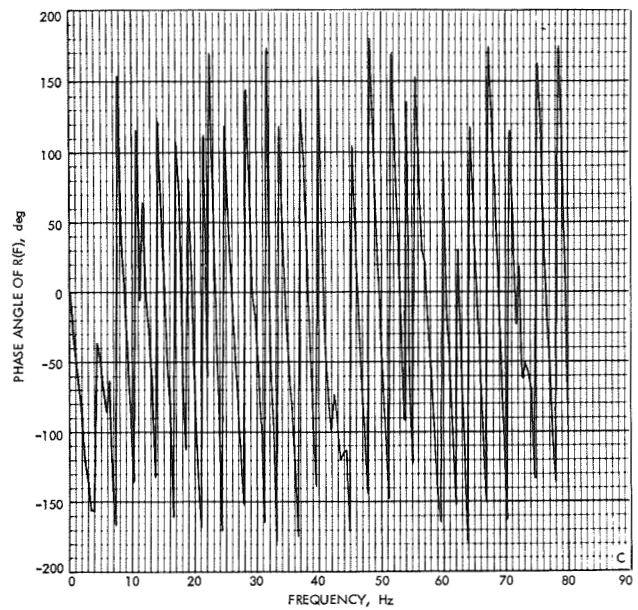
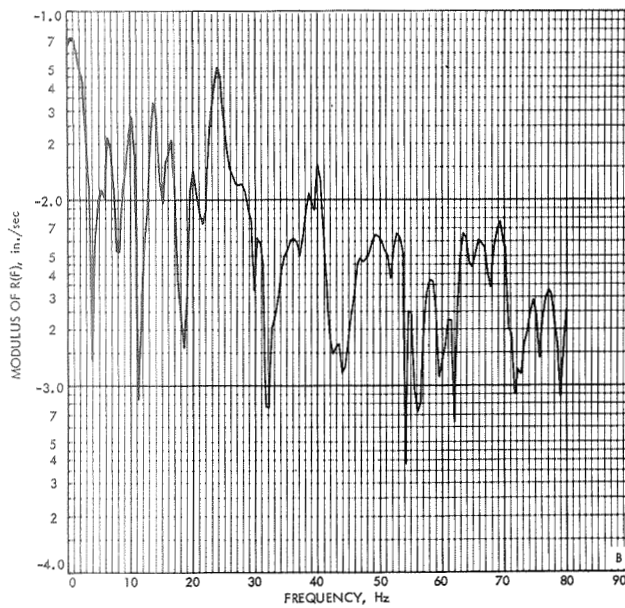
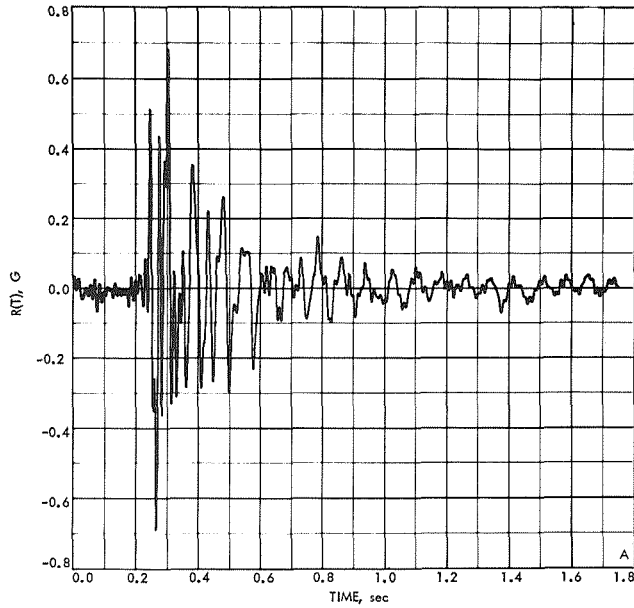


Fig. 32. Gridpoint 8, Viking acceleration response in X-direction at base of Viking truss adapter predicted from the forcing function derived from Mariner VII (AC-19) MECO flight data



- A. VIKING ACCELERATION RESPONSE, TIME HISTORY
- B. VIKING ACCELERATION RESPONSE, FOURIER TRANSFORM
- C. VIKING ACCELERATION RESPONSE, FOURIER TRANSFORM, PHASE ANGLE

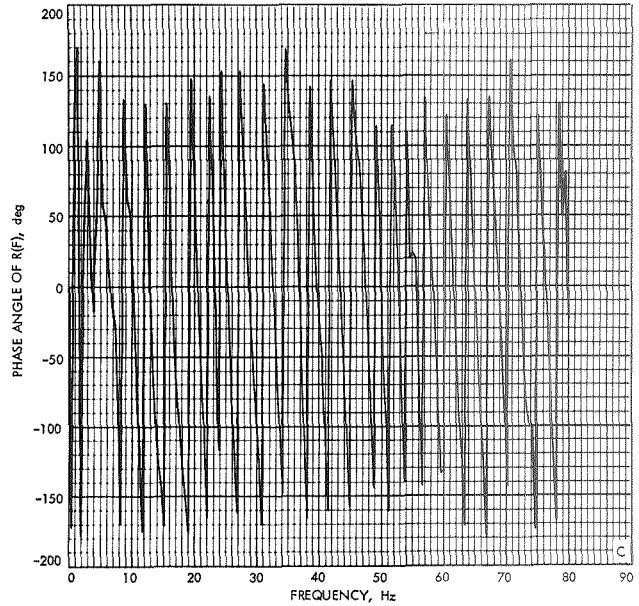
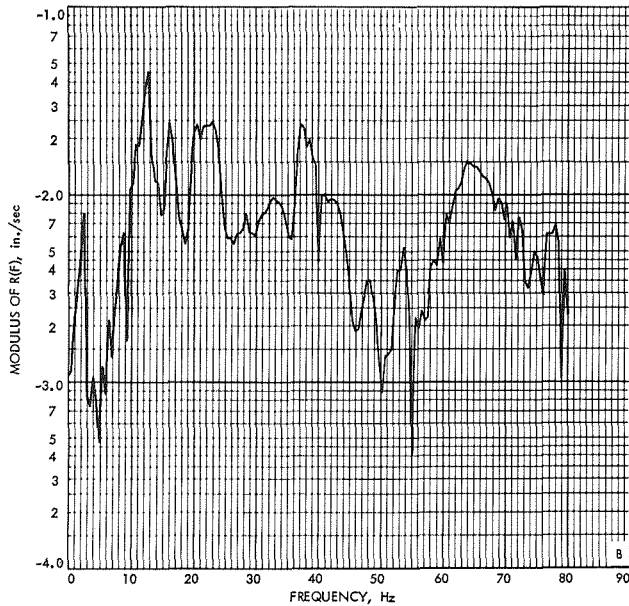
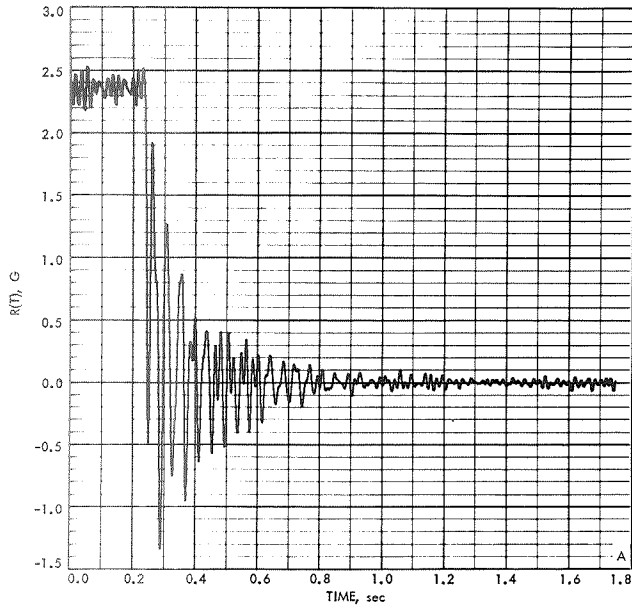


Fig. 33. Gridpoint 8, Viking acceleration response in Y-direction at base of Viking truss adapter predicted from the forcing function derived from Mariner VII (AC-19) MECO flight data



- A. VIKING ACCELERATION RESPONSE, TIME HISTORY
- B. VIKING ACCELERATION RESPONSE, FOURIER TRANSFORM
- C. VIKING ACCELERATION RESPONSE, FOURIER TRANSFORM, PHASE ANGLE

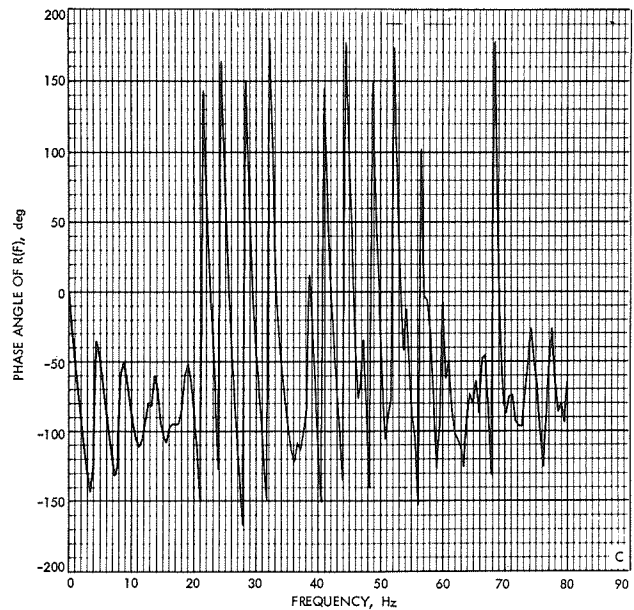
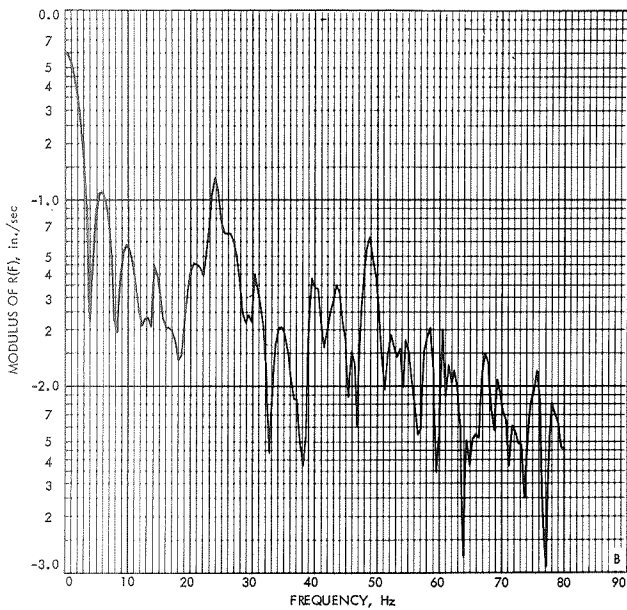
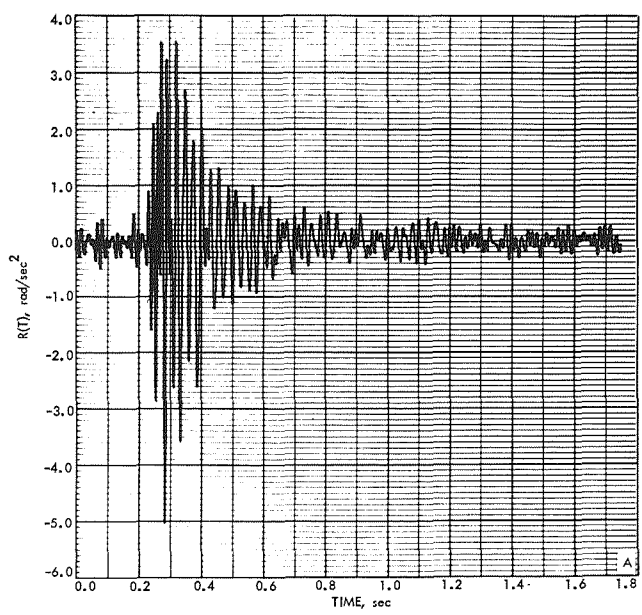


Fig. 34. Gridpoint 8, Viking acceleration response in Z-direction at base of Viking truss adapter predicted from the forcing function derived from Mariner VII (AC-19) MECO flight data



- A. VIKING ROTATIONAL RESPONSE, TIME HISTORY
- B. VIKING ROTATIONAL RESPONSE, FOURIER TRANSFORM
- C. VIKING ROTATIONAL RESPONSE, FOURIER TRANSFORM, PHASE ANGLE

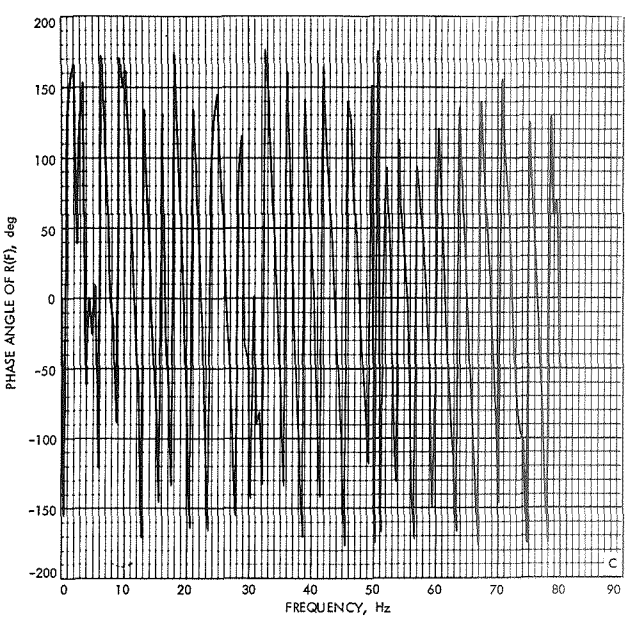
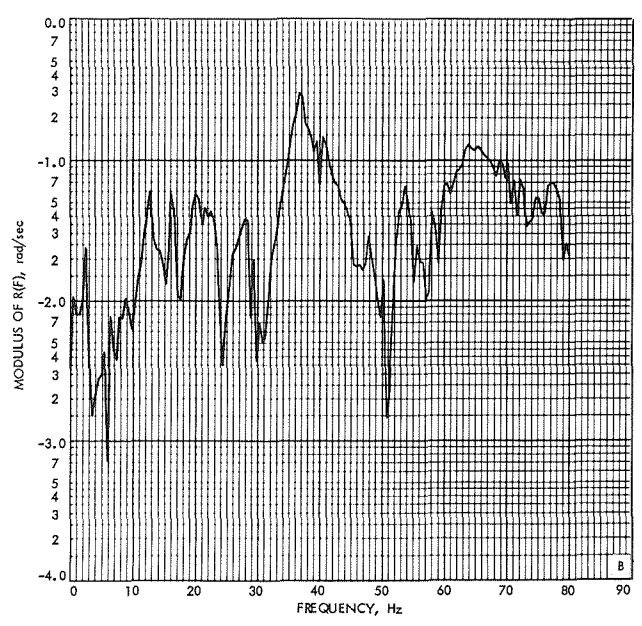
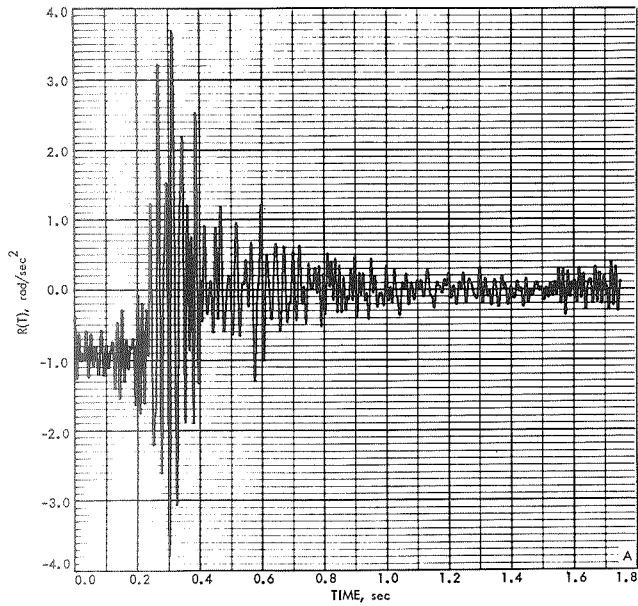


Fig. 35. Gridpoint 8, Viking rotational acceleration response in θ_x -direction at base of Viking truss adapter predicted from the forcing function derived from Mariner VII (AC-19) MECO flight data



- A. VIKING ROTATIONAL RESPONSE, TIME HISTORY
- B. VIKING ROTATIONAL RESPONSE, FOURIER TRANSFORM
- C. VIKING ROTATIONAL RESPONSE, FOURIER TRANSFORM, PHASE ANGLE

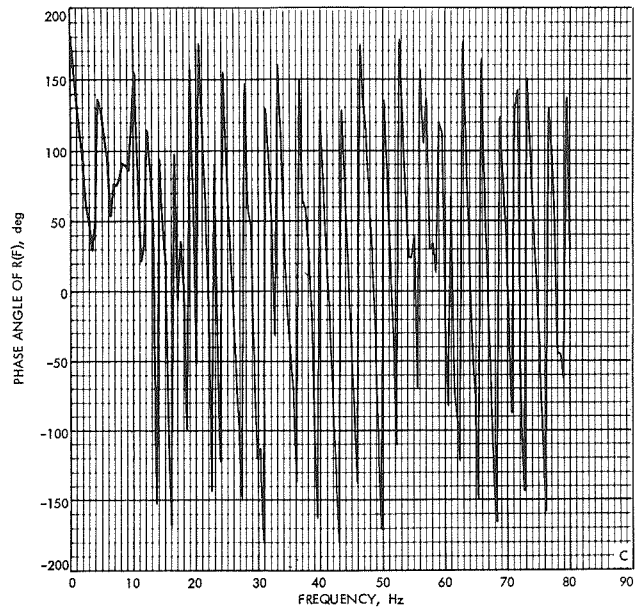
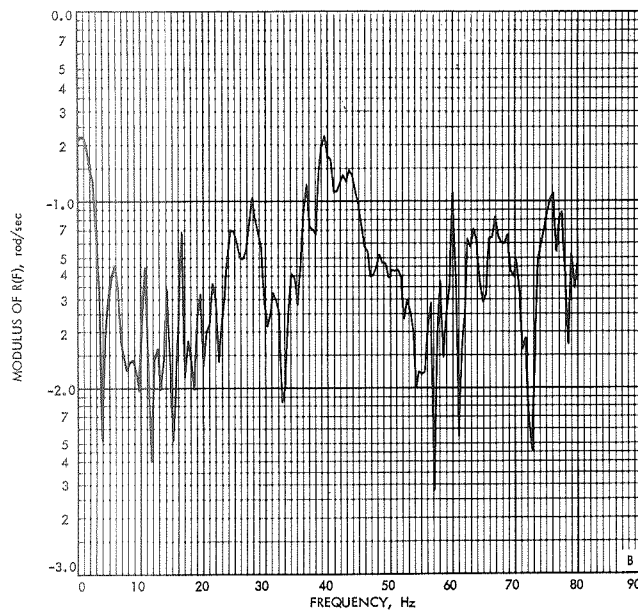
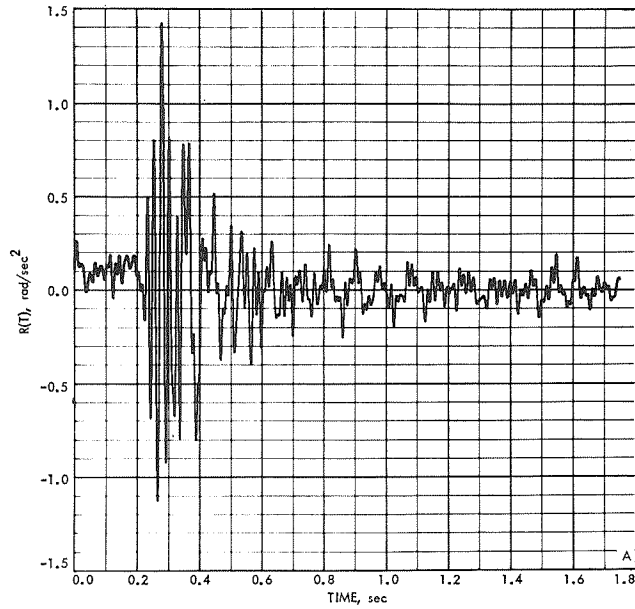


Fig. 36. Gridpoint 8, Viking rotational acceleration response in θ_y -direction at base of Viking truss adapter predicted from the forcing function derived from Mariner VII (AC-19) MECO flight data



- A. VIKING TORSIONAL RESPONSE, TIME HISTORY
- B. VIKING TORSIONAL RESPONSE, FOURIER TRANSFORM
- C. VIKING TORSIONAL RESPONSE, FOURIER TRANSFORM, PHASE ANGLE

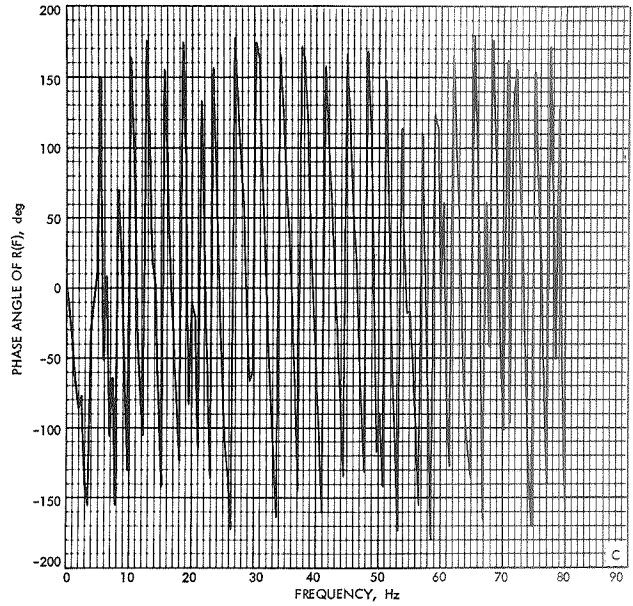
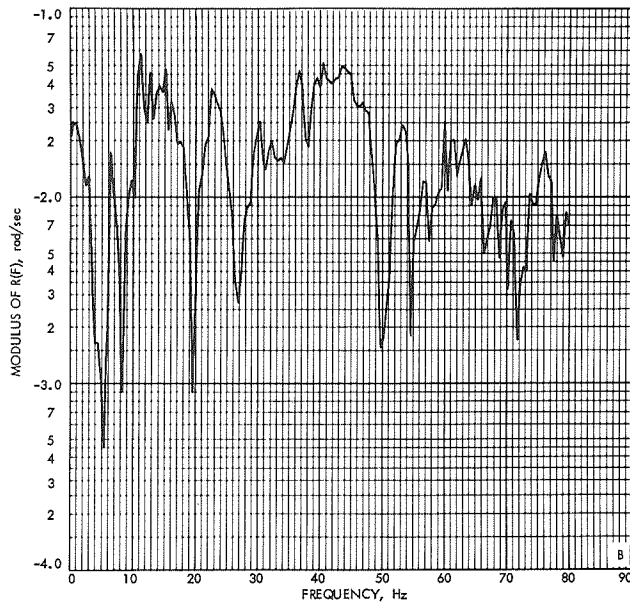
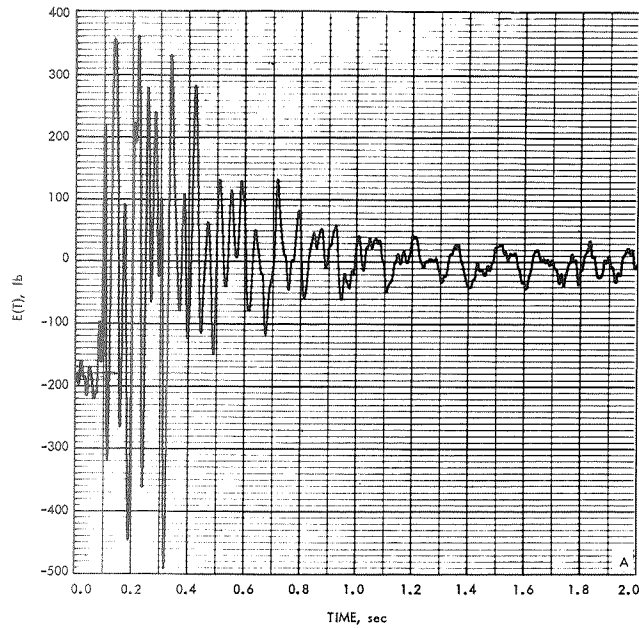


Fig. 37. Gridpoint 8, Viking torsional acceleration response in θ_z -direction at base of Viking truss adapter predicted from the forcing function derived from Mariner VII (AC-19) MECO flight data



- A. SEPARATION PLANE FORCE, TIME HISTORY
- B. SEPARATION PLANE FORCE, FOURIER TRANSFORM, MODULUS
- C. SEPARATION PLANE FORCE, FOURIER TRANSFORM, PHASE ANGLE

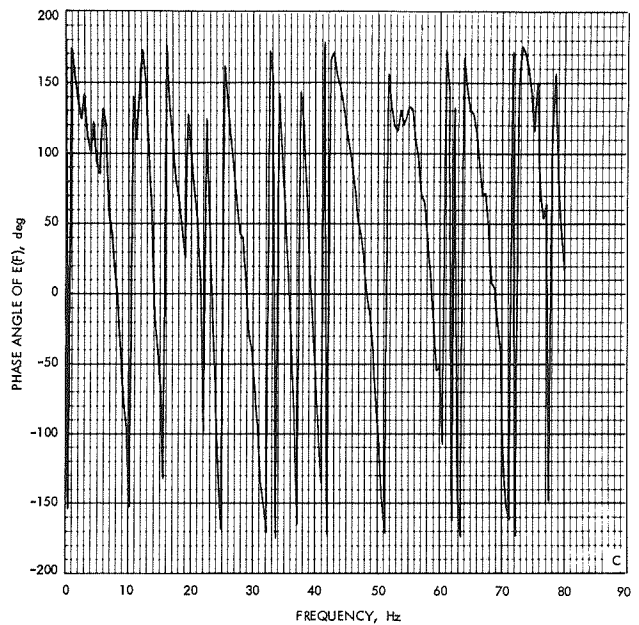
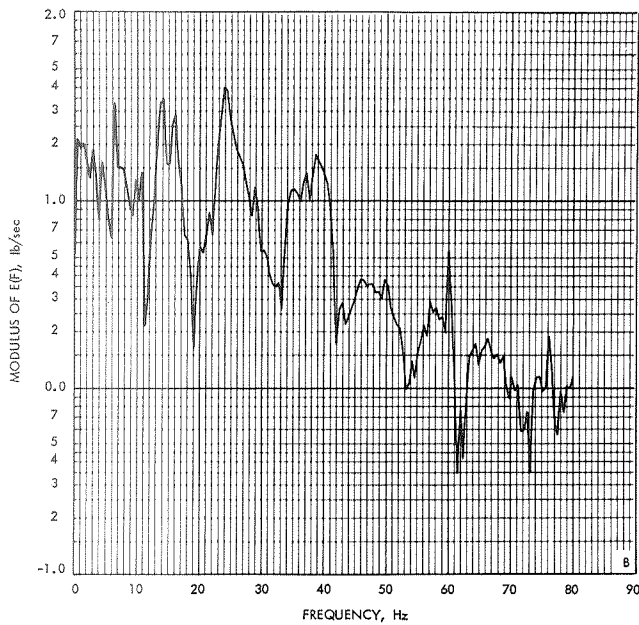
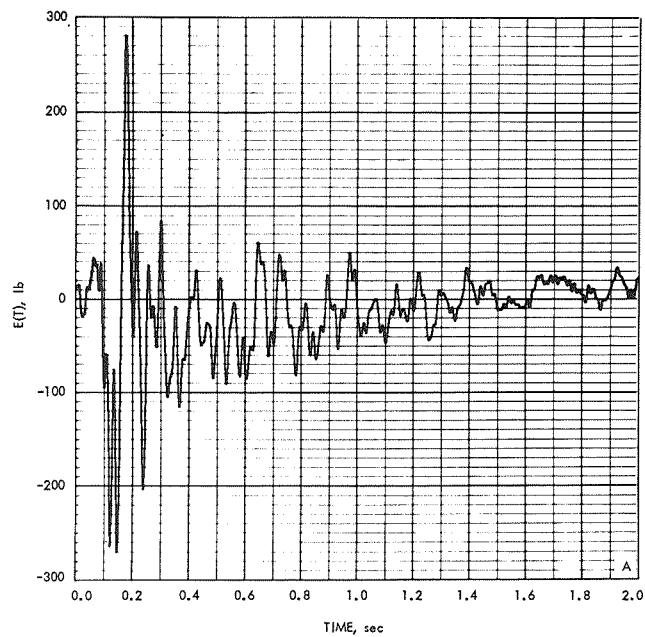


Fig. 38. Gridpoint 8, Viking reaction force in X-direction at base of Viking truss adapter predicted from the forcing function derived from Mariner VI (AC-20) MECO flight data



- A. SEPARATION PLANE FORCE, TIME HISTORY
- B. SEPARATION PLANE FORCE, FOURIER TRANSFORM, MODULUS
- C. SEPARATION PLANE FORCE, FOURIER TRANSFORM, PHASE ANGLE

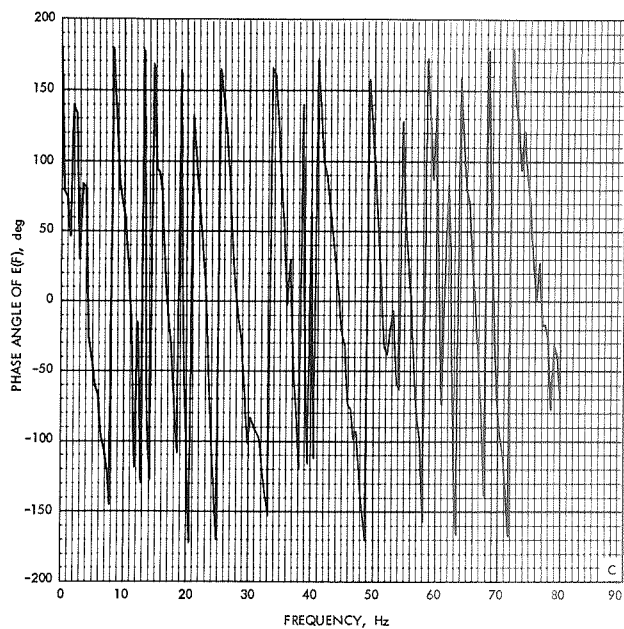
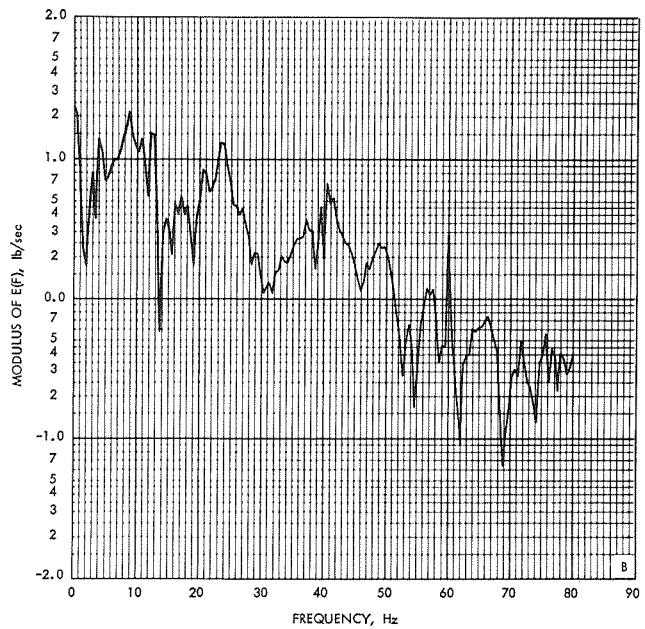
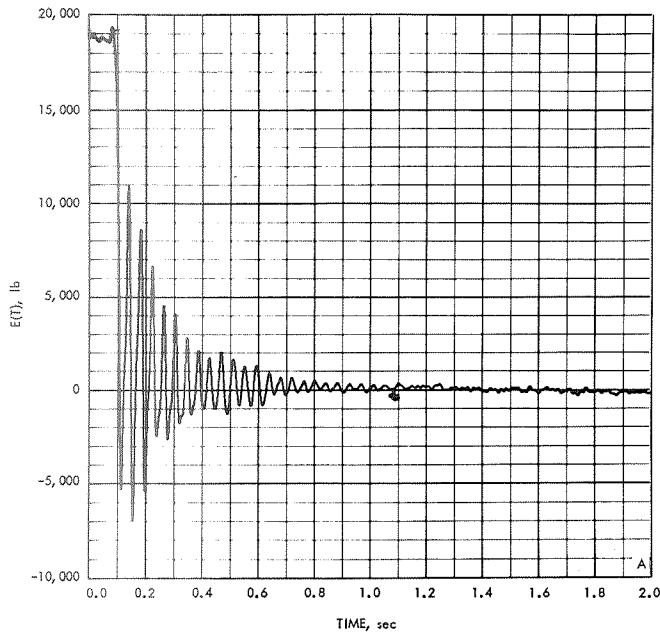


Fig. 39. Gridpoint 8, Viking reaction force in Y-direction at base of Viking truss adapter predicted from the forcing function derived from Mariner VI (AC-20) MECO flight data



- A. SEPARATION PLANE FORCE, TIME HISTORY
- B. SEPARATION PLANE FORCE, FOURIER TRANSFORM, MODULUS
- C. SEPARATION PLANE FORCE, FOURIER TRANSFORM, PHASE ANGLE

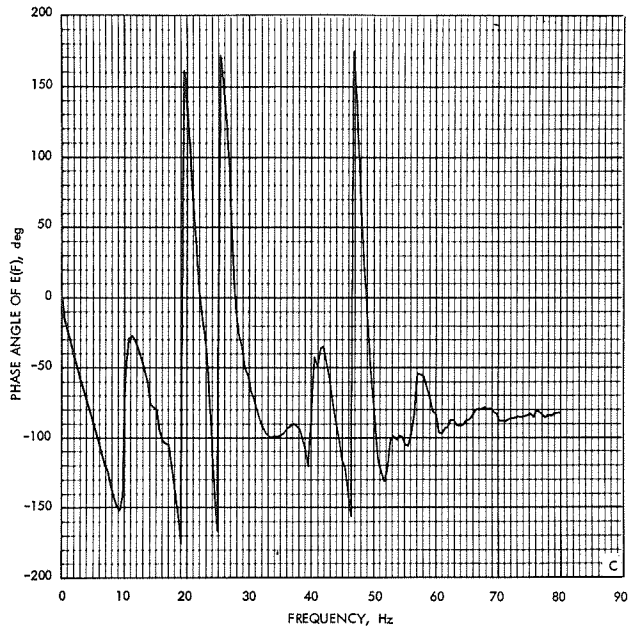
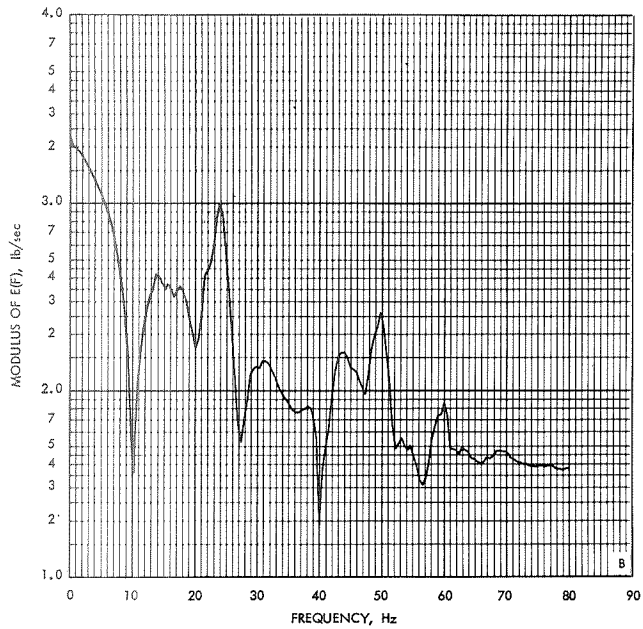
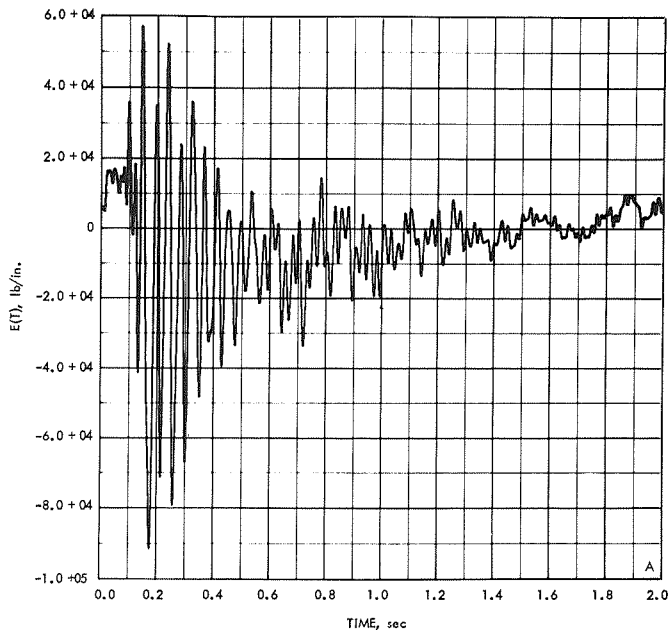


Fig. 40. Gridpoint 8, Viking reaction force in Z-direction at base of Viking truss adapter predicted from the forcing function derived from Mariner VI (AC-20) MECO flight data



- A. SEPARATION PLANE MOMENT, TIME HISTORY
- B. SEPARATION PLANE MOMENT, FOURIER TRANSFORM, MODULUS
- C. SEPARATION PLANE MOMENT, FOURIER TRANSFORM, PHASE ANGLE

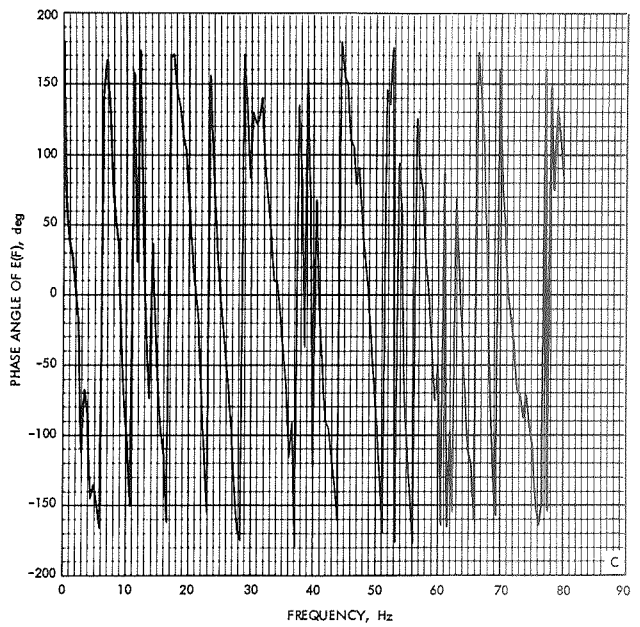
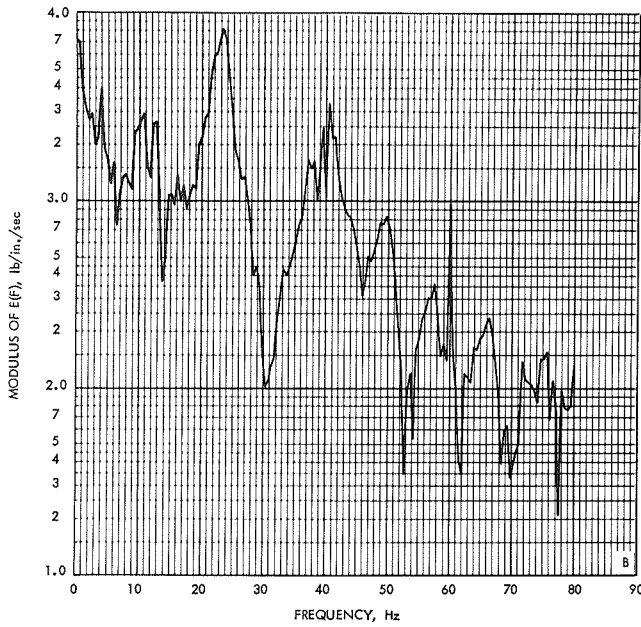
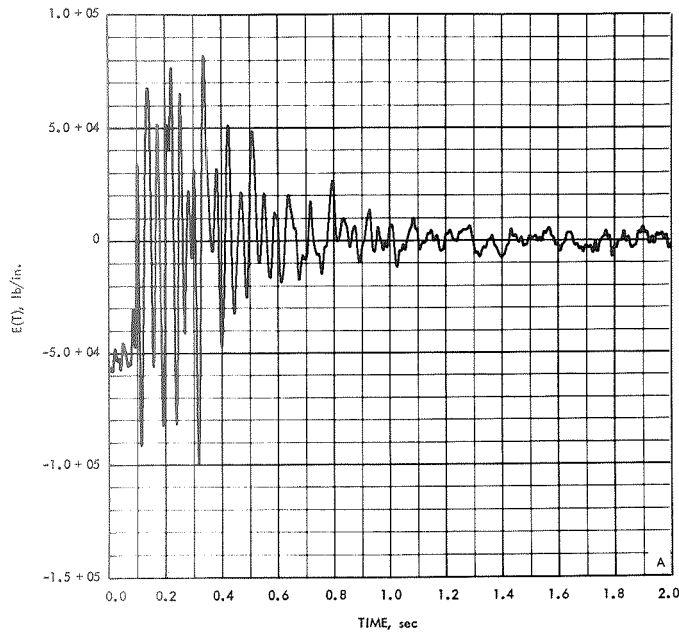


Fig. 41. Gridpoint 8, Viking reaction moment in θ_x -direction at base of Viking truss adapter predicted from the forcing function derived from Mariner VI (AC-20) MECO flight data



- A. SEPARATION PLANE MOMENT, TIME HISTORY
- B. SEPARATION PLANE MOMENT, FOURIER TRANSFORM, MODULUS
- C. SEPARATION PLANE MOMENT, FOURIER TRANSFORM, PHASE ANGLE

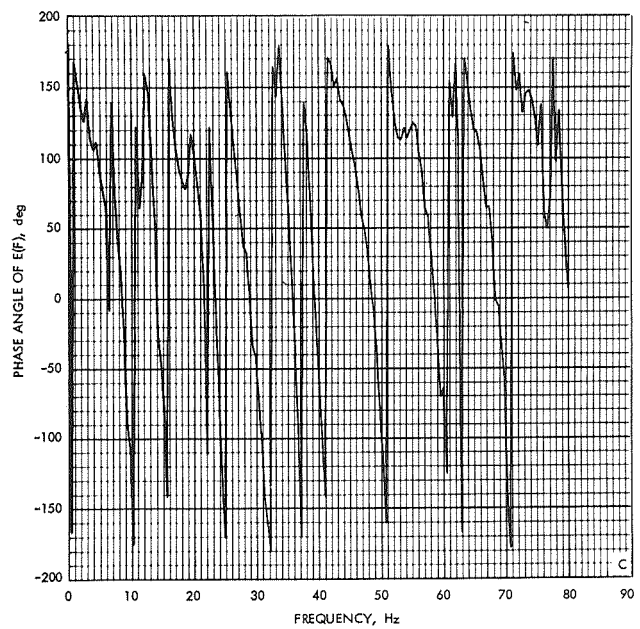
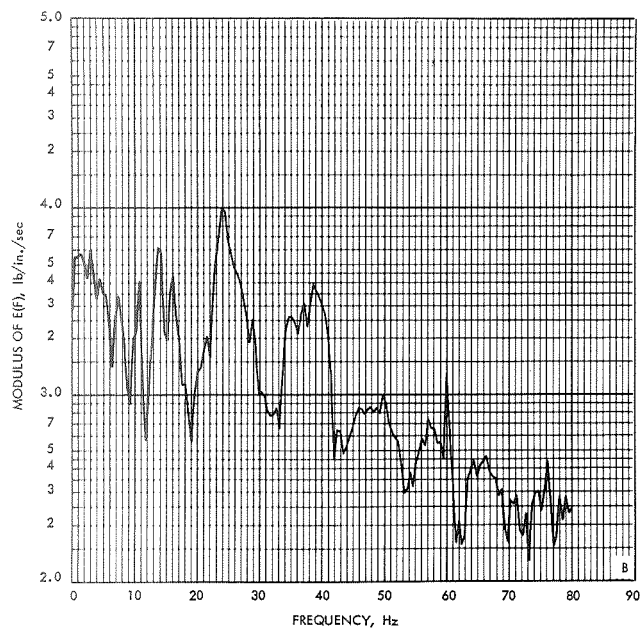


Fig. 42. Gridpoint 8, Viking reaction moment in θ_y -direction at base of Viking truss adapter predicted from the forcing function derived from Mariner VI (AC-20) MECO flight data

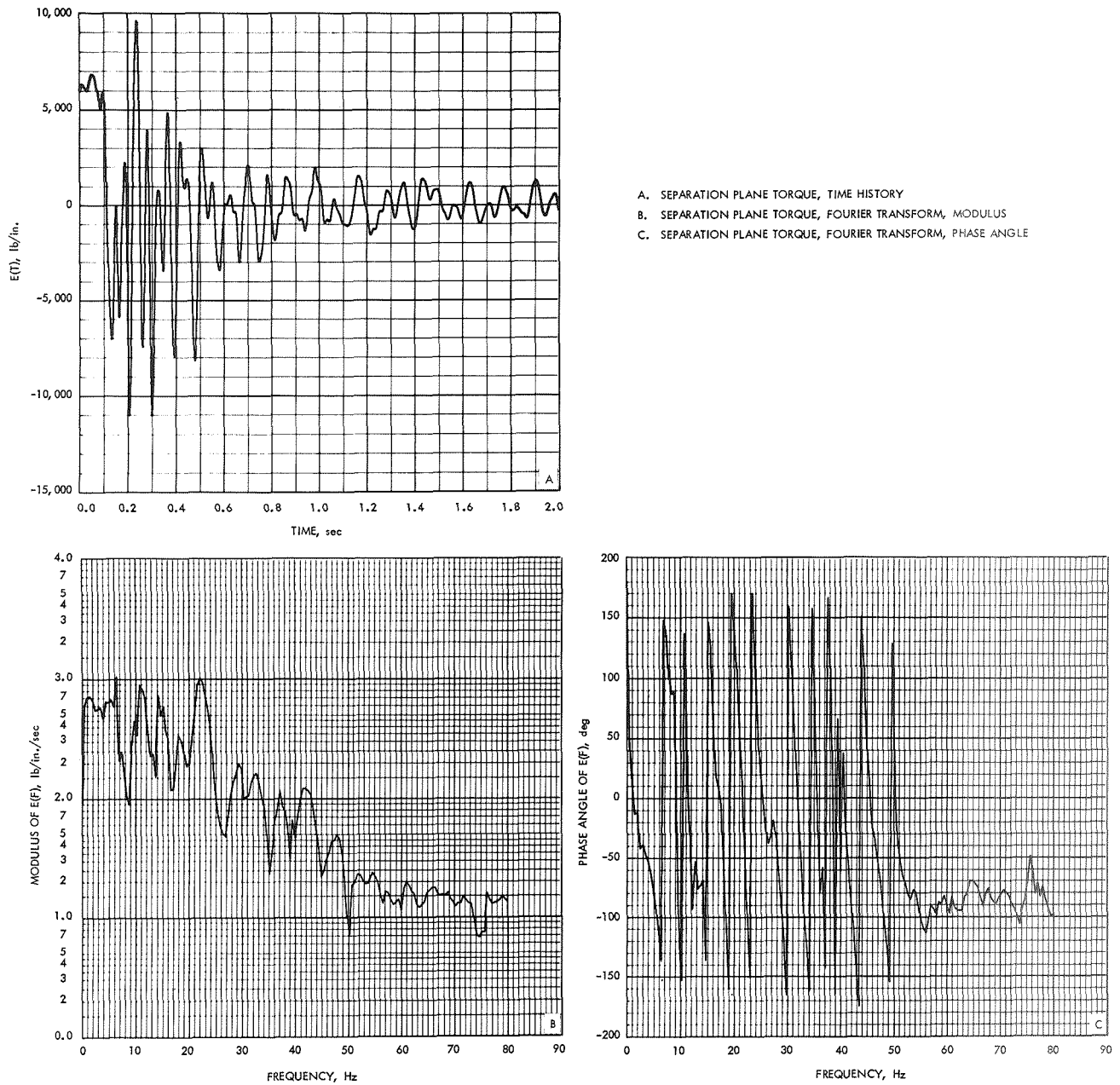
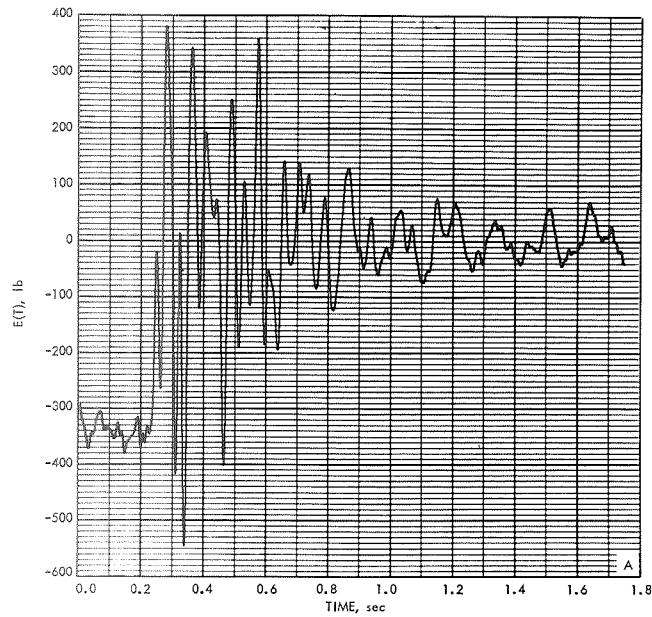


Fig. 43. Gridpoint 8, Viking reaction moment in θ_z -direction at base of Viking truss adapter predicted from the forcing function derived from Mariner VI (AC-20) MECO flight data



- A. SEPARATION PLANE FORCE, TIME HISTORY
- B. SEPARATION PLANE FORCE, FOURIER TRANSFORM, MODULUS
- C. SEPARATION PLANE FORCE, FOURIER TRANSFORM, PHASE ANGLE

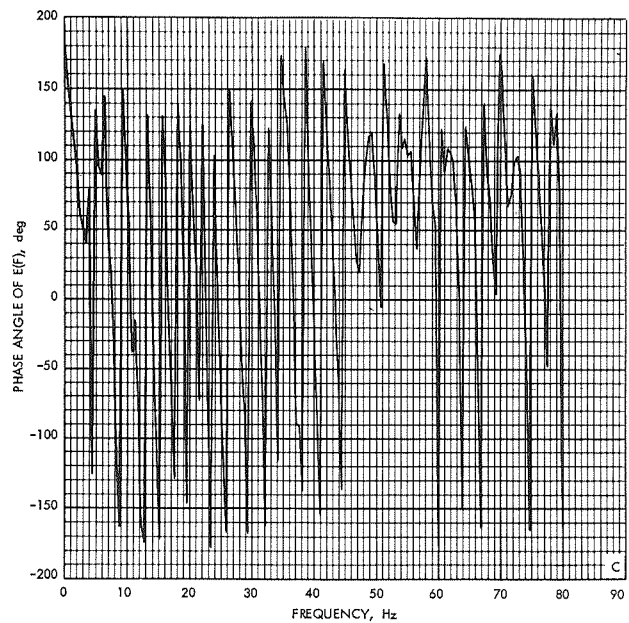
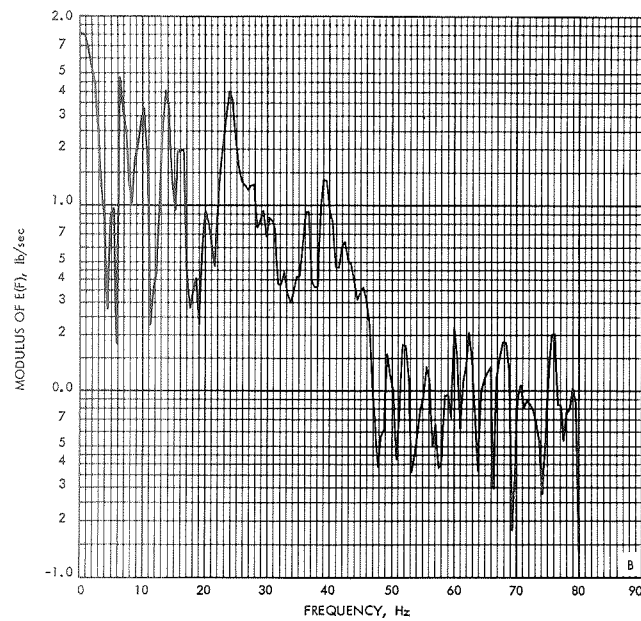
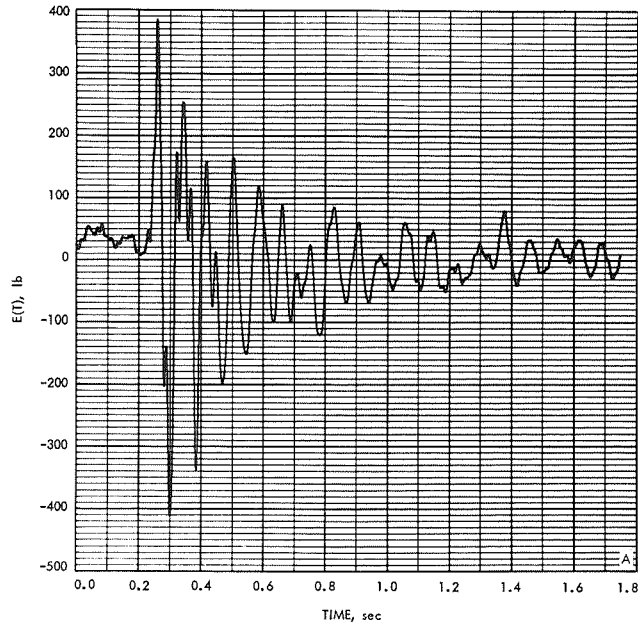


Fig. 44. Gridpoint 8, Viking reaction force in X-direction at base of Viking truss adapter predicted from the forcing function derived from Mariner VII (AC-19) MECO flight data



- A. SEPARATION PLANE FORCE, TIME HISTORY
- B. SEPARATION PLANE FORCE, FOURIER TRANSFORM, MODULUS
- C. SEPARATION PLANE FORCE, FOURIER TRANSFORM, PHASE ANGLE

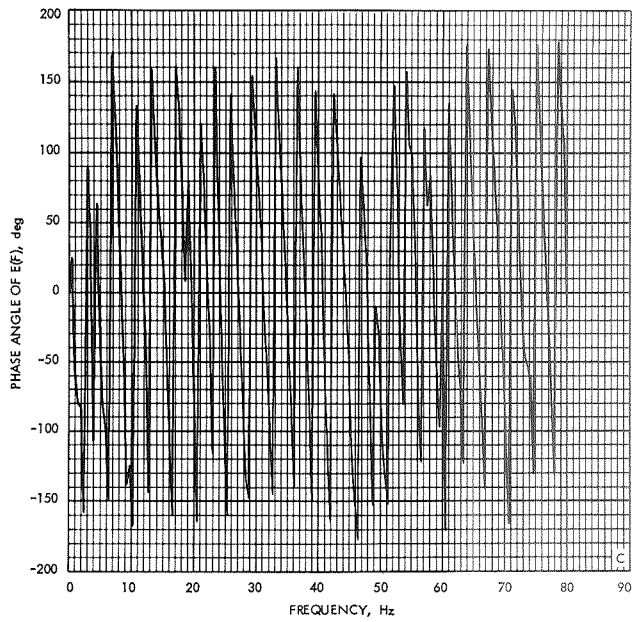
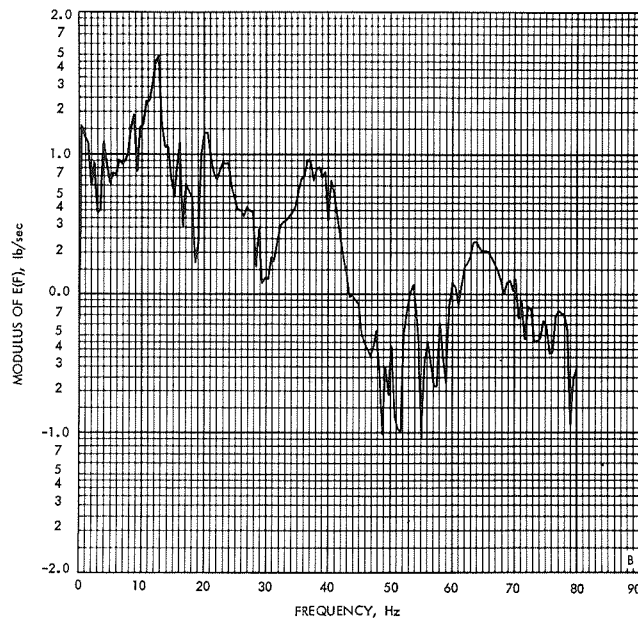
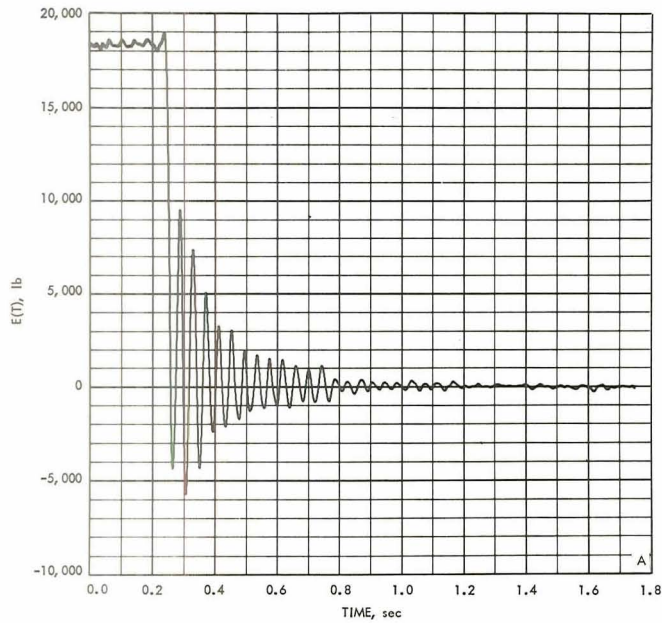


Fig. 45. Gridpoint 8, Viking reaction force in Y-direction at base of Viking truss adapter predicted from the forcing function derived from Mariner VII (AC-19) MECO flight data



- A. SEPARATION PLANE FORCE, TIME HISTORY
- B. SEPARATION PLANE FORCE, FOURIER TRANSFORM, MODULUS
- C. SEPARATION PLANE FORCE, FOURIER TRANSFORM, PHASE ANGLE

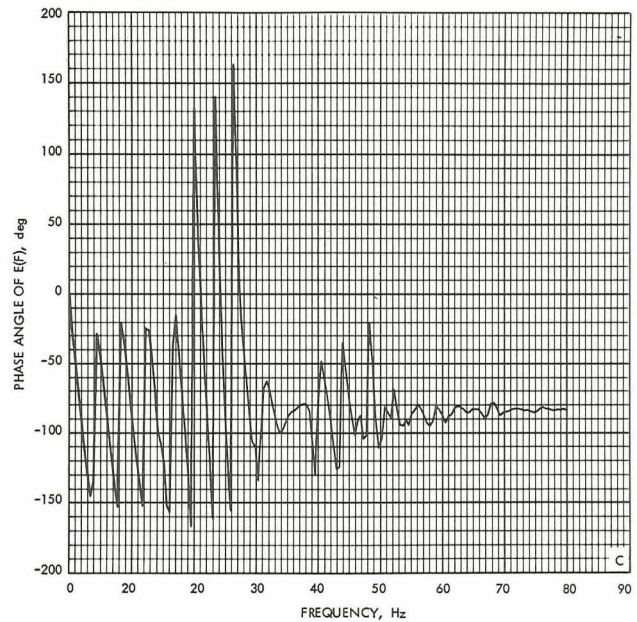
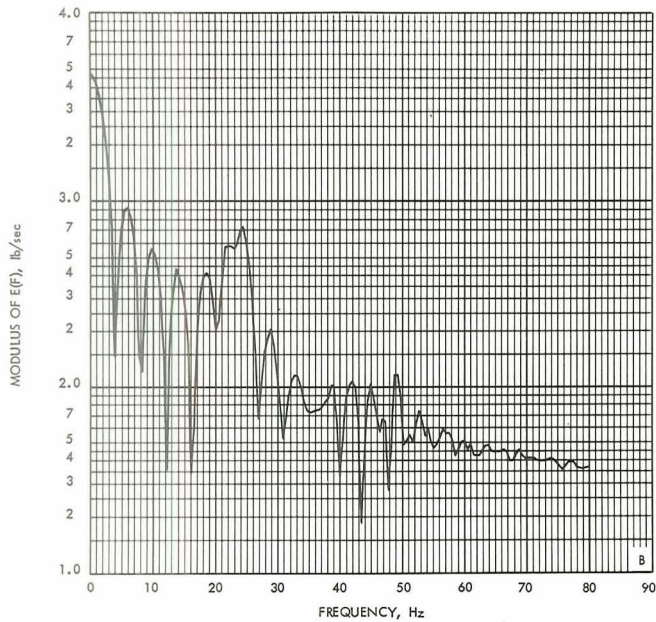
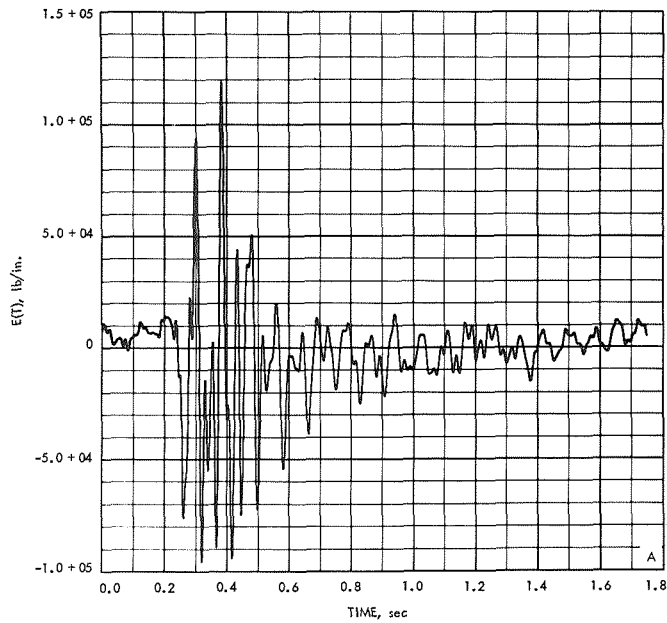


Fig. 46. Gridpoint 8, Viking reaction force in Z-direction at base of Viking truss adapter predicted from the forcing function derived from Mariner VII (AC-19) MECO flight data



- A. SEPARATION PLANE MOMENT, TIME HISTORY
- B. SEPARATION PLANE MOMENT, FOURIER TRANSFORM, MODULUS
- C. SEPARATION PLANE MOMENT, FOURIER TRANSFORM, PHASE ANGLE

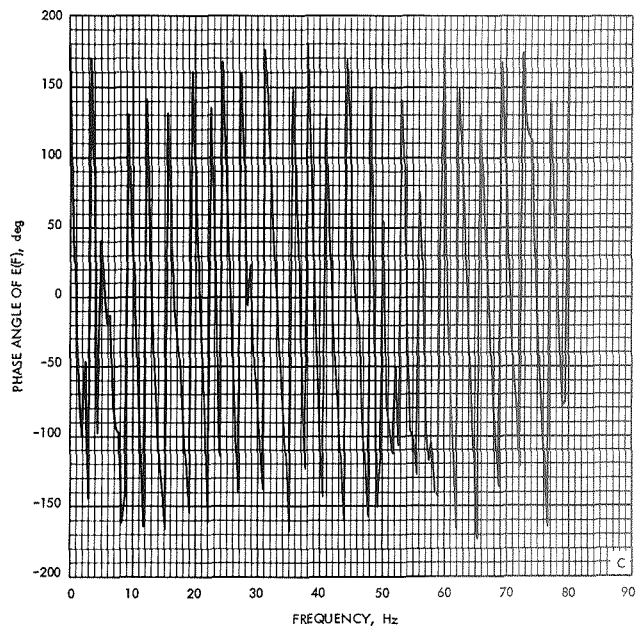
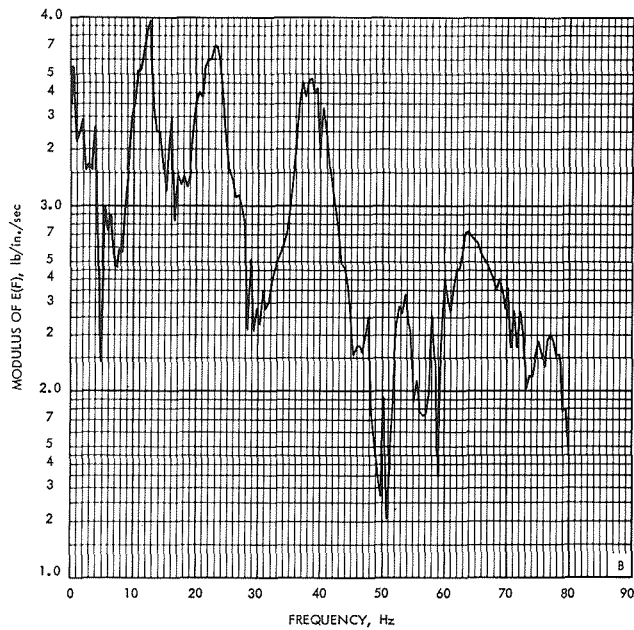
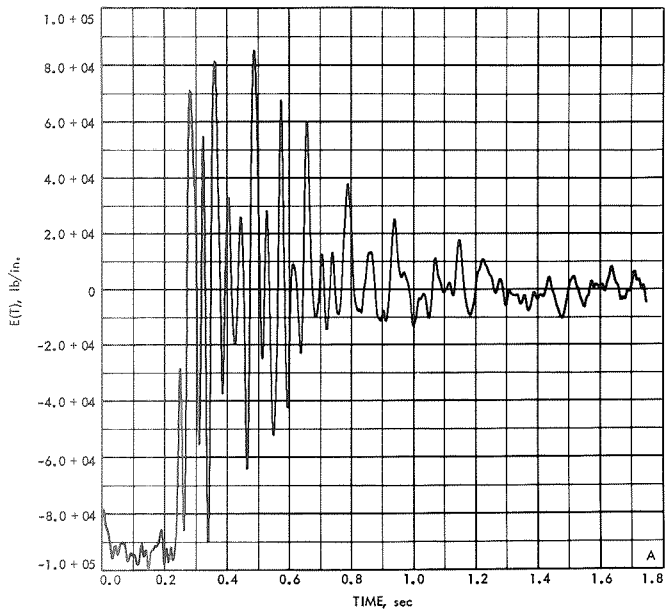


Fig. 47. Gridpoint 8, Viking reaction moment in θ_x -direction at base of Viking truss adapter predicted from the forcing function derived from Mariner VII (AC-19) MECO flight data



- A. SEPARATION PLANE MOMENT, TIME HISTORY
- B. SEPARATION PLANE MOMENT, FOURIER TRANSFORM, MODULUS
- C. SEPARATION PLANE MOMENT, FOURIER TRANSFORM, PHASE ANGLE

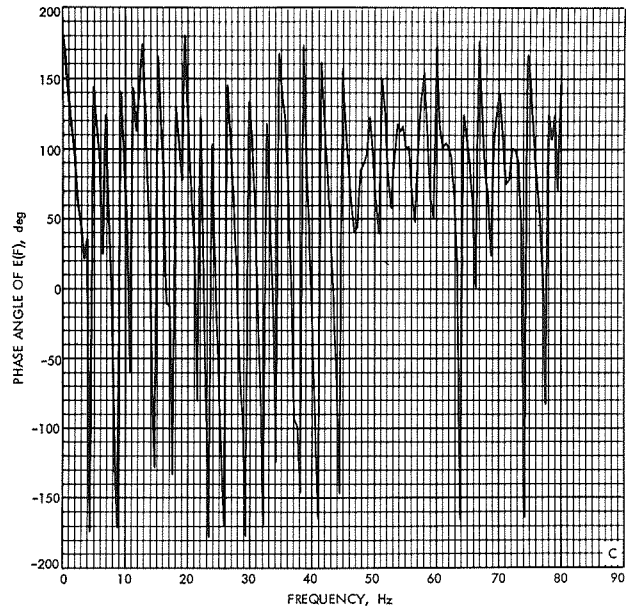
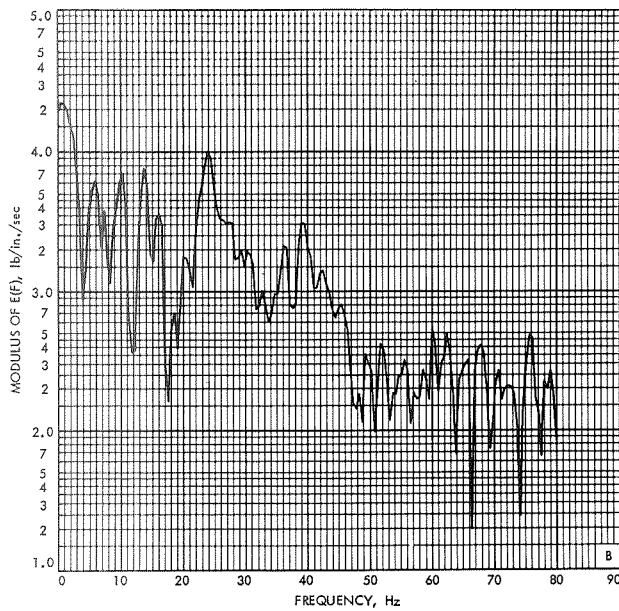
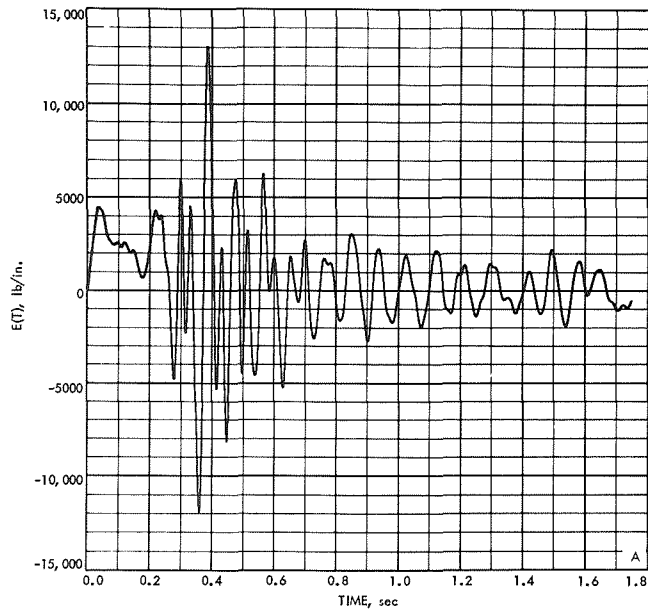


Fig. 48. Gridpoint 8, Viking reaction moment in θ_y -direction at base of Viking truss adapter predicted from the forcing function derived from Mariner VII (AC-19) MECO flight data



- A. SEPARATION PLANE TORQUE, TIME HISTORY
- B. SEPARATION PLANE TORQUE, FOURIER TRANSFORM, MODULUS
- C. SEPARATION PLANE TORQUE, FOURIER TRANSFORM, PHASE ANGLE

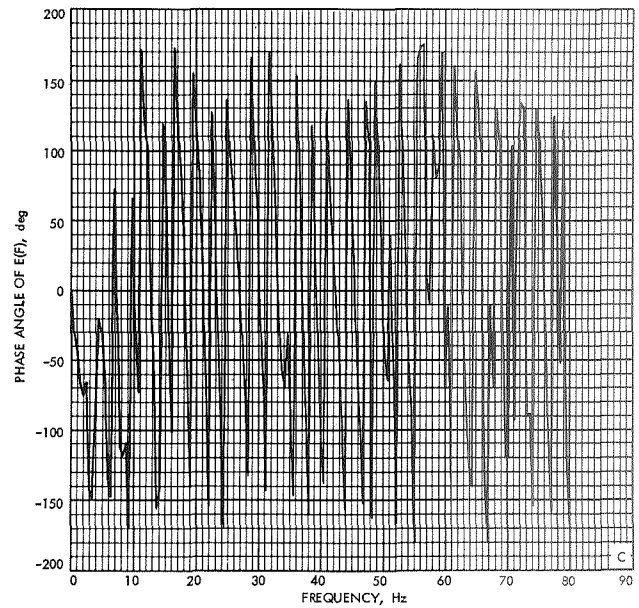
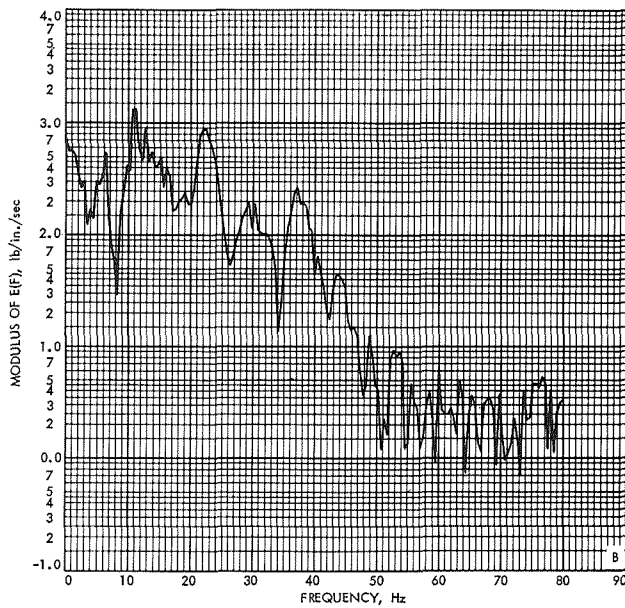


Fig. 49. Gridpoint 8, Viking reaction moment in θ_z -direction at base of Viking truss adapter predicted from the forcing function derived from Mariner VII (AC-19) MECO flight data